

FABRICATION AND STRUCTURAL  
PROPERTIES OF PEEK COMPOSITES  
USING FUNCTIONALIZED  
MULTIWALL NANOTUBES

NURUL HUDA BINTI ZAILANI

MASTER OF SCIENCE  
CHEMICAL ENGINEERING

UNIVERSITI TEKNOLOGI PETRONAS

MAY 2013



## STATUS OF THESIS

Title of thesis

**Fabrication and Structural Properties of PEEK Composites  
Using Functionalized Multiwall Nanotubes**

I NURUL HUDA BINTI ZAILANI

hereby allow my thesis to be placed at the Information Resource Center (IRC) of  
Universiti Teknologi PETRONAS (UTP) with the following conditions:

1. The thesis becomes the property of UTP
2. The IRC of UTP may make copies of the thesis for academic purposes only
3. This thesis is classified as

☐

Confidential

☐

Non-confidential

If this thesis is confidential, please state the reason:

---

---

The content of the thesis will remain confidential for \_\_\_\_\_ years.

Remarks on disclosure:

---

---

Endorsed by

Nurul Huda Binti Zailani  
No 9, Lorong IM 2/21,  
Bandar Indera Mahkota,  
25200 Kuantan, Pahang.

Date:

Assoc. Prof. Dr. Anita Ramli

Date:

UNIVERSITI TEKNOLOGI PETRONAS

FABRICATION AND STRUCTURAL PROPERTIES OF PEEK COMPOSITES  
USING FUNCTIONALIZED MULTIWALL NANOTUBES

by

NURUL HUDA BINTI ZAILANI

The undersigned certify that they have read, and recommend to The Postgraduate Studies Programme for acceptance this thesis for the fulfillment of the requirements for the degree of Master of Science in Chemical Engineering.

Signature:

Main Supervisor:

\_\_\_\_\_  
Assoc. Prof. Dr. Anita binti Ramli

Date:

\_\_\_\_\_

Signature:

Co-Supervisor:

\_\_\_\_\_  
Assoc. Prof. Dr. Zakaria bin Man

Date:

\_\_\_\_\_

Signature:

Head of Department:

\_\_\_\_\_  
Assoc. Prof. Dr. Mohd Azmi bin Bustam @ Khalil

Date:

\_\_\_\_\_



UNIVERSITI TEKNOLOGI PETRONAS

FABRICATION AND STRUCTURAL PROPERTIES OF PEEK COMPOSITES  
USING FUNCTIONALIZED MULTIWALL NANOTUBES

by

NURUL HUDA BINTI ZAILANI

A Thesis

Submitted to the Postgraduate Studies Programme  
as a Requirement for the Degree of

MASTER OF SCIENCE  
CHEMICAL ENGINEERING  
UNIVERSITI TEKNOLOGI PETRONAS  
BANDAR SRI ISKANDAR  
PERAK

MAY 2013

## DECLARATION OF THESIS

Title of thesis

**Fabrication and Structural Properties of PEEK Composites  
Using Functionalized Multiwall Nanotubes**

I NURUL HUDA BINTI ZAILANI

hereby declare that the thesis is based on my original work except for quotations and citations which have been duly acknowledged. I also declare that it has not been previously or concurrently submitted for any other degree at UTP or other institutions.

Witnessed by

\_\_\_\_\_  
Nurul Huda Binti Zailani  
No 9, Lorong IM 2/21,  
Bandar Indera Mahkota,  
25200 Kuantan, Pahang.  
Date: \_\_\_\_\_

\_\_\_\_\_  
Assoc. Prof. Dr. Anita Ramli

Date: \_\_\_\_\_

*Dedicated to my beloved Parents and Husband*

## ACKNOWLEDGEMENT

In the name of ALLAH, the Most Gracious and the Most Merciful

Alhamdulillah, all praises to Allah for the strengths and His blessings in completing this thesis. Special appreciation goes to my supervisor, Assoc. Prof. Dr. Anita Ramli, for her supervision and support. Her invaluable help of constructive comments and suggestions throughout the thesis works have contributed to the success of this research. Not forgotten, my appreciation to Dr. Moulay Rachid Babaa for his support and knowledge regarding this field as well as the supply of materials utilized throughout the experimental works.

I would like to thank all the technicians in the Chemical Engineering and Mechanical Engineering Departments for the help and assistants on the use of the facilities in the CE Lab and ME Lab. My acknowledgement also goes to all the office staffs of Chemical Engineering for their co-operations.

Sincere thanks to all my friends especially Ruzanna Ibrahim, Noor Diana bt. Abdul Majid, Nurul Shahida bt. Mohamed Zi, Nurhidayah bt. Mohammad, Siti Eda Eliana bt. Misi, Nurulhuda Mohd Yunus, Muhammad Hafiz Azahari and others for their kindness and moral support during my study. Thank you very much for the friendship and memories.

My deepest gratitude goes to my parents; Mr. Zailani b. Abd Manan and Mrs. Hasnah bt. Mohd Taha and also to my siblings for their endless love, prayers and encouragement. Last but not least, I would like to thank my husband, Mr. Nurul Sharifulizam b. Muhamad Saripudin for always be there for me and cheer me up. Your love, support and constant patience have taught me so much about sacrifice and discipline.

Finally, I would like to thank everybody who was important to the successful realization of this thesis, and expressing my apology that I could not mention personally one by one.

## TABLE OF CONTENTS

|                             | PAGE |
|-----------------------------|------|
| STATUS OF THESIS .....      | i    |
| APPROVAL PAGE .....         | ii   |
| TITLE PAGE .....            | iii  |
| DECLARATION OF THESIS ..... | iv   |
| DEDICATION .....            | v    |
| ACKNOWLEDGEMENT .....       | vi   |
| TABLE OF CONTENTS .....     | viii |
| ABSTRACT .....              | xi   |
| ABSTRAK .....               | xiii |
| COPYRIGHT PAGE.....         | xv   |
| LIST OF TABLES .....        | xvi  |
| LIST OF FIGURES.....        | xvii |
| LIST OF ABBREVIATIONS ..... | xix  |

### Chapter

|                                       |    |
|---------------------------------------|----|
| 1. INTRODUCTION.....                  | 1  |
| 1.1 Background of the Study.....      | 1  |
| 1.2 Problem Statement .....           | 4  |
| 1.3 Objectives of the Study .....     | 5  |
| 1.4 Scope of the Study .....          | 6  |
| 1.5 Outline of the Thesis .....       | 6  |
| 2. LITERATURE REVIEW.....             | 8  |
| 2.1 Carbon Nanotubes (CNTs).....      | 8  |
| 2.1.1 Types of CNTs.....              | 8  |
| 2.1.2 Synthesis of CNTs .....         | 10 |
| 2.1.3 Functionalization of CNTs ..... | 12 |

|   |        |
|---|--------|
| 2.1.3.1 Covalent Functionalization.....   | 12     |
| 2.1.3.2 Non-covalent Functionalization.....   | 14     |
| 2.1.4 Characterization of CNTs and functionalized CNTs.....                                 | 15     |
| 2.1.4.1 Scanning electron microscopy (SEM) and Transmission electron microscopy (TEM) ..... | 15     |
| 2.1.4.2 X-Ray Diffraction (XRD).....  | 17     |
| 2.1.4.3 Thermogravimetric Analysis (TGA) .....  | 18     |
| 2.1.5 Potential Applications .....  | 19     |
| 2.2 Poly(ether ether ketone) (PEEK) .....   | 20     |
| 2.2.1 Characterization of PEEK .....  | 22     |
| 2.2.2 Applications.....   | 23     |
| 2.3 Polymer Nanocomposites .....  | 23     |
| 2.3.1 Fabrication of polymer/CNTs nanocomposites.....                                       | 27     |
| 2.3.2 Structural Properties .....   | 27     |
| 2.3.3 Thermal Properties .....  | 29     |
| 2.3.4 Mechanical Properties .....   | 33     |
| <br>3. EXPERIMENTAL.....  | <br>35 |
| 3.1 Materials and Apparatus .....   | 35     |
| 3.2 Preparation of sulfonated PEEK (SPEEK) .....  | 36     |
| 3.3 Preparation of Oxidized Multiwalled Nanotubes (ox-MWNTs) .....                          | 37     |
| 3.4 Preparation of SPEEK-MWNTs.....   | 37     |
| 3.5 Preparation of MWNTs/PEEK Composites.....   | 39     |
| 3.6 Sample Characterization .....   | 40     |
| 3.6.1 Structural Properties .....   | 40     |
| 3.6.1.1 Field Emission Scanning Electron Microscopy (FE-SEM)....                            | 40     |
| 3.6.1.2 Transmission Electron Microscopy (TEM) .....  | 40     |
| 3.6.1.3 X-Ray Powder Diffraction (XRD).....   | 41     |
| 3.6.2 Thermal Properties .....  | 41     |
| 3.6.2.1 Differential Scanning Calorimeter (DSC) .....                                       | 41     |
| 3.6.2.2 Thermogravimetric Analysis (TGA) .....  | 41     |
| 3.6.3 Mechanical Properties .....   | 42     |

|  |    |
|--|----|
| 4. RESULTS AND DISCUSSIONS .....                         | 43 |
| 4.1 Multi-walled Carbon Nanotubes .....                  | 43 |
| 4.1.1 Structural Properties of MWNTs.....                | 43 |
| 4.1.2 Thermal Properties of MWNTs .....                  | 50 |
| 4.2 Structural Properties of MWNTs/PEEK Composites ..... | 51 |
| 4.2.1 XRD Results of MWNTs/PEEK Composites .....         | 51 |
| 4.2.2 FE-SEM on p-MWNTs/PEEK Composites .....            | 54 |
| 4.2.3 FE-SEM on ox-MWNTs/PEEK Composites .....           | 58 |
| 4.2.4 FE-SEM on SPEEK-MWNTs/PEEK Composites .....        | 60 |
| 4.3 Thermal Properties of PEEK Composites.....           | 62 |
| 4.3.1 TGA Results .....                                  | 62 |
| 4.3.1.1 TGA Results of p-MWNTs/PEEK Composites.....      | 62 |
| 4.3.1.2 TGA Results of ox-MWNTs/PEEK Composites.....     | 66 |
| 4.3.1.3 TGA Results of SPEEK-MWNTs/PEEK Composites ..... | 67 |
| 4.3.2 DSC Results.....                                   | 69 |
| 4.3.2.1 DSC Results of p-MWNTs/PEEK Composites .....     | 69 |
| 4.3.2.2 DSC Results of ox-MWNTs/PEEK Composites .....    | 73 |
| 4.3.2.3 DSC Results of SPEEK-MWNTs/PEEK Composites.....  | 75 |
| 4.4 Mechanical Properties of PEEK Composites.....        | 77 |
| 5. CONCLUSIONS AND RECOMMENDATIONS .....                 | 80 |
| 5.1 Conclusions .....                                    | 80 |
| 5.2 Recommendations .....                                | 81 |
| REFERENCES.....  | 83 |

## APPENDICES

- A. MSDS 1,6-Hexanediamine (HDA)
- B. MSDS N,N'-Dicyclohexylcarbodiimide (DCC)
- C. FT-IR Spectroscopy Results of p-MWNTs and ox-MWNTs



## ABSTRACT

Incorporation of carbon nanotubes (CNTs) into a polymer matrix can provide structural materials with dramatically increased mechanical and electrical properties. These properties combined with their low density makes them useful for the transport industry, especially for aerospace structures, where the reduction of weight is one of the main goals in order to reduce fuel consumption. However, several limitations exist firstly related to the dispersion of nanotubes and their compatibility with the matrix and secondarily to the nature of the binding between nanotubes and the polymer chains. These setbacks need to be resolved prior to successful applications.

In this work, two main approaches are considered for fabricating CNTs / poly (ether ether ketone) (PEEK) composites. In the first case, multiwalled carbon nanotubes (MWNTs) were functionalized with carboxyl group (-COOH) through oxidation process and then were incorporated in PEEK matrix using compression moulding process. In order to obtain a covalent linking between nanotubes and the matrix, another approach has been used based on the use of both chemically modified MWNTs and polymer. The attachment of oxidized MWNTs and sulphonated PEEK (SPEEK) was possible using a diamine as an interlinking molecule. The functionalization is required to improve the interfacial adhesion between MWNTs and PEEK matrix. Pristine MWNTs have been also embedded in polymer matrix without any surface modification and were used as a reference. Transmission electron microscopy (TEM), Field emission scanning electron microscopy (FE-SEM) and X-ray diffraction (XRD) techniques were used for structural investigation of the composite systems. Thermogravimetric analysis (TGA), Differential scanning calorimetry (DSC) and tensile test were done to understand the overall behavior of the composites.

FE-SEM reveals that the dispersion of MWNTs is improved after oxidation process and functionalization with SPEEK. XRD results concluded that the improvement of crystallinity after the addition of MWNTs to PEEK matrix and were confirmed with DSC scans. The thermal properties studied using TGA explained no significant amendments indicating no effects of MWNTs on the thermal properties of PEEK. On top of that, mechanical properties which is tensile modulus decreases after the addition of SPEEK-MWNTs revealing that use of bi-molecular molecule is not a suitable way to achieve a good dispersion of MWNTs in the matrix. This is due to the large nanotubes aggregations that nullify the effect of providing effective reinforcement. On the basis of the results from this research, it can be concluded that incorporation of SPEEK-MWNTs to PEEK material does not affect or improve the thermal and mechanical behavior. Hence, the author recommends further approach of fabrication method of the composites before other uses are considered.

## ABSTRAK

Penggabungan karbon nanotub (CNTs) ke dalam matriks polimer boleh menghasilkan bahan-bahan struktur dengan sifat-sifat mekanikal dan elektrik yang meningkat secara mendadak. Ciri-ciri di atas serta ciri kepadatan rendah CNTs menjadikannya berguna dalam industri pengangkutan, terutamanya bagi struktur aeroangkasa, di mana pengurangan berat adalah salah satu matlamat utama dalam usaha untuk mengurangkan penggunaan bahan api. Walau bagaimanapun, terdapat beberapa batasan pertamanya berkaitan dengan penyebaran nanotub dan keserasian mereka dengan matriks dan keduanya ialah sifat mengikat antara nanotub dan rantaian polimer. Halangan-halangan ini perlu diatasi sebelum berjaya diaplikasikan.

Dalam tesis ini, dua pendekatan utama telah dipertimbangkan untuk mereka komposit CNTs / poli(eter eter ketone) (PEEK). Langkah pertama ialah Karbon Nanotub Dinding Berlapis (MWNTs) diubahsuai dengan kumpulan karboksil (-COOH) melalui proses pengoksidaan dan kemudian telah digabungkan dalam matriks PEEK menggunakan proses pengacuan mampatan. Pendekatan lain telah digunakan berdasarkan penggunaan kedua-dua MWNTs yang telah diubahsuai secara kimia dan polimer untuk mendapatkan hubungan kovalen antara MWNTs dan matriks PEEK. Percantuman antara MWNTs teroksida dan PEEK tersulfon (SPEEK) boleh dilakukan dengan menggunakan diamina sebagai molekul antara-hubung. Proses pengubahsuaian adalah perlu untuk menguraikan MWNTs dan juga meningkatkan perlekatan antara muka antara MWNTs kepada PEEK matriks. MWNTs tulen juga telah digabung dalam matriks polimer tanpa sebarang pengubahsuaian permukaan dan digunakan sebagai rujukan. Mikroskop pancaran elektron (TEM), Mikroskop imbasan elektron medan pencahayaan (FE-SEM) dan teknik Pembelauan sinar-X (XRD) telah digunakan untuk memahami keseluruhan sifat-sifat sistem komposit.

FE-SEM mendedahkan bahawa penyerakan MWNTs dalam matriks PEEK bertambah baik selepas proses pengoksidaan dan pengubahsuaian menggunakan SPEEK. Keputusan XRD menyimpulkan bahawa penghabluran meningkat selepas penambahan MWNTs kepada matriks PEEK dan telah disahkan bersama imbasan DSC. Sifat haba dikaji menggunakan TGA menjelaskan tiada perubahan ketara di mana ia menunjukkan tiada kesan sifat MWNTs terhadap sifat haba PEEK. Selain itu, sifat mekanik iaitu modulus tegangan berkurangan selepas penambahan SPEEK-MWNTs. Ini menunjukkan bahawa penggunaan dwi-molekular molekul ini bukan satu cara yang sesuai untuk mencapai penyerakan MWNTs yang baik dalam matriks. Ini disebabkan oleh gumpalan besar nanotiub yang menghapuskan kesan yang menyediakan peneguhan yang berkesan. Hasil daripada kajian ini, dapat dirumuskan bahawa penggabungan SPEEK-MWNTs dengan bahan PEEK tidak menjejaskan atau memperbaiki sifat-sifat haba dan mekanik polimer tersebut. Oleh itu, penulis mencadangkan kajian lanjut cara penghasilan komposit sebelum kegunaan lain dipertimbangkan.

In compliance with the terms of the Copyright Act 1987 and the IP Policy of the university, the copyright of this thesis has been reassigned by the author to the legal entity of the university,

Institute of Technology PETRONAS Sdn Bhd.

Due acknowledgement shall always be made of the use of any material contained in, or derived from, this thesis.

© Nurul Huda Binti Zailani, 2013

Institute of Technology PETRONAS Sdn Bhd

All right reserved

## LIST OF TABLES

| Table |   | Page |
|-------|---|------|
| 2.1   | Summary table of PEEK based composites researches               | 26   |
| 3.1   | List of Chemical Utilized                                       | 35   |
| 3.2   | MWNTs/PEEK composites compositions                              | 39   |
| 4.1   | TGA data of MWNTs/PEEK Composites                               | 68   |
| 4.2   | DSC crystallization and melting data of p-MWNTs/PEEK Composites | 72   |
| 4.3   | DSC data of ox-MWNTs/PEEK Composites                            | 75   |
| 4.4   | DSC data of SPEEK-MWNTs/PEEK Composites                         | 77   |
| 4.5   | Mechanical properties of PEEK and MWNTs/PEEK Composites         | 78   |

## LIST OF FIGURES

| Figure |  | Page |
|--------|--|------|
| 2.1    | Transmission electron micrographs (TEMs) of the first observed MWNTs by Iijima in 1991 (a) Tube consisting of five graphitic sheets, diameter 6.7 nm (b) Two-sheet tube, diameter 5.5 nm (c) Seven-sheet tube, diameter 6.5 nm. [43] | 10   |
| 2.2    | Schematic preparation of the functionalized carbon nanotubes containing isocyanate groups. [52]  | 13   |
| 2.3    | Covalent modification of MWNTs with lipase. [53]   | 14   |
| 2.4    | Covalent modification of MWNTs with alkyl group. [54]  | 14   |
| 2.5    | (a) SEM images of Poly(L-lactide)/functionalized MWNTs and (b) TEM images of Poly(L-lactide)/functionalized MWNTs [20]   | 16   |
| 2.6    | Molecular Structure of PEEK  | 21   |
| 3.1    | Schematic illustration of the synthesis of SPEEK   | 36   |
| 3.2    | Schematic preparation of oxidation process of MWNTs  | 37   |
| 3.3    | Schematic presentation of functionalization reactions  | 38   |
| 4.1    | (a and b) FE-SEM images of p-MWNTs, (c and d) FE-SEM images of SPEEK-MWNTs   | 45   |
| 4.2    | TEM images of MWNTs; (a) p-MWNTs, (b) ox-MWNTs, (c) SPEEK-MWNTs  | 47   |
| 4.3    | XRD pattern of MWNTs and functionalized MWNTs  | 49   |
| 4.4    | XRD pattern of ZTP powder, pure SPEEK membrane and SPEEK/ZTP composite membrane. [99]  | 49   |

|      |   |    |
|------|---|----|
| 4.5  | TGA of p-MWNTs  | 50 |
| 4.6  | XRD pattern of p-MWNTs/PEEK composites  | 52 |
| 4.7  | XRD of ox-MWNTs/PEEK composites   | 53 |
| 4.8  | XRD of (SPEEK-MWNTs)/PEEK Composites  | 54 |
| 4.9  | FE-SEM Image of 100% PEEK and p-MWNTs/PEEK Composites; (a) Pure PEEK, (b) 0.5 MP and (c and d) 2 MP | 57 |
| 4.10 | FE-SEM images of ox-MWNTs / PEEK Composites; (a) 0.5 OMP and (b and c) 2 OMP                        | 60 |
| 4.11 | FESEM images of SPEEK-MWNTs/PEEK composites; (a) 0.5 SMP and (b) 2 SMP                              | 61 |
| 4.12 | TGA of Pure PEEK  | 63 |
| 4.13 | TGA of p-MWNTs/PEEK Composites  | 65 |
| 4.14 | TGA of ox-MWNTs/PEEK Composites   | 66 |
| 4.15 | TGA of SPEEK-MWNTs/PEEK Composites  | 67 |
| 4.16 | DSC scans of p-MWNTs/PEEK composites. (a) Heating and (b) cooling curves.                           | 70 |
| 4.17 | DSC scans of ox-MWNTs/PEEK composites. (a) Heating and (b) cooling curves.                          | 74 |
| 4.18 | DSC scans of SPEEK-MWNTs/PEEK composites. (a) Heating and (b) cooling curves.                       | 76 |



## LIST OF ABBREVIATIONS

|                                |   |
|--------------------------------|---|
| $\Delta H_c$                   | Crystallization Enthalpy                    |
| $(1-\lambda)_c$                | Degree of Crystallinity                     |
| AFM                            | Atomic Force Microscopy                     |
| CNTs                           | Carbon Nanotubes                            |
| CVD                            | Chemical vapour deposition                  |
| DCC                            | N,N'-dicyclohexylcarbodiimide               |
| DMF                            | Dimethylformamide                           |
| DSC                            | Differential Scanning Calorimetry           |
| DWNTs                          | Double-walled Nanotubes                     |
| FE-SEM                         | Field Emission Scanning Electron Microscopy |
| H <sub>2</sub> SO <sub>4</sub> | Sulphuric Acid                              |
| HDA                            | 1,6-hexane diamine                          |
| HNO <sub>3</sub>               | Nitric Acid                                 |
| LCP                            | Liquid Crystalline Polymer                  |
| MWNTs                          | Multi-walled Nanotubes                      |
| NaOH                           | Sodium Hydroxide                            |
| nm                             | nanometers                                  |
| p-MWNTs                        | Pristine Multi-walled Nanotubes             |
| ox-MWNTs                       | Oxidized Multi-walled Nanotubes             |
| PBT                            | Poly(butylenes Terephthalate)               |
| PEEK                           | Poly(ether ether ketone)                    |

|                  |  |
|------------------|--|
| PLLA             | Poly (L-lactide)                         |
| PMMA             | Poly(methyl methacrylate)                |
| PP               | Polypropylene                            |
| PS               | Polystyrene                              |
| PVA              | Poly(vinyl alcohol)                      |
| SiO <sub>2</sub> | Silicon Dioxide                          |
| SPEEK-MWNTs      | Sulphonated PEEK-Multiwall Nanotubes     |
| SWNTs            | Single-walled Nanotubes                  |
| TEM              | Transmission Electron Microscopy         |
| T <sub>c</sub>   | Crystalline Temperature                  |
| T <sub>g</sub>   | Glass Transition Temperature             |
| T <sub>m</sub>   | Melting Temperature                      |
| TGA              | Thermogravimetry Analysis                |
| UHMWPE           | Ultra High Molecular Weight Polyethylene |
| XRD              | X-ray Diffraction                        |

## CHAPTER 1

### INTRODUCTION

#### 1.1 Background of the Study

Carbon nanotubes (CNTs) have proven to exhibit extraordinary mechanical and electronic properties that make them useful and attractive to be used in a wide range of applications especially as reinforcement in composite materials [1]. CNTs are categorized as single-walled carbon nanotubes (SWNTs), double-walled carbon nanotubes (DWNTs) and multi-walled carbon nanotubes (MWNTs). However, a major difficulty remains in the control of the dispersion of these CNTs in the polymer matrix and the interaction between the polymer matrix and the CNTs charges. Thus, functionalization of CNTs surface is one interesting way to improve both the ability to disperse the nanotubes homogeneously throughout the matrix and the load transfer from the matrix to nanotubes [2].

Poly (ether ether ketone) (PEEK) is a semycrystalline, high performance thermoplastic polymer with a polyarylether group [3-4]. It has excellent thermal stability and mechanical properties, thus is being used in wide range of application such as in aerospace and marine industries. PEEK has been established in 1981 with many publications reported on the morphology and structure [3, 5], mechanical [3, 6-7], thermal [4-5, 8] and electrical [3] characteristics of the thermoplastic material. Recent publications reported on functionalization of multiwalled nanotubes with sulphonated PEEK to facilitate incorporation of CNTs in PEEK matrix [5-6, 9].

Thermoplastic materials like PEEK offer quite a range of advantages. PEEK have unlimited shelf life, short process cycle time, and it is able to reform after melted. In addition, PEEK has increased moisture resistance and increased

toughness and impact resistance. However, thermoplastic materials do have several disadvantages where the processing temperature is higher than those required for polyepoxy composite materials. The present cost of thermoplastic materials and performs for advanced composites is high. In fact, the manufacture of thermoplastic prepreg and other preform is much more difficult [10].

Oil crisis in the 1970's have forced the aerospace making companies to upgrade and design the aircraft that consume less fuel [11]. What's more, the oil crisis becomes even greater nowadays due to reduced source of oil. In other words, the aircraft should have more efficient engines, reduced aircraft weight and improved aerodynamics. The reduced aircraft weight is where the role of plastics or polymers comes in place. The weight of the aircraft is crucial because more fuel will be required to power it if the vehicle is heavier. The polymers not only save fuel consumption but also in terms of money because of their smooth contours that is able to improve the aerodynamics along with less upkeep required and easier to repair [11]. According to the above matters, PEEK will be expected to be the key material in the future.

Nanocomposites are defined as multi component solid materials where the size of at least one of the components are smaller than 100 nanometers (nm), or consists of structures having nano-scale repeat distances between the different phases that made up the material. As a result, the nanocomposites will have new and improved properties compared to the virgin polymer itself.

Incorporation of CNTs into a particular polymer matrix can provide structural materials with dramatically increased mechanical, thermal and electrical properties. These properties combined with their low density makes them useful for the transport industry, especially for aerospace structures, where the reduction of weight is one of the main goals in order to reduce fuel consumption. Previous researches have reported changes in morphology and consequently the properties of the polymer by the incorporation of CNTs [1-3, 5-6, 12].

Unfortunately, pristine CNTs are insoluble in most solvents. Thus, they are difficult to be dispersed evenly in polymer matrix such as PEEK and other polymers [13]. This complicates the efforts to utilize CNTs novel properties in some potential applications. To overcome this problem, chemical functional groups can be introduced to the surface of CNT without significantly changing the CNTs desirable properties so as to make CNT more dispersible in liquids [13]. On top of that, chemical functional groups such as carboxylic group, amine group, etc. are more dispersible in most common solvents, thus easier to be embedded with desired matrix. Chopping, oxidation and wrapping are examples of functionalization methods which can create more active bonding sites on the surface of CNTs [14].

Oxidation is one of the most commonly used techniques of purifying the MWNTs by refluxing the CNTs in the concentrated acidic solution [15]. Apart from purification, oxidation introduces active functional, opens end caps of CNTs and also causes damages to CNTs [15-16]. Both physical and mechanical/thermal properties of the composites are influenced by the chemical treatment of the MWNTs that is carried out before they are embedded into the polymer materials [15]. Based on Coleman et al. [19], covalent functionalization and surface chemistry of carbon nanotubes are the important factors for nanotubes processing and applications. The lack of interfacial bonding between polymer matrix and carbon nanotubes is because of the smooth graphene structure of nanotubes [17-18]. Coleman et al. [19] also reported that covalent attachments can decrease the maximum buckling force of nanotubes by 15% and also reduce the mechanical properties of the final nanotubes composite.

## **1.2 Problem Statement**

CNTs possess unique physical properties which have attracted great deal of interest in various fields such as composites, electronics and consumer products. Physical properties like mechanical strength, electrical and thermal conductivity of CNTs can be utilized to improve the comprehensive properties of a particular matrix. The

microsize material tends to have a large surface area per unit volume which results in very good load transfer to the nanotube network.

CNTs have a potential to be used as reinforcing material especially in polymer materials for development of new improved material with better mechanical properties but still maintains the production costs to be relatively low. The CNTs loading can be a minimum of 0.01 % to a maximum of 5 % depending on the type of polymer to be upgraded. Different polymers have different optimum loading of CNTs. The tube-like molecule structure of CNTs offers a large surface area which in return creates bonding with polymer matrix providing network to transfer load to CNTs.

Nevertheless, a major difficulty remains in the dispersion of these CNTs in polymer matrix and interaction between the matrix and nanotubes. CNTs tend to agglomerate among themselves. Their small size and the large surface area make them susceptible to van der Waals forces that promote aggregation [20].

Thus, many techniques have been applied in order to break these agglomerations and enhance the dispersion of CNTs in polymer matrices. Functionalization of CNTs surface is an interesting way to improve the ability to disperse the nanotubes homogeneously throughout the matrix and the load transfer from the matrix to nanotubes. The technique through covalent bonding by chemical functionalization on the surface of CNTs would improve the interfacial bonding between CNTs and polymer matrix. The low forces existing between the wrapping macromolecules and nanotubes are considered as a disadvantage to the load transfer between them.

PEEK has been used in aerospace industries, specifically aircraft exterior and aircraft interior components for its weight. For example, a new line of wiring and tubing clamps have been created from PEEK coupled with a proprietary silicone overmolding process. The new clamps delivered significant weight as well as cost savings on the aircrafts. Other applications are insulation cover films, impeller blades and aircraft door handles [73]. It is crucial to upgrade PEEK in order to improve its physical properties. Consequently, the product would be produced

utilizing smaller amount of polymer but with same strength. Less oil consumption can be achieved with better aerodynamic design, reduction in aircraft weight and improvement in composite polymer properties. The incorporation of CNTs would be expected to improve the physical properties of PEEK. On top of that, treatments of CNTs are required to improve their dispersion in a particular matrix which in return would result in significant improvement in their mechanical properties.

In the study, functional groups such as carboxyl group (-COOH) and sulphonated PEEK (-SPEEK) chain have been proposed. Carboxyl group is the most attractive functional group for CNTs as its ability to be readily used for further functionalization with other functional groups and also to be incorporated in a polymer. Carboxyl group were introduced to CNTs via oxidation process by refluxing CNTs in concentrated acidic solution [15]. Hence, COOH-CNTs could be called oxidized CNTs, ox-CNTs.

MWNTs have been selected as the reinforcing material because they are able to be produced in much larger amount at lower cost eventhough having lower mechanical performance than SWNTs. On top of that, MWNTs are longer than SWNTs and more rigid because their section is much larger.

### **1.3 Objectives of the Study**

The general objective of this research is to prepare PEEK composites with MWNTs as the reinforcing material and to study the effect of chemical modification of MWNTs on the physical properties of the MWNTs/PEEK composite. To achieve these general objectives, the specific objectives have been outline as:

- i) To functionalize and characterize MWNTs with carboxyl group and SPEEK.
- ii) To fabricate PEEK composites with ox-MWNTs and SPEEK-MWNTs.
- iii) To characterize the structural, thermal and mechanical properties of functionalized CNTs / polymer (PEEK) nanocomposite materials.

## **1.4 Scope of the Study**

In order to accomplish the objectives of the research, the scope of work has been divided into several sections as listed below;

- i. Functionalization of MWNTs with carboxyl group and SPEEK respectively and their characterization.
- ii. Fabrication of PEEK composites with ox-MWNTs and SPEEK-MWNTs using melt process.
- iii. Characterization of structural, thermal and mechanical properties using Transmission Electron Microscopy (TEM), Field Emission Scanning Electron Microscopy (FE-SEM), Powder X-ray Diffraction (XRD), Thermogravimetry Analysis (TGA), Differential Scanning Calorimetry (DSC) and tensile test.

## **1.5 Outline of the Thesis**

This thesis is organized as follows:

- Chapter 1 explains the introduction of the study comprising the background of the study, problem statement, objective and scope of the study also the outline of the thesis.
- Chapter 2 describes the relevant background information of carbon nanotubes, the polymer, i.e. PEEK, as well as an introduction to the polymer nanocomposites and its approaches. Additionally, Chapter 2 presents several applications of the composites and also the properties concerning the composites.
- Chapter 3 presents the syntheses of surface functionalization of MWNTs and the fabrication approaches of the nanocomposites.
- Chapter 4 presents the main part of the thesis, namely the testing of the properties of the composites. The properties discussed are structural,



thermal and mechanical properties of the fabricated composites. Prior to the properties of the composites, the effect of surface modification of MWNTs are studied and addressed in this chapter.

- Chapter 5 presents the conclusions of this thesis and recommendations for the future works. This is followed by references.

The sufficient information and findings from this thesis can be used as a future reference for the development of composite materials especially on the functionalization of CNTs and the fabrication method of the composite materials.

## CHAPTER 2

### LITERATURE REVIEW

#### 2.1 Carbon Nanotubes (CNTs)

Carbon nanotube is a number of sheets of graphite rolled into a cylinder with several microns size of length and a few nanometers of diameter [12, 21-22]. Bonding in CNTs is essentially  $sp_2$ . However, the circular curvature cause quantum continuement and  $\alpha$ - $\pi$  rehybridization in which 3  $\alpha$  bonds are slightly out of plane. This makes CNTs mechanically stronger, electrically and thermally more conductive and chemically and biologically more active than graphite [23].

Carbon nanotubes possess unique mechanical, thermal properties and structural properties [3, 24-30]. Since the first discovery of CNTs by Iijima in 1991, many studies were carried out on the elaboration of composite materials especially polymer composites [3, 24, 26, 31-32]. These extraordinary properties of CNTs such as high strength and good thermal conductivity create great interests to be applied in diverse fields from electronic industry to aeronautic industry [5, 12, 15, 24, 29, 33-34]. CNTs can be considered to have diameters ranging from 0.9 nm to 50 nm [35].

##### 2.1.1 Types of CNTs

Nanotubes are in three forms; single-walled, double-walled and multi-walled [12, 36]. Single-walled nanotubes consist of one layer of carbon atoms through the thickness of the cylindrical wall. On the other hand, multi-walled nanotubes consist of concentric cylinders around a common central hollow with a constant separation between layers close to the graphite interlayer spacing, 0.34 nm and double-walled

nanotubes consist of two cylinders [12, 33, 37]. Many of the properties of MW tubes are already quite close to graphite. While the MWNTs have a wide range of application, they are less well defined from their structural and hence electronic properties due to many possible numbers of layers [23]. The purity of CNTs depends on the technique utilized. Putting SWNTs and MWNTs side by side, MWNTs have lower mechanical performance yet is able to be produced in much larger amount at lower cost. MWNTs are longer than SWNTs and more rigid because their section is much larger [36].

Theoretically, the elastic modulus of CNTs is able to exceed 1.0 TPa which is higher than the elastic modulus of steel; 0.2 TPa ; diamond is 1.2 TPa [12, 26, 38-39]. Meanwhile, the tensile strength is around 10-50 GPa (0.25 GPa for steel). The thermal conductivity of CNTs is able to have as high as 3000 W/m.K which is approximately seven times higher than copper, 385 W/m.K [12].

Hence, mechanical properties and thermal transport of a particular material can be enhanced by using carbon nanotubes as fillers [29, 40]. Possessing good thermal conductivity suggests their use in composites for thermal management [39]. It is typical for the structure of CNTs to be entangled and agglomerate to each other [29, 32, 34, 41]. This is strongly affected by van der Waals forces due to their small size and large surface area [5, 12, 37]. As a solution, oxidation and chemical functionalization of CNTs as well as covalent attachment of polymer chains to the CNTs can improve the dispersion of CNTs and the strength of interfacial bonding between CNTs and polymer matrices will be stronger [29, 32-33, 39].

Iijima initially observed only MWNTs with between two and 20 layers. However, subsequent publication in 1993, he confirmed the existence of SWNTs and elucidated their structure [42]. Figure 2.1 below shows the MWNTs discovered by Iijima in 1991.

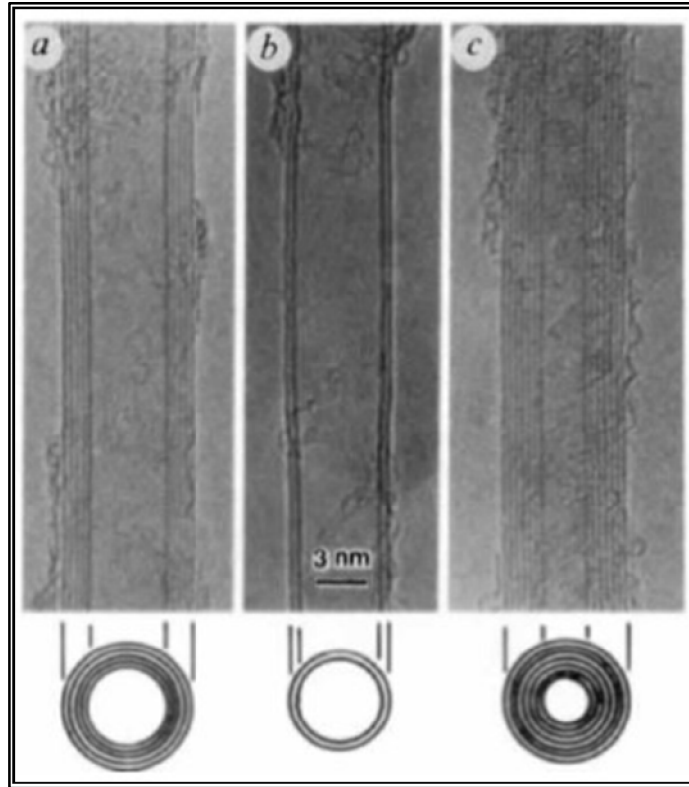


Figure 2.1: Transmission electron micrographs (TEMs) of the first observed MWNTs by Iijima in 1991 (a) Tube consisting of five graphitic sheets, diameter 6.7 nm (b) Two-sheet tube, diameter 5.5 nm (c) Seven-sheet tube, diameter 6.5 nm. [43]

### 2.1.2 Synthesis of CNTs

Most early properties measurements were carried out on MWNTs long before SWNTs. This is due to MWNTs proved they are far easier to manufacture in large scale than SWNTs and are thus farther along in terms of material development. Besides, the first mass production of MWNTs was reported less than a year after Iijima's finding. The development of the synthesis of CNTs is now available in wider range from high temperature methods which occurring near the focus of a high-powered laser, in between two arcing graphite electrodes, or even in the middle of a flame, nanotubes form, given the right condition [36, 42, 44].

The first method to produce SWNTs and MWNTs was the arc discharge and it has been optimised to be able to produce small scaled quantity of either of the CNTs. Arc discharge is similar to the Kratschmer-Huffman method which is used to generate fullerenes as well as the procedure to make carbon whiskers developed by Roger Bacon 30 years ago. First discovery of MWNTs by the method found that nanotubes are formed on the cathode, along the soot and fullerenes. Two years later, SWNT were reported by Iijima and Ichihashi and Bethune et al. They learned that SWNT could only be formed by adding metal catalyst to the anode [42]. Generally, nanotubes produced by the synthesis method require extensive purification before usage. Nevertheless, both SWNTs and MWNTs made from the process are now commercially available relatively reasonably priced [45].

Laser ablation and arc discharge follows the similar principle as both uses a metal impregnated graphite target to produce SWNTs also both produce MWNTs and fullerenes when pure graphite is used instead. SWNTs made by the method have the diameter roughly between 1.0 and 1.6 nm [45-46].

Chemical vapour deposition (CVD) was first reported in 1993 by Endo et al. to produce defective MWNTs. The CVD process covers a wide range of synthesis techniques from the gram quantity bulk formation of nanotubes materials to the formation of individual aligned SWNTs on SiO<sub>2</sub> substrates for electronic purposes. CVD can also fabricate aligned vertical MWNTs for use as high-performance field emitters. In addition, various forms of CVD produce SWNTs material of higher atomic quality and higher percent yield than the other currently available and as such represents a significant advance in SWNTs production [47-48].

Flame synthesis has the potential to become an extremely cheap and simple way to produce nanotubes even though it is still not a viable method for the production of high quality SWNTs. Flames have been shown to produce MWNTs since early 1990s. First production of SWNTs revealed by Vander Wal et al. [49], a hydrocarbon flame composed of ~10% ethylene or acetylene with Fe or Co particles interspersed and diluted in H<sub>2</sub> and either He or Ar was ignited by the researchers. Ever since, many groups have been able to produce SWNTs. There was also a brief

review written by Height et al. on the specifics of various methods for MWNTs and SWNTs production. Though the current yields are very low, the synthesis is extremely attractive and potentially very cheap to be able to produce nanotubes with technology no more complicated than fire [46].

### **2.1.3 Functionalization of CNTs**

Researches were done in recent years focusing on polymer composite with CNTs as fillers because of their potential to reduce the unit cost of production. CNTs / Polymer composite is able to form the conductive path at a relatively very low content if compared to composites filled with carbon black or carbon fiber [15]. This is because the CNTs have high aspect ratio of 100-1000 and high specific surface areas [15, 37]. CNTs produced by thermal methods have an amount of impurities up to 30 to 40%. Impurities in CNTs product are metallic catalyst particles and carbonaceous materials like amorphous carbon, spheroidal fullerenes and non-crystalline graphite species. The existence of impurities impairs the properties of CNTs thus also having bad effect on the composites which causes dispersion of CNTs in polymer to be poor. Hence, purification of CNTs is essential for CNTs to be useful in wide application [15].

Suggs and Wang [50] carried out studies to investigate the techniques to disentangling the CNTs bundles while improving their interfacial adhesion to the matrix. The techniques utilized are covalent and non-covalent functionalization [31, 44, 50-51].

#### **2.1.3.1 Covalent Functionalization**

Covalent functionalization which is the covalent attachment of functional groups to the walls of CNTs is able to be achieved by multitude of chemical and physical methods [46]. However, this introduces defects on the walls of the perfect structure of CNTs and reduces the strength of the reinforcing component [44]. More

homogeneous distribution of the reinforcement can be obtained by wrapping the CNTs with polymer [50]. There are numerous tested covalent modifications of CNTs have been reported since its discovery. The major approaches include the amidation or esterification of carboxylated CNTs and also the direct side-wall covalent attachment of functional groups to the pristine CNTs [52]. In situ polymerization where the polymer macromolecules are grafted onto the walls of CNTs is also one of the main approaches for the preparation of polymer grafted nanotubes [19].

Based on Coleman et al. [19], covalent functionalization and surface chemistry of carbon nanotubes are the important factors for nanotubes processing and applications. The lack of interfacial bonding between polymer matrix and carbon nanotubes is because of the smooth graphene structure of nanotubes [17-18]. Coleman et al. [19] also reported that covalent attachments can decrease the maximum buckling force of nanotubes by 15% and also reduce the mechanical properties of the final nanotubes composite.

Zhao et al. [52] described a covalent process for side-wall functionalization of MWNTs with isocyanate groups with high reactivity and can react with a number of chemicals like alcohols, amines and carboxylic acid, etc (Figure 2.2). The functionalized CNTs containing isocyanate groups are able to extend nanotubes chemistry based of the wealth chemistry of isocyanate groups and may be hopeful to be prepared.

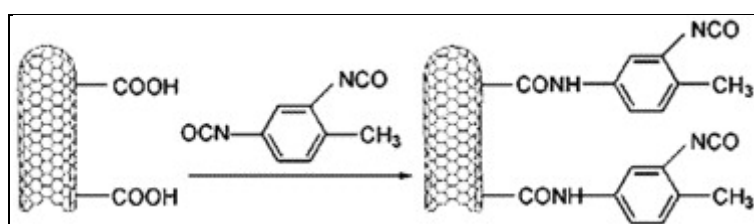


Figure 2.2: Schematic preparation of the functionalized carbon nanotubes containing isocyanate groups. [52]

Another study by Shi et al. [53] reported that the covalent functionalization of MWNTs by lipase showed higher solubility in several organic solvents than that of

the pristine MWNTs (Figure 2.3). Lipase itself exhibit drastically higher interfacial activity compared to esterases upon lipid-water interface contacts. The similar results were obtained by Jung et al. [54] on MWNTs functionalized with alkyl group to be embedded to poly (3-hydroxybutyrate) (PHB) (Figure 2.4). The alkylated MWNTs improve the properties of PHB.

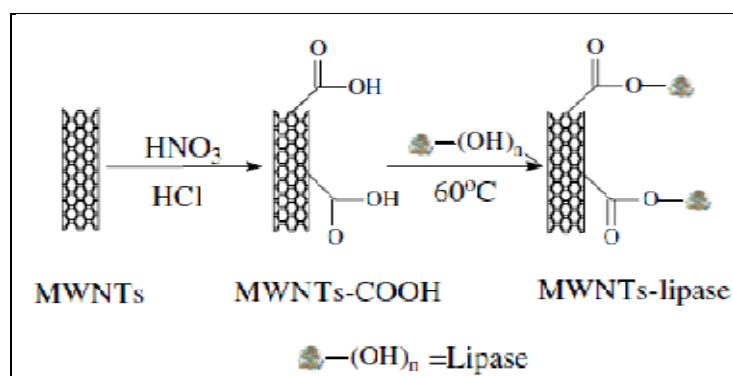


Figure 2.3: Covalent modification of MWNTs with lipase. [53]

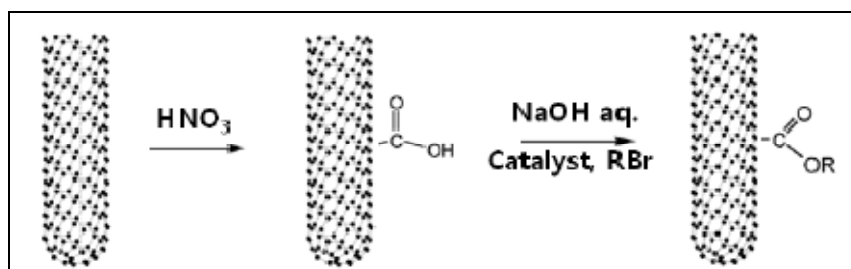


Figure 2.4: Covalent modification of MWNTs with alkyl group. [54]

### 2.1.3.2 Non-covalent Functionalization

The non-covalent attachment leads to only weak interfacial van der Waals forces where the perfect structure of the CNTs is not altered and their overall mechanical properties remains.

Studies of SWNTs are hindered by overcoming difficulties due to the insolubility of SWNTs. In other words, the poor dispersion of SWNTs in common solvents and polymer matrices [55]. Carboxyl group is among the attractive functional groups because of its ability to be readily used for further covalent or non-covalent



functionalization. Carboxylation is usually conducted via oxidation of the surface of the SWNTs by strong oxidants [51, 55].

Oxidation is one of the most commonly used techniques of purifying the MWNTs by refluxing the CNTs in the concentrated acidic solution [15]. Apart from purification, oxidation introduces active functional, opens end caps of CNTs and also causes damages to CNTs [15-16]. The extent of the above effects depends on the oxidation conditions yet influences the physical and electrical properties of the composites [15, 34]. Both physical and mechanical/thermal properties of the composites are influenced by the chemical treatment of the MWNTs that is carried out before they are embedded into the polymer materials [15].

Zhao et al. [56] utilized organic molecules including benzene, cyclohexane and 2,3-dichloro-5,6-dicyano-1,4-benzoquinone to be functionalized with CNTs. The organic molecules are used to control the electronic properties of the CNTs.

#### **2.1.4 Characterization of CNTs and Functionalized CNTs**

Tools for characterization are crucial in research of emerging materials to assess their full potential in various applications and also to understand their basic physical and chemical properties. There are various techniques that have aided to reveal some of the essential properties of CNTs.

##### *2.1.4.1 Scanning electron microscopy (SEM) and Transmission electron microscopy (TEM)*

The first technique is the electron microscopy. Different electron microscopy method enables one to investigate structure of CNTs in detail as well as identify their growth mechanism. This may gain the insight of the improvement of the nanotubes growth processes and modification of its structure. Scanning electron microscopy (SEM) illustrates the rope of SWNTs in a sample or imaged the highly oriented

forest of MWNTs. The typical resolution of a SEM is in range from 2 to 5 nm [47-48, 57].

Transmission electron microscopy (TEM) is another common technique that allows one to determine the number of walls in a single MWNT or image the isolated SWNTs residing inside a SWNTs bundle. Techniques of electron microscopic (EM) are priceless for nanotubes characterization. EM will play the significant role in future studies of nanotubes research [48, 57]. Figure 2.5 below are the SEM and TEM images of SWNTs and MWNTs from previous researches.

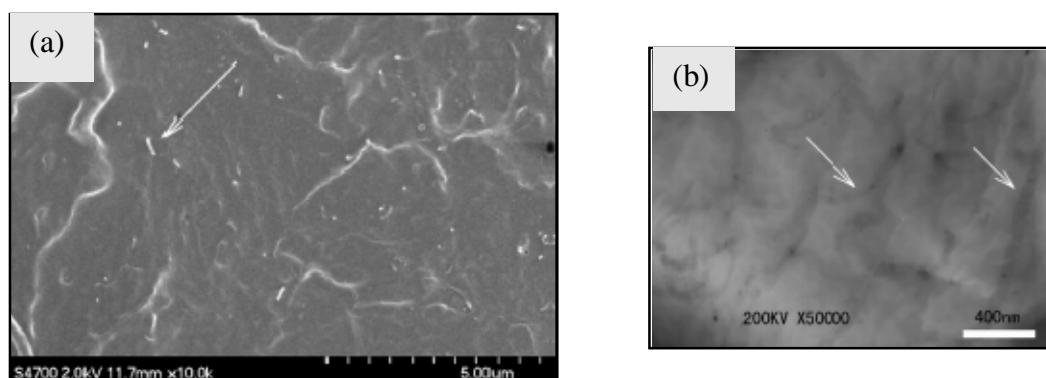


Figure 2.5: (a) SEM images of Poly(L-lactide) / functionalized MWNTs and (b) TEM images of Poly(L-lactide) / functionalized MWNTs. [20]

Through SEM and TEM images, pristine MWNTs (p-MWNTs) were highly tangled with each other with very small traces of impurities and rarely visible ends. The entanglement is because of the van der Waals forces between the nanotubes [5, 15, 25]. Observation on p-MWNTs and ox-MWNTs by Choi et al. [21] suggests that the treatment did not damage the MWNTs severely. Babaa et al. [9] functionalize the MWNTs with SPEEK and give results of the shorter length tubes and are wrapped by a layer of polymer.

Banerjee and Wong [25] pointed out that the aggressive oxidation condition can open the caps of MWNTs and remove the outer layers of the tubes. On the other hand, the chemically treated MWNTs dispersed better. This owes to the functional groups and negative charges formed at the surface of MWNTs. The metallic catalyst and carbonaceous materials comprises assorted shapes and molecular organizations

which impair properties of MWNTs itself and the composites derived with MWNTs; agreed with Sloan et al. as reported by Kim et al. [15]. Strong acid condition is able to remove the impurities completely as displayed in TEM images. The amount of damage caused by the oxidation process depends on the degree of acidity or basicity, the treatment time and temperature, applied mechanical forces, the degree of CNTs crystallinity and others.

Pirlot et al. [58] managed to reveal the presence of long individual MWNTs, the linear types that are averagely 4 and 13 nm of inner and outer diameters. The intertube distance of 3.4 Å showed that there are 13 graphitic layers of MWNTs. The degree of dispersion of MWNTs in the polymer matrix is assessed using low resolution of TEM. It can be seen that the aggregates of MWNTs appeared as well as some isolated nanotubes. Ruan et al. [59] ran TEM that showed the average diameters of the MWNTs are ~15 nm.

#### *2.1.4.2 X-Ray Diffraction (XRD)*

Historically, X-ray diffraction (XRD) has provided structural information for an infinite number of crystals. Nevertheless, the technique has found relatively limited success for research in CNTs [48].

The XRD patterns characterizing MWNTs have four peaks at  $2\theta = 25.8^\circ$ ,  $43.1^\circ$ ,  $54.0^\circ$  and  $78.5^\circ$  corresponding to the (002), (100), (004) and (110) crystal face diffraction peaks, respectively [60]. A literature by Pirlot, C. et al. [58] discussing on the XRD pattern of MWNTs showed two obvious peaks at  $25.8^\circ$  and  $42.8^\circ$  corresponding interlayer spacing which is 0.34 nm, d002 and d100 reflection of the carbon atoms. The band at  $42.8^\circ$  is asymmetric due to the turbostratic nature of nanotubes where the basal plane has slipped sideways to each other. The increased intensity of the peaks assigned to the MWNTs in the composite as a consequence of the increase in the charge of the MWNTs in the film. They concluded the preparation approach did not cause alteration of the structure of the MWNTs.

#### 2.1.4.3 Thermogravimetric Analysis (TGA)

TGA measurement was carried out by Chen et al. [55] on purified SWNTs showed little weight loss which is less than 5 wt%. From the literature of Chen et al. [61], the MWNTs were dispersed in concentrated acid mixture for three hours to achieve moderate oxidation and maintain high aspect ratio. Chen et al. [61] also agreed the small amount of amorphous carbon and impurities represent the minor mass loss from TGA. The oxidized MWNTs shows 7% mass fraction of organic groups chemically bonded to MWNTs were eliminated at 600°C.

Cheng et al. [16] studied the CNTs / epoxy composites and found out that the CNTs are thermally stable in nitrogen gas environment below 1000°C. However, Díez-Pascual et al. [5] stated that the SWNTs start to degrade at temperature above 600°C under nitrogen condition. The CNTs are thermally more stable under inert conditions rather than in an oxidative condition which is agreed by Díez-Pascual et al. [5].

On the other hand, the thermal behavior of the CNTs is measured by TGA [52]. The onset temperature of oxidized MWNTs, 460°C become dramatically lower than pristine MWNTs, 615°C due to the organic contents attached. Li et al. [62] also did thermogravimetric analysis on the p-MWNTs and at 600°C, only 5 wt% of initial weight indicating their high thermal properties. Chen et al. [55] also reported TGA trace of purified SWNTs shows little weight loss indicates that the trace amount of impurities in the SWNTs.

MWNTs are used more often today due to its cost [1, 63]. Two practical advantages of dispersing CNTs into PP compared to dispersing clay or silica into polyolefins are; i) the clay and silica often require organic treatment on their surfaces and / or ii) a compatibilizing polymer modifier, e.g. PP grafted with malice anhydride (PP-g-MA). On the other hand, CNTs are organophilic which can be dispersed directly into the polymer [63].

### 2.1.5 Potential Applications

The rapid development of the CNTs science and technology can be witnessed since its primary findings. The impressive progress of the fabrication, manipulation and characterization also the modelling of the nanostructures based CNTs made it is utilized in various application areas such as devices, energy, materials and other sectors. In particular, CNTs shows potentials varying from composites, energy storage, nanoelectronics and other solid-state devices, to sensors and actuators [44, 64]. Devices like sensors based on CNTs continuously expanding and widening. Example of CNTs based sensors are chemical, flow, mass, optical, pressure and thermal sensors. The mechanism of this application involves the modulation of the electronic properties of the CNTs itself [44]. For example, gas sensor fabricated by simple casting of SWNTs on an interdigitated electrode was studied by Li et al. [65]. The response shows reproducible linear behaviour and have detection limit of <44 ppb for NO<sub>2</sub> and 262 ppb for nitrotoluene.

High flexibility of CNTs comes together with high strength and high stiffness if compared to other carbon materials, i.e. steel [50]. Hence, a new generation of high performance light weight polymer composites become useful for structural reinforcement due to the above properties. A great deal of research is done and keeps going to investigate the ability of CNTs to stiffen and strengthen the polymers. The reinforcement depends on the load transfer to the CNTs aggregates. If the adhesion between the matrix and the CNTs is not strong enough to sustain high loads, the advantage of high tensile strength of CNTs loss. The mechanical properties of CNTs will be imitated in composites once a good load transfer between the matrix and the outer surface of CNTs is obtained [44].

Recently, CNTs probes in AFM have become well-known as data in literature is sufficient to demonstrate the enhanced resolution and the performance of CNTs probes. SWNTs probe shows impressive resolution where a tip with a radius of curvature as small as 1 nm demonstrated. However, the attachment of SWNTs to the Si probe requires improvement to enhance stability. On the other hand, MWNTs probes have demonstrated for high aspect ratio imaging application which resolves

deep and narrow features with CD in the sub-100-nm range. The attachment of MWNTs to the surface of Si probe is strengthened by current-induced welding that leads to enhancement on the stability of probe [48].

Others than the above, CNTs is also applied within molecular electronics and chemical and biological sensor. The development of the biosensors is due to the intention to detect various diseases at early stage. Until now, studies on the application of CNTs in biosensing are still in full swing. The advancement of the approach to deliver the drugs in a fast, durable, in time and safe ways are progressing as well aiming to lower the side effect [44].

CNTs emitter is another potential application where any system that uses an electron source could host a CNTs field emission device. CNTs field emitters are suitable for high efficiency, fast switching or ultrahigh frequency modulation and very high current densities. Several applications of CNTs emitters are vacuum microelectronics, x-ray tubes and microwave amplifiers [66-67].

## **2.2 Poly(ether ether ketone) (PEEK)**

Polymer is defined as a long-chain molecule of very high molecular weight, often measured in the hundreds of thousands of gram for every mole of the molecule [68]. Introduction to Physical Polymer Science Handbook define polymer in its simplest form can be regarded as comprising molecules with molecular weight of at least  $2000 \text{ g mol}^{-1}$  [68].

PEEK, an aromatic polyketone is a high performance thermoplastic material that is able to retain its good mechanical properties such as elastic modulus, strength and toughness and elevated temperature even at high temperature [3-5, 7, 44]. Thermoplastic materials have one or two dimensional molecular structure (Figure 2.6) and it soften at high temperature and melt. The softening process is reversible to regain its properties during cooling which assists the molding technique to mold the material [10].

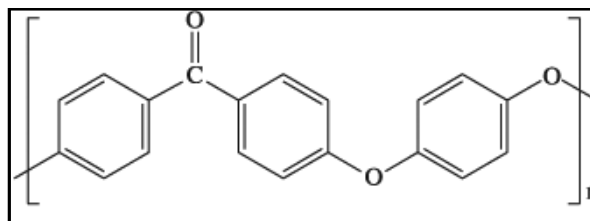


Figure 2.6 : Molecular Structure of PEEK

The semicrystalline polymer shows good thermal and chemical stability as well as storage stability without freezing device, cycling usage ability and in situ adaptability [3, 5, 7-8]. On top of the above, PEEK have relatively high viscosity which is widely used for aerospace and marine industries as load bearing structural material [3, 5]. Many studies have been done on polymer composites and its characterization. However, majority of previous work done are materials degradation and decomposition in order to obtain and understand the kinetic parameters of the processes involved during decomposition [4].

Thermoplastic materials like PEEK offer quite a range of advantages. PEEK have unlimited shelf life, short process cycle time, and it is able to reform after melted. In addition, PEEK has increased moisture resistance and increased toughness and impact resistance. However, thermoplastic materials do have several disadvantages where the processing temperature is higher than those required for polyepoxy composite materials. The present cost of thermoplastic materials and performs for advanced composites is high. In fact, the manufacture of thermoplastic prepreg and other preform is much more difficult [10].

Oil crisis in the 1970's have forced the aerospace making companies to upgrade and design the aircraft that consume less fuel [11]. What's more, the oil crisis becomes even greater nowadays due to reduced source of oil. In other words, the aircraft should have more efficient engines, reduced aircraft weight and improved aerodynamics. The reduced aircraft weight is where the role of plastics or polymers comes in place. The weight of the aircraft is crucial because more fuel will be required to power it if the vehicle is heavier. The polymers not only save fuel consumption but also in terms of money because of their smooth contours that is able

to improve the aerodynamics along with less upkeep required and easier to repair [11]. According to the above matters, PEEK will be expected to be the key material in the future.

### **2.2.1 Characterization of PEEK**

PEEK itself have high mechanical and thermal properties. However, several improvements on the mechanical properties shall be seen plus the effect of reinforcement on the thermal stability.

Yin et al. [69] discussed the X-ray diffraction of PEEK where PEEK has the orthorhombic uniform structure. The sharp and diffuse patterns for PEEK showed the characteristics of semicrystalline polymers. The character peak of PEEK is at  $18.76^\circ$ ,  $20.70^\circ$ ,  $22.84^\circ$  and  $28.77^\circ$  with the interplanar distance of 4.72, 4.28, 3.88 and 3.09Å respectively.

The tensile properties were done by Deng et al. [3] where the tensile modulus at room temperature is 4 GPa. Song et al. [70] fabricated SWNT paper reinforced PEEK nanocomposites studied the static mechanical properties at room temperature. The Young's Modulus, failure strength and elongation at break are 2.67 GPa, 113.21 MPa and 6.45 % respectively.

Heat of combustion of PEEK measured using bomb calorimeter is 31.28 kJ/g [4]. PEEK has superior thermal degradation resistance with continuous use temperature of up to  $260^\circ\text{C}$  [4, 71] and melting point of  $343^\circ\text{C}$  [4, 10]. The glass transition temperature is  $143^\circ\text{C}$  [10, 71]. An onset decomposition temperature of PEEK is  $575^\circ\text{C}$  in nitrogen. The thermal decomposition of PEEK differs in oxygen and nitrogen environment but both shows two step of decomposition. The first step is the random chain scission of ether and ketone bonds which is the main mechanism. Carbonyl bond cleavage leads to more stable radical intermediates because of resonance effects and predominate. Volatilisation of about 45% of polymer mass occurs rapidly just below  $600^\circ\text{C}$  with major mass loss and carbonaceous char is the



remaining polymer mass [4, 71-72]. The decomposition products are phenols, carbon monoxide, carbon dioxide and some other aromatic ethers [4]. The factor influencing thermal resistance is the intermolecular forces between chains [10].

### **2.2.2 Applications**

Polymer composite materials become more preferable materials as structural materials for construction of aircraft and spacecraft [73]. Examples of applicability of PEEK are insulation film tape, tubing clamps, compression valve components and hinge bracket. More than that, because of the great thermal stability, PEEK is utilized for the interior cabin parts replacing steel. The replacement of steel with high performance polymer is to reduce the weight of the aircraft which in turn will utilize less oil consumption.

PEEK is also used for structural orthopaedic implants reviewed in Streicher [44]. The character of PEEK as stronger than steel but does not corrode and lighter weight is suitable to be used for structural implant material. The application of PEEK is expanding more and more for medical application.

Not only is medical and aircraft field, PEEK is utilized in telecommunication and electronics areas. PEEK is used as insulator, connectors, and wire coating. In semiconductor production, PEEK is gradually more used for transport and storage of semiconductors during production.

## **2.3 Polymer Nanocomposites**

Generally, a composite is a combination of two or more separate materials to form a useful material with a combination of properties that is not in the original material. Hence, nanocomposites material combines two or more separate materials where at least one of the components is in nanometer length scale. Nanocomposites are developed because of the unique properties that are not accomplished by traditional composites. The properties are improved from their small size, large surface area

and the unique properties of the fillers itself. Up to 2010, research and development of nanocomposites has increased significantly and the production of nanofillers increasing and improved to make use of the properties [10, 17].

The main purposes of reinforcement addition are property enhancement, overall cost reduction and improving and controlling of processing characteristics. The fillers character of being much stiffer and stronger than the polymer is believed to improve its modulus and strength. Therefore, the mechanical property modification is the primary function apart from the effect on the thermal stability, thermal expansion, etc. There are some parameters that can affect the properties of the polymer composites including the properties of the reinforcement, the composition of the reinforcement, the interaction of components at the phase boundaries and also the fabrication method utilized [10, 74].

Bringing the aim of enhancing the strength and mechanical resistance of a particular polymer, the usage of CNTs as reinforcement to high strength polymers looks like a promising route. Instead of carbon fibre, CNTs is used for composites fabrication owing to its tremendous properties. Nevertheless, the difficulties associated with the dispersion of CNTs and their compatibility in the matrix and also the nature of the bonding between the CNTs and the matrix should be overcome before practically utilized. Based on the previous papers on CNTs and polymer composites related, the fundamental challenges need to be tackled which is a complex issue with numerous competing factors. The factors start from the production and purification of CNTs, functionalization of the CNTs, the properties of CNTs based composites and the composite fabrication method [44].

The crystallinity of a semicrystalline polymer may have affected upon the incorporation of any substance as well as the properties of CNTs composites. The substitution between the individual strength of the interface, the nanotubes and the composites should be kept upright. The portion of CNTs substitution is necessary to attain significant changes on the properties of the composite and its processibility apart from the polymer, the CNTs and any functionalization. Much approach has been applied to have a strong interface between CNTs and polymer matrix [44].

Early application of polymer / CNTs composite, the composites are prepared by mechanical dispersion. However, the increment in tensile strength and Young's Modulus are not remarkable due to the reinforcement was achieved through adhesion and weak van der Waals forces. Strong bonding between CNTs chains and polymer chains is necessary to have a high stress transfer via chemical functionalization on the CNTs [44]. Unfortunately, excessive functionalization of CNTs can ruin the tubular framework and reduce its mechanical strength. Carboxylic acid group introduction on the surface of CNTs could improve the processibility and performance of nanocomposite that leads to stabilization in polar solvents and helps covalently link polymers [21, 34]. Mylvaganam and Zhang [34] also have the opinion on different polymers synthesis, different initiators that follow different mechanisms are used. Viswanathan et al. work was reported by Mylvaganam and Zhang [34] regarding the introduction of negative charges on CNTs surface helps to exfoliate the CNTs bundles. With 0.05 wt% CNTs loading in polystyrene (PS) grafted composite, the glass transition temperature,  $T_g$  of the composite increased by 15% which attributed to decrease in chain mobility due to attachment of polymer chains to the nanotubes.

Mangalgiri [73] makes reviews on the application of composites as structural material that shows significant growth of usage. Issues discussed are impact tolerance, damage tolerance, environmental degradation and long term durability. Polymer has become the key role as materials of construction of aerospace vehicles and components. PEEK that is able to withstand elevated temperature is a very promising polymer and utilizes CNTs as reinforcement. PEEK / CNTs composites possess higher mechanical and thermal properties with lighter weight, reduced energy usage (fuel consumption) cost and maintenance.

Streicher [44] reviewed Babaa et al. study using PEEK as a matrix material to produce composite for structural orthopaedic implants. The CNTs is chemically functionalized by using difunctional molecules which is covalent bonding with the purpose for a better bonding between CNTs and the polymer.

Based on Mikitaev, Kozlov and Zaikov [75], CNT bundles dispersion method by formation covalent bonds CNTs / polymer composite is effective at small CNTs contents only. Composite with more than 5 wt% CNTs loading is insufficiently effective because of the level of interfacial adhesion and van der Waals interactions between the polymer and CNTs [75]. Numerous studies (Table 2.1) have been done on composites with thermoplastic polymer, PEEK as matrix in order to increase its properties for a particular application.

Table 2.1: Summary table of PEEK based composites researches

| Filler   | Polymer      | Study (Ref)                 | Year | Remarks                                 |
|--|--------------|-----------------------------|------|---|
| Knitted carbon                                     | PEEK         | Fujihara et al. [76]        | 2004 | For orthopedic bone plates applications |
| SiO <sub>2</sub><br>Al <sub>2</sub> O <sub>3</sub> | PEEK<br>PEEK | Kuo et al. [77]             | 2005 |   |
| Aluminium Nitrate                                  | PEEK         | Goyal et al. [78]           | 2005 |   |
| Carbon fibre                                       | PEEK         | Davim and Cardoso [79]      | 2006 |   |
| Nanometer Al <sub>2</sub> O <sub>3</sub>           | PEEK         | Qiao et al. [80]            | 2007 |   |
| Al <sub>2</sub> O <sub>3</sub>                     | PEEK         | Goyal et al. [81]           | 2008 |   |
| MWNTs  | PEEK         | Bangarusam path et al. [82] | 2009 |   |
| CNTs   | PEEK         | Mohiuddin and Van Hoa [83]  | 2010 | Manufacturing pressure sensing element  |
| SWNTs  | PEEK         | Diez-Pascual et al. [5]     | 2010 |   |
| Carbon fibre                                       | PEEK         | Vacogne and Wise [84]       | 2011 |   |
| MWNTs  | PEEK         | Ogasawara et al. [85]       | 2011 |   |
| MWNTs  | PEEK         | Tsuda et al. [86]           | 2011 |   |

### **2.3.1 Fabrication of polymer / CNTs nanocomposites**

Thermoplastic materials are prepared by hot melt or solution processes. However, the product is stiff with no drape and tack which can be improved by slightly melting the material during hand lay-up procedure. The equipment must be able to withstand high temperature and pressure [10].

Extrusion is commonly used to manufacture thermoplastic composites into standard shapes such as channels, structures and plates. Traditional matched-die molding combined with a preheating step can be used for thermoforming thermoplastic composites since they have high melt temperature with high viscosity [10].

An alternative technique to deal with thermoplastic polymers is melt processing where it softens when heated. It is required to process semicrystalline polymers above their melt temperature to induce sufficient softening. Melt processing involves the melting of polymer pellets or powder to form a viscous liquid. Bulk samples can be fabricated by techniques like compression molding, injection molding or extrusion [19].

### **2.3.2 Structural Properties**

The morphology and dispersion of fabricated composites are assessed by examining the fractured film composites with FE-SEM. The samples were metalized with ~5nm Au-Pd overlayer to get better view of the composites. The dispersion of p-MWNTs in PEEK matrix seem to severely agglomerate yet randomly oriented in Zhao et al. [20]. Choi et al. [87] fabricated polystyrene / MWNTs composites and the morphology of the composites were investigated. The PS / MWNTs nanocomposite produced was black in color with only 1 wt% of MWNT addition. The MWNTs used in the study exhibited a distinct curved shape in all three dimensions as a result of interlocking between the MWNTs. Choi et al. [87] concluded that the structure and shape of nanotubes are randomly oriented in the polymer matrix [88].

Fracture surfaces of the composites showed the CNTs perform was locally distributed in the composites. Most parts of the sample were pure epoxy and showed features of brittle fracture. It can be seen that the CNTs were either pulled out of broken from the matrix during the tensile testing. The liquid epoxy wetted the CNTs perform very well during epoxy infiltration even though the CNTs is not chemically modified. There was good adhesion between the matrix and the CNTs. SEM images of the composites displayed the CNTs perform was locally distributed in the composite and the amount of CNTs was clearly higher than the sample with lower overall CNTs content [16].

Kim et al. [15] discussed on the epoxy composites with oxidized MWNTs in terms of the morphology resulted very good dispersion of oxidized MWNTs in all the composites. The van der Waals force between the MWNTs and the hydrogen bonding occurred between the opened epoxide rings of the matrix and the carbonyl groups contribute to the good dispersion of MWNTs in the epoxy matrix regardless of whether or not there is any CNTs damage or impurities [15, 29]. Even though 1 wt% of MWNTs were added, the color of PS / MWNTs nanocomposite produced was black [87]. Distinct curved shape in all three dimensions exhibited as a result of interlocking between the MWNTs. As a conclusion, the structure and shape of nanotubes are randomly oriented [87-88].

Mago et al. [88] reported that the crystals begin to grow perpendicularly to the surface of the nanotubes resulting in nanohybrid-shish-kebab-like-structure especially for various types of semicrystalline polymers. The spherulitic morphologies that cover the surface of the nanotubes appear to have cultivated upon the nucleation of multiple polymer chains on any nanotubes surface.

Zhao et al. [20] who fabricated poly(L-lactide) (PLLA) / functionalized MWNTs explained the factors attributed to the difference in the dispersion of p-MWNTs and functionalized MWNTs in the PLLA matrix. The major factor is the electrostatic and van der Waals interactions between the MWNTs alone that lead to aggregation of the MWNTs. On the other hand, as the MWNTs is functionalized, the existence of the carbonyl groups on the surface of MWNTs assists a lot to improve the

compatibility between functionalized MWNTs and the PLLA matrix. Hence, this prevents the apparent aggregation of MWNTs. As agreed with Zhao et al. [20], the load transfer takes place efficiently from the matrix to the nanotubes [6]. This strong interfacial adhesion is accredited for the improvement of mechanical properties that associate with the hydrophilicity of the PEEK macromolecules, while hydrophobic polymers like polypropylene usually possess weak bond to the nanotubes [70].

Recent research on PEEK / carbon nanotube composites by Díez-Pascual et al. [5] which manipulated the fabrication method generally gives similar XRD results as pure PEEK in section 2.2.1. The sharp and diffuse patterns for PEEK show the characteristics of semicrystalline polymers [69]. Yin et al. [69] discussed the X-ray diffraction of PEEK where PEEK has the orthorhombic uniform structure. The sharp and diffuse patterns for PEEK showed the characteristics of semicrystalline polymers. The character peak of PEEK is at 18.76°, 20.70°, 22.84° and 28.77° represents the interplanar distance of 4.72, 4.28, 3.88 and 3.09 Å respectively. Small loading of pristine MWNTs increases the crystallinity ratio of the polymer. However, the crystallinity ratio reduces little by little as the loading of p-MWNTs increases.

### **2.3.3 Thermal Properties**

Fujihara et al. [8] did a study on carbon fibers reinforced PEEK composites also analyze the thermal stability of the system and the onset temperature is 561°C. However, the onset of thermal degradation by Patel et al. [4] resulting in mass loss occurs between 575 to 580°C. Díez-Pascual et al. [5] suggested that the decomposition takes place in a single stage only involving decarboxylation, decarbonylation and dehydration processes. These processes lead to the formation of phenol groups, carbon dioxide and water leaving the ether and aromatic structures to remain in the residue at elevated temperatures. The residual weight obtained from the study is relatively similar with results of Díez-Pascual et al. [5] which is about

46%. However, the initial degradation temperature of pure PEEK experimentally obtained is increases up to 20°C as well as the onset temperature.

PEEK has superior thermal degradation resistance with continuous use temperature of up to 260°C [4, 71] and melting point of 343°C [4]. The glass transition temperature is 143°C [71]. Onset decomposition temperature of PEEK is 575°C in nitrogen. The thermal decomposition of PEEK differs in oxygen and nitrogen environment but both shows two step of decomposition. The first step is the random chain scission of ether and ketone bonds which is the main mechanism. Carbonyl bond cleavage leads to more stable radical intermediates because of resonance effects and predominate. Volatilisation of about 45% of polymer mass occurs rapidly just below 600°C with major mass loss and carbonaceous char is the remaining polymer mass [4, 71-72].

Choi et al. [87] stated that the enhanced distribution of MWNTs improve the thermal stability of the polymer matrix [21] and also raises the surface area in the polymer matrix. Choi et al. [87] did the study on polystyrene (PS) / MWNTs composites. Further explanation by Choi et al. [21] that the improved interfacial interaction increases the activation energy of degradation at interface between MWNTs and the polymer. Hence, this retards the degradation at the surface of the composites as a result of great thermal conductivity of CNTs [21].

Similar results can be observed on Silica-SWNT composites [32]. Díez-Pascual et al. [5] explains that the incorporation of small amount of SWNTs that is uniformly and well disperse can stabilize the composite in an oxidative environment, raise the matrix  $T_i$  and delays the  $T_{mr}$  which progressively increase with increasing MWNTs loading. Furthermore, Nayak et al. [6] mentioned that the chain mobility of polymer matrix is reduced with the incorporation of CNTs by imposing numbers of restriction sites which reduces the thermal vibration of the C-C bond. Hence, more thermal energy is required for the degradation of polymer matrix which in turn increases their thermal stability. Another reason is the formation of char acting as the physical barrier between the polymer and the superficial zone where the combustion of the polymer is occurring.



$$\text{Degree of crystallinity } (1-\lambda)_c (\%) = \Delta H_c / (\Delta \hat{H}_c \times [\text{wt \% of PEEK composition}]) \text{ ---(1)}$$

The apparent crystallization enthalphy,  $\Delta H_c$  (J/g) is calculated as the normalized integral of the crystallization peak [5, 88]. On the basis of heat of fusion of 100% crystalline PEEK,  $\Delta \hat{H}_c$  which is 130 J/g, the degree of crystallinity,  $(1-\lambda)_c$  of PEEK and its composite are determined by the ratio of the crystallization enthalphy of the samples to that of 100% crystalline PEEK. The degree of crystallinity obtained for pure PEEK sample is 19.63 %.

Both the melting and crystallization scans of PEEK / p-MWNTs composites are narrower compared to pure PEEK. This indicates a narrower crystallite size distribution in the matrix; hence heat will be evenly distributed in the matrix [40]. Similar observations can be seen in Bhattacharyya et al. [40] who produced PP / SWNTs which having narrower melting and crystallization peaks for the composites. The character of MWNTs for having higher thermal conductivity than the polymer shall contribute to the sharper crystallization and melting peaks. DSC analysis on Polypropylene / MWNTs filaments resulted slight increment of heat of fusion of the composites due to more ordered polymer packing obtained for the composites [21]. Choi et al. [21] discussed the crystallization of polymer consist of primary nucleation and spherulitic growth which does affect the crystallization temperature as MWNTs were added.

According to Díez-Pascual et al. [5], the network of CNTs enforces a confinement on the polymer chain diffusion and crystal growth. This decelerates the overall process for crystallization leading to lower  $T_c$  for the composites. Anyhow, results from this study are coherent with the behavior mentioned by Díez-Pascual et al. [5] regarding DSC analysis on PEEK / SWNTs composites. The opposite observation is documented by Choi et al. [21] where the crystalline temperature increased around 4.5°C as 1% MWNTs was incorporated and also Vega et al. [41] who fabricated HDPE / 0.54% MWNTs composite having 1°C increment of crystallization temperature. The small increment is significant in view of high nucleation density of polyethylene. Nevertheless, the  $T_m$  and crystallinity remain the same even by the presence of MWNTs [41]. Regarding the  $T_c$ , Vega et al. [41]

found that the process of crystallization occurs earlier than the neat HDPE, overall, the entire crystallization process occurs faster.

Mago et al. [88] have got the similar observation where the melting temperature of poly (butylenes terephthalate) (PBT) / MWNTs reduced slightly from 208.6°C for pure PBT to 202.3°C for PBT / 2% MWNT. However, Díez-Pascual et al. [5] obtained 343°C in average of melting temperature and it remains for all PEEK / SWNTs composites. The values of  $T_g$ s are approximately 153.7°C in the composites and are lower than of the pure PEEK.

The increment of crystallinity of PEEK is important before and after the MWNTs additions [20-21, 88]. Zhao et al. [20] ran DSC scans on the poly (L-lactide) (PLLA) / MWNTs composites found that the addition of MWNTs shows slight effect on the  $T_m$  and  $T_c$  of PLLA, and increases the  $\Delta H_c$ ,  $\Delta H_m$ , and  $(1-\lambda)_c$  significantly. Mago et al. [88] suggest that the increase of degree of crystallinity does play an important part on the enhancement of various ultimate properties of the particular polymer. The incorporation of ox-MWNTs is seen to be more efficient than p-MWNTs in enhancing the crystallization of PEEK as in agreement with Zhao et al. [20]. Du, Fischer and Winey [89] in their study on p-SWNTs / poly(methyl methacrylate) (PMMA) composites shows that the weight loss of the polymer and the composites are at the same temperature, but the maximum mass loss rate is 61°C higher than that of pure PMMA. This reveals that the thermal stability improved at addition of only 0.5% of p-SWNTs.

Because of the moisture accumulated in intermolecular space, materials showed different behaviour. However, nanocomposites keep it back owing to intracapillary effect of the nanotubes. Moisture starts to go off from the composites at an elevated temperature ranging 446-483 K for phenylone / CNTs composites done by Burya et al. [90]. Burya et al. [90] concluded that the thermostability of the composites increased and optimumly at CNTs loading of 5 wt% [75].

### 2.3.4 Mechanical Properties

Tensile strength and modulus enhancements are continually reported by Andrews and Weisenberger [39]. However, very little of the data achieve reinforcement predicted by a rule of mixtures approach especially at loadings beyond 10 vol.%. Song et al. [70] obtained increment in the Young's Modulus up to ~40% of the neat PEEK for sandwich-like PEEK / SWNTs composites. Meanwhile, the failure strength was slightly improved by 4%. The SWNTs is in film form and as more layers of SWNT paper incorporated in PEEK film, some air bubbles are recognized in the composites. This was one of the defects and finally results in the pre-fracture of materials. Despite the defects, the mechanical properties of the composites are still better than neat PEEK. In other study, the addition of MWNTs results in increase in the elastic modulus and the yield strength but decrease in the failure strain. In the study, the tensile modulus of the pure PEEK is 4 GPa. The composites containing 15 wt% have tensile modulus of 7.55 GPa, increase by 89% [3]. Deng et al. [3] concluded that the incorporation of MWNTs improves more effective above the glass transition temperature.

Tensile test were performed on the PEEK / liquid crystalline polymer (LCP) blend system samples with MWNTs incorporation by Nayak et al. [6]. The Young's Modulus of composites is higher than the PEEK / LCP blend. The tensile modulus increased by 9% and 12% as 1 wt% MWNTs and functionalized MWNTs were added into the blend system, respectively. The tensile strength increased by 12.5 % and 38% with comparison with pure blend. However, the elongation at break decreased from 19.8% to 9.1% and 5.2%, respectively. The reduced elongation might be because of the decrease of ductility of the polymer blend as MWNTs is added [6]. The changes in crystallinity affect the mechanical properties and permeability of the semicrystalline polymer. Young's Modulus of PBT / 2% MWNTs composites increased from 1.3 GPa to 1.5 GPa as the crystallinity increased from 20.2% to 24.3%. The tensile strength at yield increases and the elongation at break decreases with increasing crystallinity of the composites [88].

Coleman et al. [38] fabricated two sets of polymer composites which are PVA / MWNTs and Cl-PP / MWNTs composites. The amount of MWNTs were up to 0.6 vol.%. For PVA / MWNTs composites, the stress-strain curves of all cases are linear at low strain and then plastic deformation in the 3% strain region. At higher strains, the film of pure polymer yield to break at 6% strain. The breaking strain tends to decrease with increasing nanotubes content and for 0.6 vol.% composite, the films breaks at approximately 4%. The Young's Modulus, strength and toughness increases by factor of x3.7, x4.3 and x1.7, respectively with increasing nanotubes content. On the other hand, the stress-strain curves of all cases for Cl-PP / MWNTs composites are linear up to 2% strain region. Necking and drawing is observed at higher strains up to breaking at 450% strain. The breaking strain tends to decrease with increasing nanotubes content and for 0.6 vol.% MWNTs addition, the yield points shifts up steadily reaching 4.3%. The Young's Modulus, strength and toughness increases by factor of x3.1, x3.9 and x4.4, respectively with increasing nanotubes content.

Chang et al. [91] studied PP / SWNTs composites and obtained the tensile modulus increase sharply by  $\sim x3.0$  with addition of 1% SWNTs. However, the tensile modulus increases much slower with further addition of SWNTs. The tensile stiffness increases by  $\sim 45\%$  when the concentration of SWNTs increases from 1% to 4-5 wt%. Ruan et al. [59] study on the UHMWPE / 1 wt% MWNTs composites results on 25% increase in Young's Modulus and 47.6% increase in yielding stress.

## CHAPTER 3

### EXPERIMENTAL

#### 3.1 Materials and Apparatus

Raw materials required for the study are multiwalled carbon nanotubes (MWNTs) and Poly(ether ether ketone) (PEEK). MWNTs (Nanocyl-7000 at 90% purity) were purchased from Nanocyl. The diameter distribution is ranged from 4 nm to 15 nm. Commercially available PEEK was a Victrex® PEEK 150 PF kindly provided by Victrex.

Chemicals used during the study are as follows:

Table 3.1: List of Chemical Utilized

| Chemicals  | Manufacturer                        |
|--|-------------------------------------|
| Dimethylformamid (DMF, 99%)                              | Sigma-Aldrich Chemical Company, Inc |
| 1,6-hexane diamine (HDA, 99%)                            | Sigma-Aldrich Chemical Company, Inc |
| N,N'-dicyclohexylcarbodiimide (DCC, 99%)                 | Sigma-Aldrich Chemical Company, Inc |
| Sulphuric acid (H <sub>2</sub> SO <sub>4</sub> , 95-98%) | Sigma-Aldrich Chemical Company, Inc |
| Nitric acid (HNO <sub>3</sub> , 70%)                     | Sigma-Aldrich Chemical Company, Inc |
| Sodium hydroxide (NaOH)                                  | Sigma-Aldrich Chemical Company, Inc |
| Acetone (99.5%)  | Sigma-Aldrich Chemical Company, Inc |

### 3.2 Preparation of sulfonated PEEK (SPEEK)

*Sulfonation Reaction;* The sulfonation reaction was performed using  $\text{H}_2\text{SO}_4$  treatment as in literature of Huang et al. [59]. The schematic illustration is shown in Figure 3.1. Initially, 20 g of PEEK was dried in a vacuum oven at  $100^\circ\text{C}$  and subsequently dissolved in 500 ml of concentrated sulfuric acid ( $\text{H}_2\text{SO}_4$ , 98%) under vigorous stirring [92]. The sulfonation degree (DS) in this study is around 70% [9]. The DS was estimated by titration technique as in a publication of Huang et al. [93].

*Neutralization of the Sulfonated Poly (Ether Ether Ketone) (SPEEK-H);* The wet SPEEK-H was immersed in a 50/50 (v/v) aqueous acetone solution 5 min and then in pure acetone 10 min to remove water from the SPEEK-H. Finally, the acetone-wet SPEEK-H was air dried. A sample of about 0.5 g was then neutralized in 200 mL of 0.01 M sodium hydroxide aqueous solution for 3 days, so that the SPEEK-H was fully converted into its sodium salt form SPEEK-Na [93].

*Backtitration of NaOH Solution;* Dilute sulfuric acid (0.003 M) is employed to back titrate the NaOH aqueous solution, which has been partially neutralized by the SPEEK-H. Universal indicator is adopted to predict the neutral point [93].

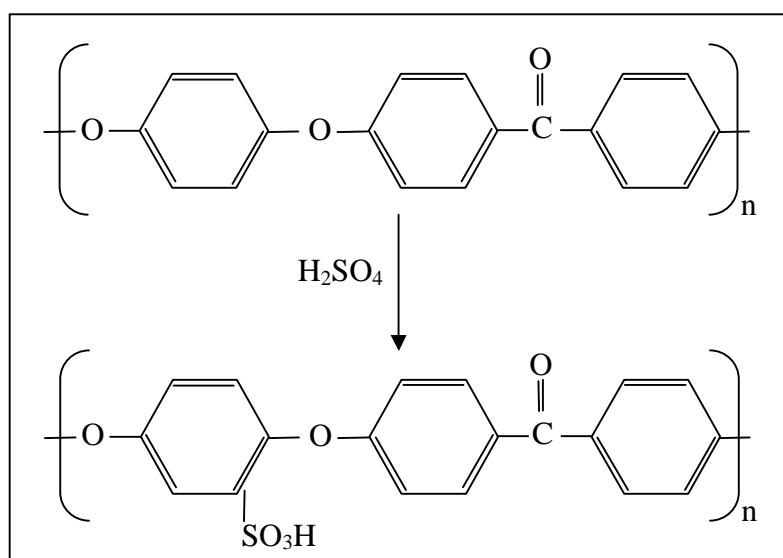


Figure 3.1: Schematic illustration of the synthesis of SPEEK

### 3.3 Preparation of Oxidized Multiwalled Nanotubes (ox-MWNTs)

Purpose of oxidation process to MWNTs in this study is to create chemistry on the surface of MWNTs to be ready to be functionalized. 60 mg of pristine CNTs were dispersed in 250 ml of  $\text{HNO}_3$  (69%) using ultrasonication for 45 minutes. Then, the dispersion was refluxing at  $100^\circ\text{C}$  for 3 hours. The oxidized CNTs were filtered using cellulose nitrate filter ( $0.45\ \mu\text{m}$ ) and washed repeatedly using distilled water. After filtration and washing, the oxidized CNTs were stored in the oven at  $100^\circ\text{C}$  for 24 hours. The schematic preparation of oxidized MWNTs is shown below.

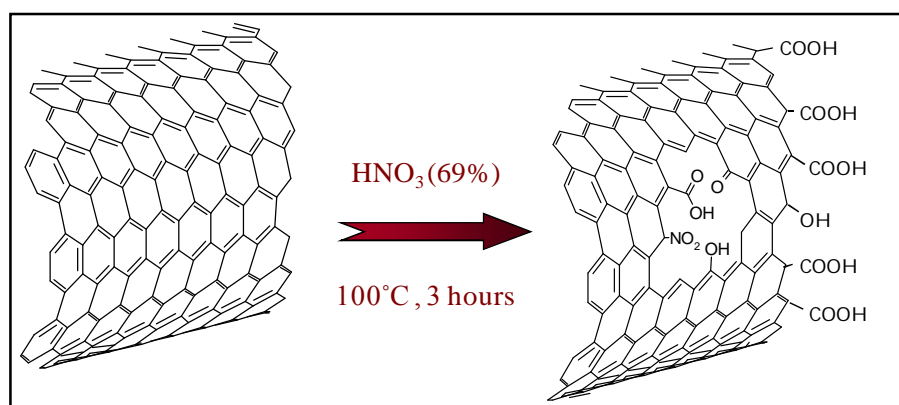


Figure 3.2: Schematic preparation of oxidation process of MWNTs

### 3.4 Preparation of SPEEK-MWNTs

About 50 mg of ox-MWNTs were dispersed in 250 ml DMF by ultrasonication for 2 hours. 50 mg of HDA and 50 mg of DCC as coupling agent were simultaneously added. The mixture was heated at  $40^\circ\text{C}$  to dissolve DCC (melting point of  $35^\circ\text{C}$ ) and vigorously stirred for 24 hours. After washing and filtration, functionalized MWNTs with HDA (HDA-MWNTs) were dispersed in DMF by ultrasonication for 2 hours. 50 mg of SPEEK and 50 mg of DCC were simultaneously added. The mixture was heated at  $40^\circ\text{C}$  and vigorously stirred for 24 hours. After washing and filtration, functionalized MWNTs with SPEEK was stored in the oven at  $100^\circ\text{C}$  for 24 hours [9], [92]. The schematic preparation of SPEEK-MWNTs is shown in Figure 3.3.

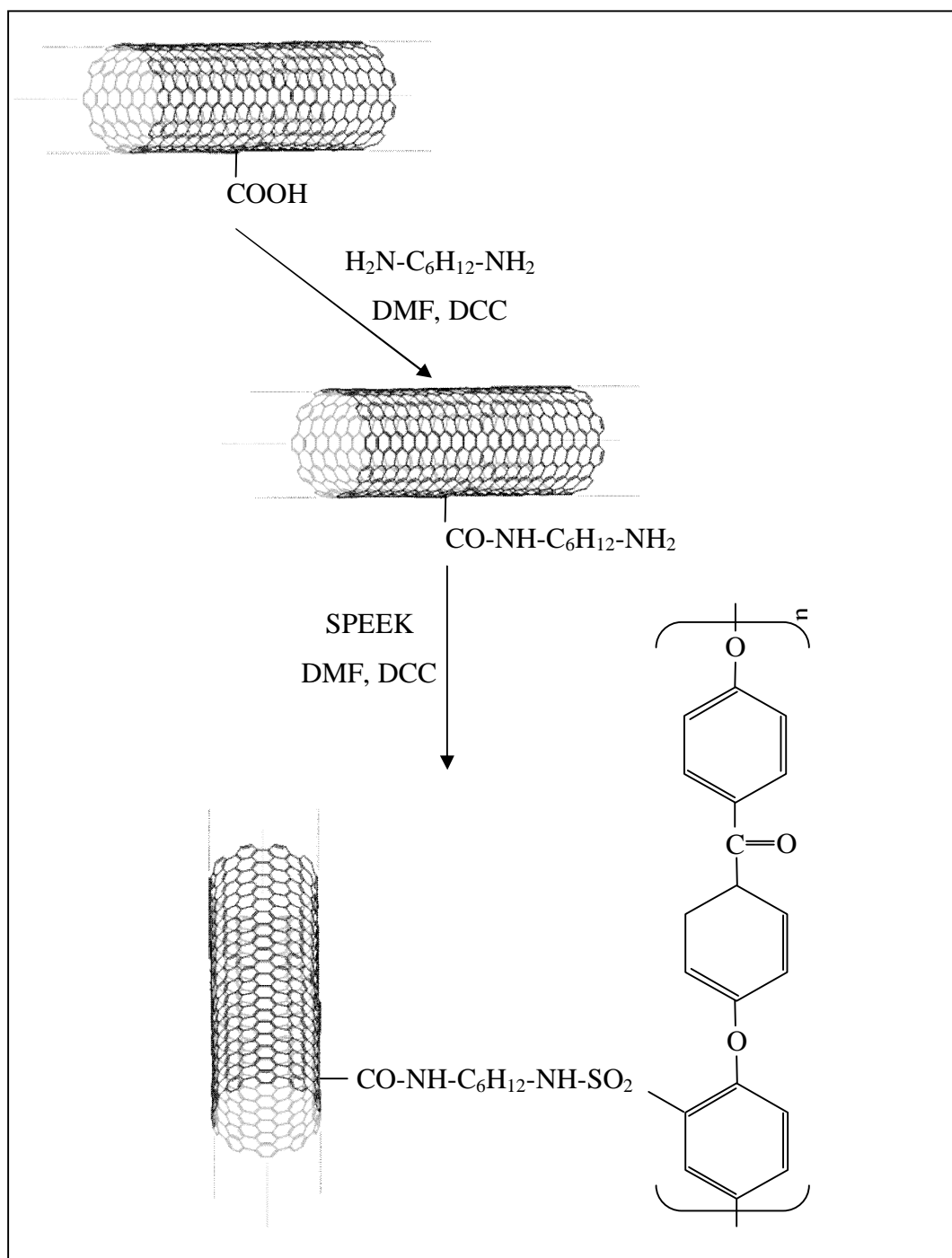


Figure 3.3: Schematic presentation of functionalization reactions



### 3.5 Preparation of MWNTs / PEEK Composites

PEEK was vacuum-dried at 120°C for 4 hours and stored in a dry environment before blending. Composites were prepared by mixing the MWNTs / PEEK mixture in a mortar grinder for 2 minutes. This method was utilized because the required equipment is not functioning. All samples were compression molded at 350°C under a pressure of 2.5 metric tons for 30 minutes [8, 22, 70].

The composition of MWNTs and PEEK were prepared as in the table below along with the notation of each MWNTs / PEEK composites. The MWNTs loading chosen was low loading up to 2% loading. It is not necessary to add more than 2% since it has been reported that the optimum properties are at low MWNTs loading [75].

Table 3.2: MWNTs / PEEK composites compositions

| Composites                    | %MWNTs | % PEEK | Notations |
|-------------------------------|--------|--------|-----------|
| p-MWNTs / PEEK composites     | 0.5    | 99.5   | 0.5 MP    |
|                               | 2      | 98     | 2 MP      |
| ox-MWNTs / PEEK composites    | 0.5    | 99.5   | 0.5 OMP   |
|                               | 2      | 98     | 2 OMP     |
| SPEEK-MWNTs / PEEK composites | 0.5    | 99.5   | 0.5 SMP   |
|                               | 2      | 98     | 2 SMP     |

## 3.6 Sample Characterization

### 3.6.1 Structural Properties

#### 3.6.1.1 Field Emission Scanning Electron Microscopy (FE-SEM)

FE-SEM measurements were performed with a Zeiss Supra 55 VP FE-SEM microscope using a voltage of 25 kV and an intensity of  $9 \times 10^{-9}$  A. The composite film samples were covered with an approximately 5 nm overlayer of an Au alloy in Balzers using a covering time of 3 min at 20 mA in order to avoid charging during electron irradiation. At least 5 FE-SEM images of each composite sample were taken at different magnification to assess the state of dispersion of the CNTs in the polymer matrices [5].

#### 3.6.1.2 Transmission Electron Microscopy (TEM)

Transmission Electron Microscopy (TEM), a microscopy technique where a beam of electrons is transmitted through an ultra thin specimen, interacts with the specimen as it passes through. The TEM analysis was performed with a Zeiss Libra 200FE TEM using 200 kV Schottky field emitter with Koehler illumination system with in-column corrected OMEGA filter [100].

Prior to TEM analysis, the samples were prepared based on the form of the material. Several methods to prepare the samples are thinning, polishing, grinding, dimpling and milling. As for the study, the samples to be prepared for TEM analysis are p-MWNTs, ox-MWNTs and SPEEK-MWNTs which are in powder form. The procedure starts by dispersing the fine particles in a volatile liquid (isopropanol) according to the material specific requirements. The agglomerated particles are sonicated to separate and ensure a homogenous suspension. A dilution step is often required to obtain very low concentrations of the material, so that the particles on the

support film remain isolated. A droplet of the suspension was placed on the coated grid. The specimen is ready for observation after complete evaporation or drying.

#### *3.6.1.3 X-Ray Powder Diffraction (XRD)*

Powder diffraction or XRD is an analytical technique used for phase identification, crystallite size (grain size), and preferred orientation of a crystalline material samples. The XRD patterns were recorded with a D8 Advance Bruker AXS Diffractometer equipped with a Göbel mirror and Vantec PSD detector, with a voltage of 40kV and intensity of 40mA, using Ni-filtered Cu K $\alpha$  ( $\lambda=0.15418$  nm) radiation, with an aperture of 0.6 mm. Diffractograms were registered on films or powder, in the angular region of  $2\theta$  from 2° to 80°, at room temperature with a scan speed of 0.2s and angular increment of 0.02° [5]

### **3.6.2 Thermal Properties**

#### *3.6.2.1 Differential Scanning Calorimeter (DSC)*

The crystallization and melting behavior of the composites were investigated by DSC operating under nitrogen flow. Before the heating and cooling scans, composites were melted at 350°C and maintained at this temperature for 5 min to erase the thermal history of the material. Subsequently, they were cooled from 350 to 30°C at a rate of 10°C/min and then heated from 30 to 350°C at 10°/min.

#### *3.6.2.2 Thermogravimetric Analysis (TGA)*

The thermal stability of the MWNTs and the composites was analyzed by Thermal Gravimetric Analysis (TGA). The measurements were carried out using Perkin Elmer Pyris 1 TGA at heating rate of 10°C/min under nitrogen atmosphere. The analysis was performed on samples with an average mass of 10 mg, under

dynamic conditions from room temperature to 900°C with a gas purge of 15 ml/min [5]. Sample of around 5-10 mg are required for each sample for the analysis.

### **3.6.3 Mechanical Properties**

Young's Modulus, E or also known as tensile modulus is a constant of proportionality in the Hooke's Law where it represent by the formula  $\sigma = E\epsilon$ . Hooke's Law is a relationship between engineering stress and engineering strain for elastic deformation. Young's Modulus was determined following the ASTM D638 to study the ability of a structure to resist loads without failure because of extra stress or deformation. The measurements were carried out using a Universal Tensile Machine, INSTRON 1331 (Montpellier, France) at 2 mm/min of crosshead speed. All tests were repeated three times and a mean value obtained.

## CHAPTER 4

### RESULTS AND DISCUSSIONS

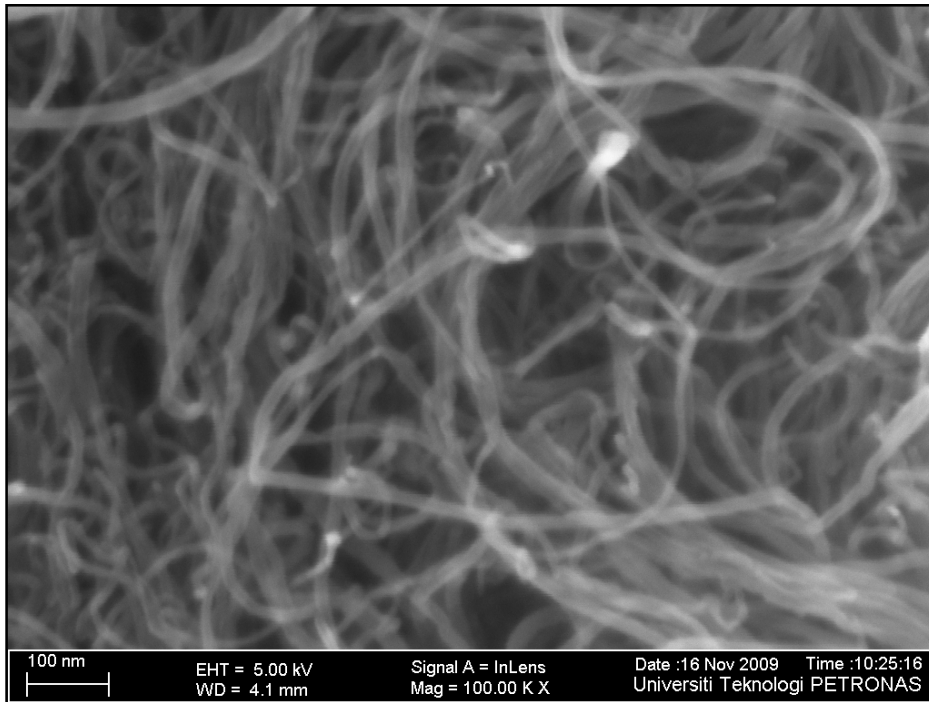
#### 4.1 Multi-walled Carbon Nanotubes

##### 4.1.1 Structural Properties of MWNTs

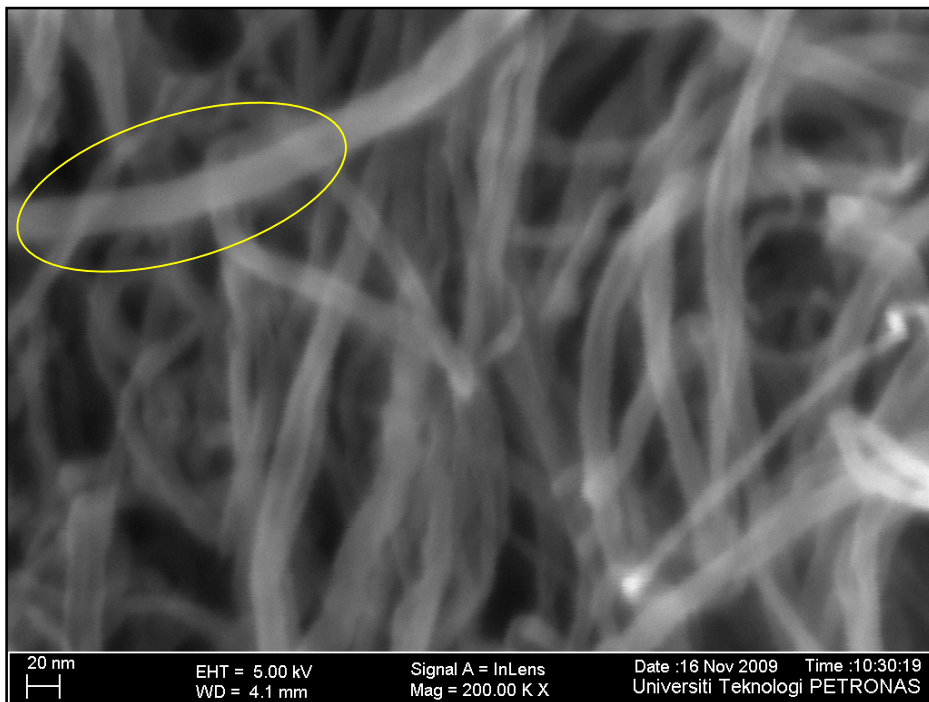
The morphology of the MWNTs was studied with scanning electron microscopy. The structure of the samples was probed with FE-SEM (Figure 4.1) and TEM (Figure 4.2). FE-SEM mainly gives the details on the surface morphology of the samples while TEM is used to measure the diameter of nanotubes in the bundles [94]. Figure 4.1(a) shows the FE-SEM images of pristine MWNTs (p-MWNTs). p-MWNTs are highly tangled with each other with rarely visible ends. The entanglement is because of the van der Waals forces between the nanotubes [5, 15, 25]. p-MWNTs also can be seen to have clean and smooth surface due to the high purity since the sample is a commercial product.

Figure 4.1(b) shows the functionalization of MWNTs with SPEEK resulted in shorter tubes length and they are seen wrapped by a layer of polymer at certain locations [9]. More visible ends can be observed as compared to those observed in p-MWNTs. The length of CNTs are shorter due to the initial step of oxidation process which cuts the tubes and introduces carboxylic functional group (-COOH) to the tubes. The surface of the SPEEK-MWNTs is relatively rough because of the grafted functional groups at certain locations. The same observation was reported by Chiu and Kao [95] with their study on polyamide 46/multi-walled carbon nanotube nanocomposites.

(a)



(b)



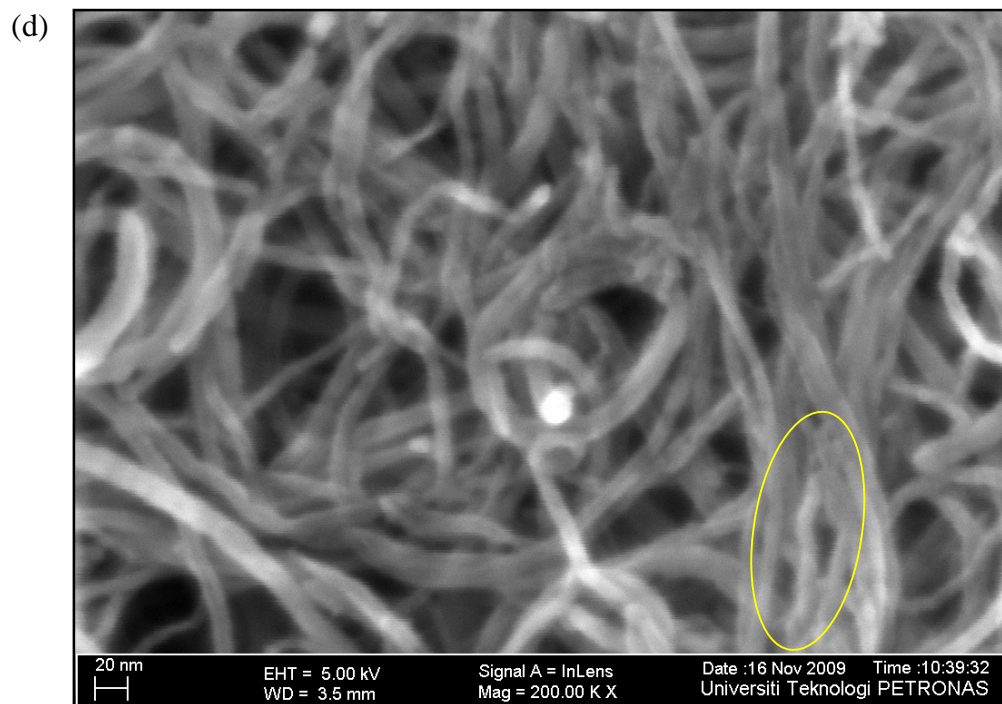
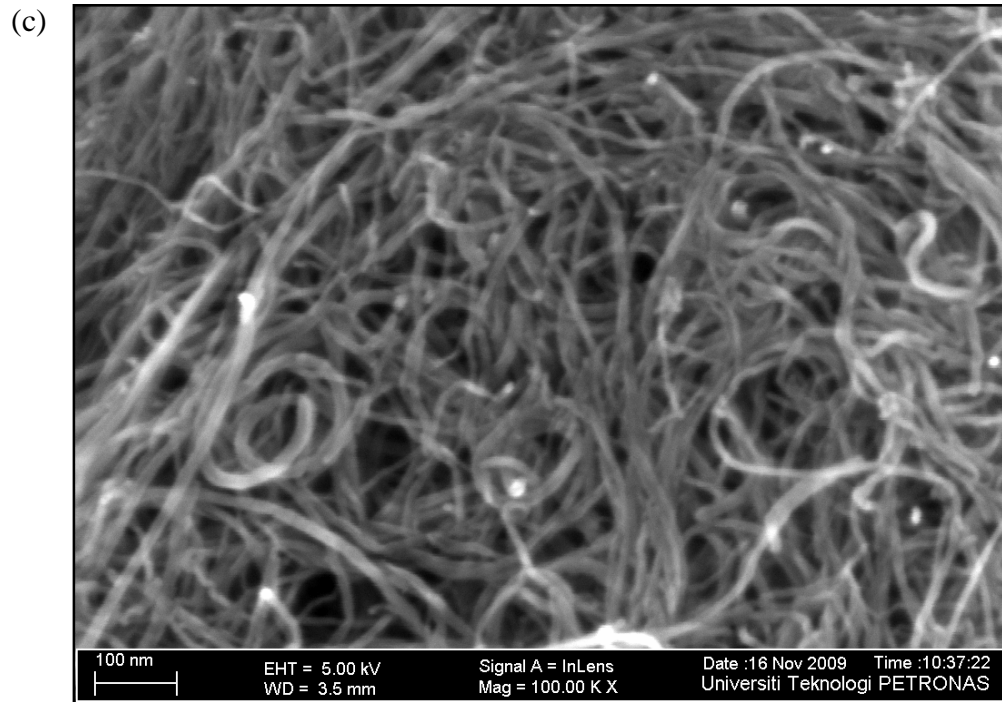
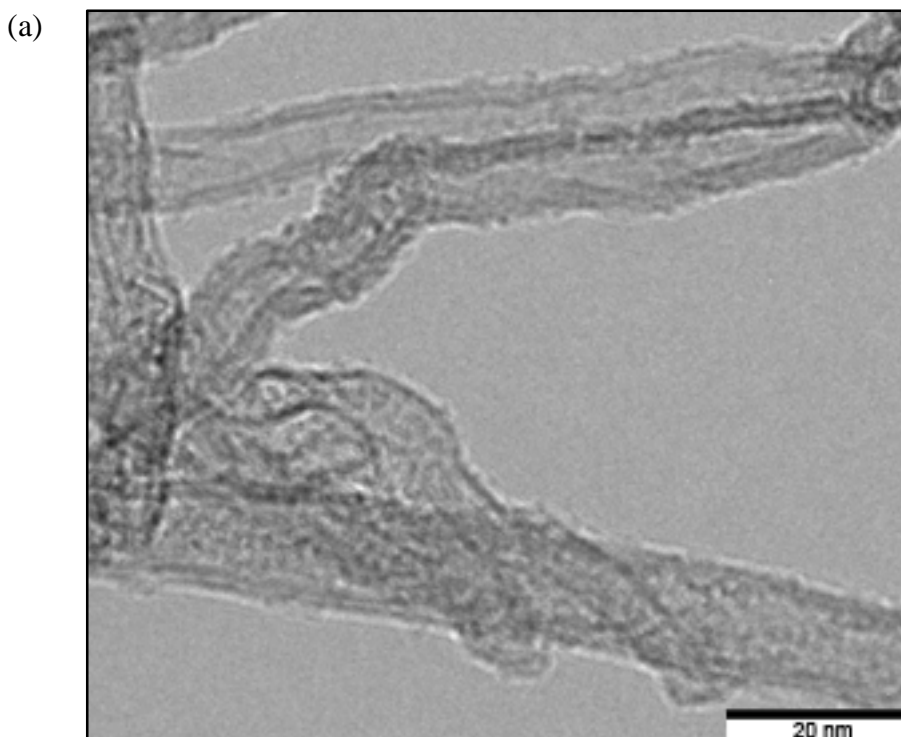


Figure 4.1: (a and b) FE-SEM images of p-MWNTs and (c and d) FE-SEM images of SPEEK-MWNTs

Figure 4.2(a) shows the TEM image of p-MWNTs which exhibit a typical structure of at least two layers rolled-up graphene sheets often many more and there was invariably closed at both ends. The diameters of the nanotubes are in the range of 7 to 13 nm with approximately 3 nm of wall thickness. However, it can be seen that the tubes have irregular diameters and wall thicknesses. After oxidation, the diameters of the tubes are in the range of 7 to 15 nm with approximately 3.2 nm of wall thickness (Figure 4.2(b)). Figure 4.2(c) illustrates the SPEEK functionalized MWNTs (SPEEK-MWNTs) where the tubes are twisted and there are extra layer of SPEEK on the surface of the tubes. Both the ox-MWNTs and SPEEK-MWNTs show some defects in the carbon-carbon bonding. Figure 4.2(c) shows the walls are opened at several locations. The defects in carbon-carbon bonding are because of the formation of carboxylic groups on the surface of MWNTs as suggested by Sahoo et al. [96]. During the defect-consuming steps, the graphene structure of the tube was destroyed and it mostly counts on the ability of the acid to destroy the graphene structure around the already oxidized carbon (-COOH) and their neighbour groups [101].





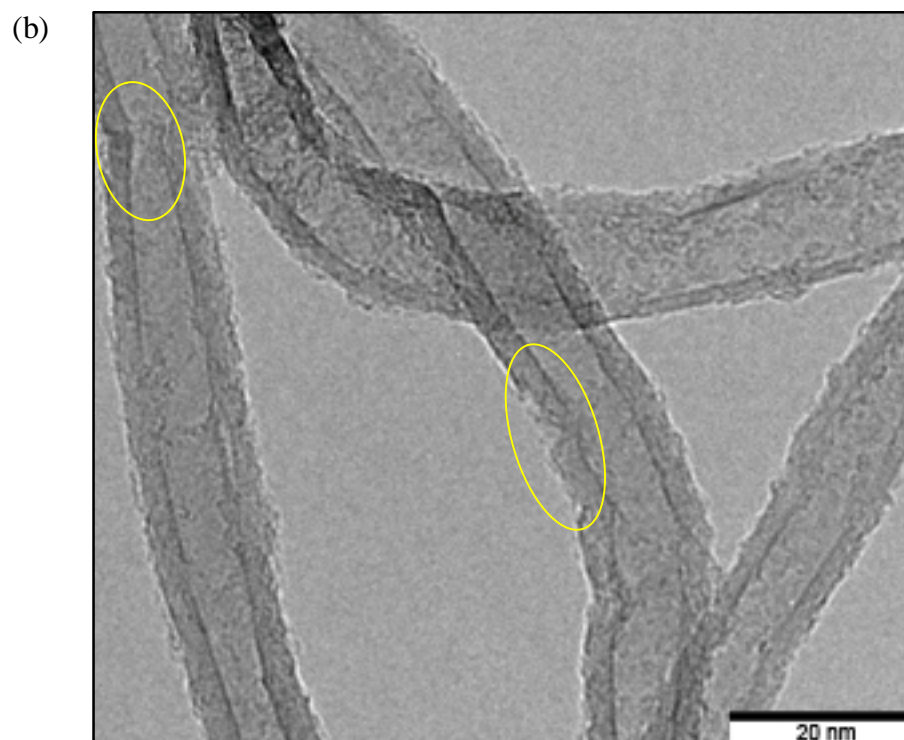


Figure 4.2: TEM images of MWNTs; (a) p-MWNTs, (b) ox-MWNTs, (c) SPEEK-MWNTs

Banerjee and Wong [25] reported that aggressive oxidation condition can open the caps of MWNTs and remove the outer layers of the tubes. The microstructures of MWNTs from TEM microscopy show the agglomeration (Figure 4.2(a)) which may be due to the van der Waals forces between the MWNTs. On the other hand, the chemically treated MWNTs dispersed better which may be due to the functional groups and negative charges formed on the surface of MWNTs. Kim et al. [15] reported that the metallic catalyst and carbonaceous materials comprises various shapes and molecular organizations which changes the properties of MWNTs itself and the composites derived with MWNTs. Strong acid condition is able to completely remove the impurities as displayed in TEM images. The amount of damage caused by the oxidation process depends on the degree of acidity or basicity, the duration of treatment and temperature, applied mechanical forces, the degree of CNTs crystallinity and others [15].

Pirlot et al. [58] reveals the presence of long individual MWNTs. On average, the inner and outer diameters of the linear types are 4 and 13 nm respectively. The intertube distance of 3.4 Å is reported to consist of 13 graphitic layers of MWNTs. Ruan et al. [59] reported that the average diameters of the MWNTs observed under TEM is ~15 nm.

The crystalline structure of p-MWNTs was characterized using powder X-ray diffraction (XRD). The XRD patterns of all MWNTs samples in Figure 4.3 displays four diffraction peaks at  $2\theta = 25.8^\circ$ ,  $43.1^\circ$ ,  $54.0^\circ$  and  $78.5^\circ$  corresponding to the (002), (100), (004) and (110) crystal phase diffraction peaks, respectively [60]. Comparison made between p-MWNTs and ox-MWNTs shows no changes in peak broadening or appearance of any new peaks. Pirlot et al. [58] suggested that two obvious peaks shown by MWNTs at  $25.8^\circ$  and  $42.8^\circ$  are corresponding to interlayer spacing which is 0.34 nm from d(002) and d(100) reflection of the carbon atoms. The band at  $42.8^\circ$  is asymmetric due to the turbostratic nature of nanotubes where the basal plane has slipped sideways to each other. Rani, Beera and Pugazhenthir [99] illustrated the XRD pattern of raw SPEEK with a peak at  $2\theta = 19.1^\circ$  in their study on SPEEK / Zirconium Titanium Phosphate (ZTP) composite membrane (Figure 4.4).

Hence, functionalization of MWNTs with SPEEK resulted in appearance of a new peak at  $2\theta = 17.5^\circ$  that is shifted, attributed to SPEEK. This indicates the existence of new phase in the SPEEK-MWNTs. The peak at  $2\theta = 25.8^\circ$  for p-MWNTs also were shifted slightly from  $2\theta = 25.8^\circ$  to  $24.7^\circ$  for SPEEK-MWNTs. Additional results of FT-IR spectroscopy were attached in Appendix C.

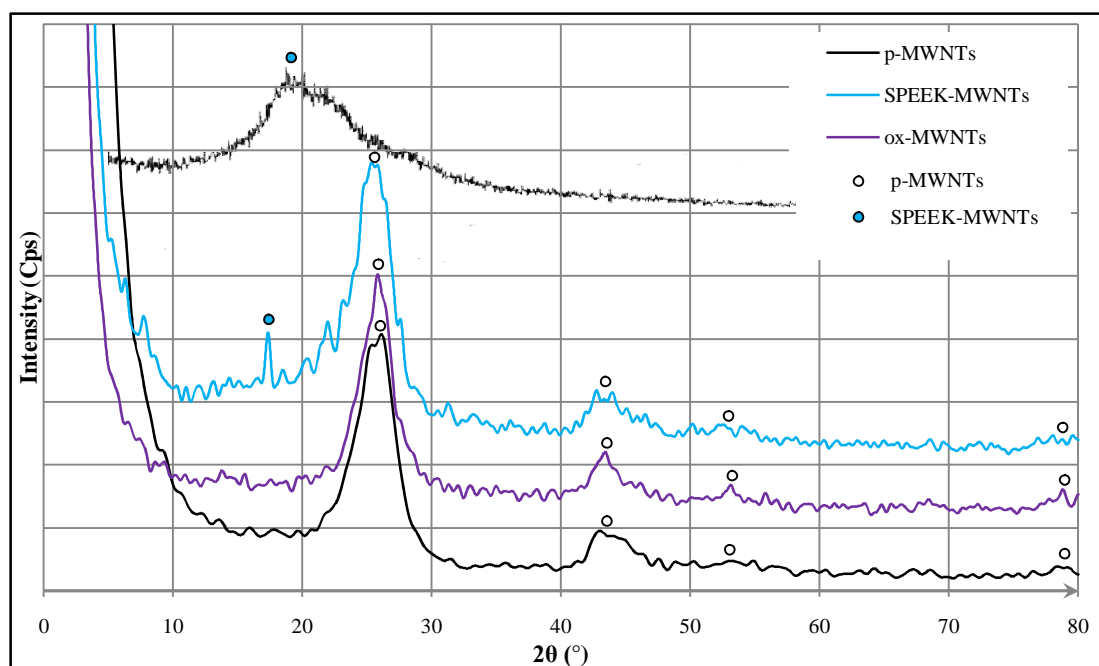


Figure 4.3: XRD pattern of MWNTs and functionalized MWNTs

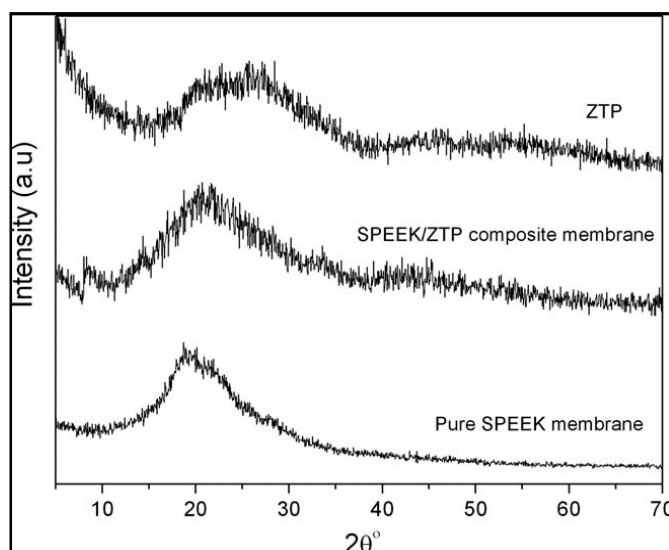


Figure 4.4: XRD pattern of ZTP powder, pure SPEEK membrane and SPEEK/ZTP composite membrane [99]

### 4.1.2 Thermal Properties of MWNTs

TGA under nitrogen environment was carried out to analyze the thermal behavior of the MWNTs and to determine their metallic residue. TGA analysis on p-MWNTs is displayed in Figure 4.5. The observed total weight loss of p-MWNTs shows the presence of small amounts of impurities and amorphous carbon as reported by Chen et al. [61]. The mass fraction of organic groups and impurities which is the total weight loss eliminated is close to 4%. This is in agreement with Chen et al. [55] which reported that mass fraction of purified SWNTs has a minor loss. Cheng et al. [16] studied the CNTs / epoxy composites and found that the CNTs are thermally stable in nitrogen gas environment below 1000°C. However, Díez-Pascual et al. [5] reported that the SWNTs start to degrade at temperature above 600°C under nitrogen condition and suggested that CNTs are thermally more stable under inert conditions rather than in an oxidative condition.

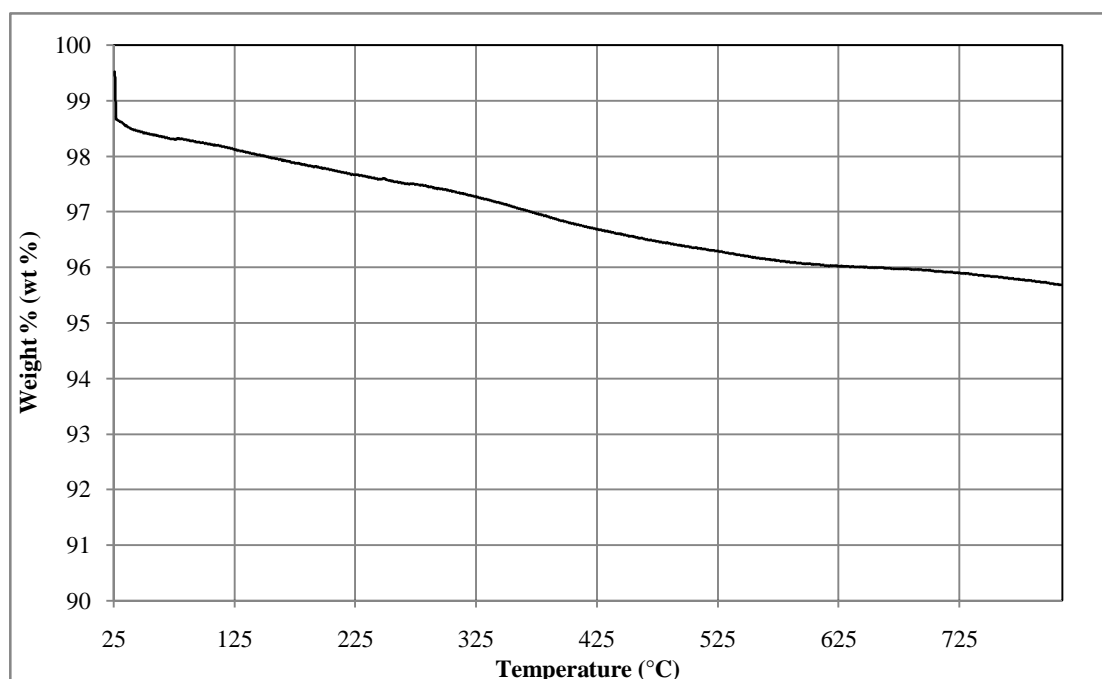


Figure 4.5: TGA of p-MWNTs

Li et al. [62] also reported a weight loss of only 5 wt% for p-MWNTs at 600°C indicating their high thermal properties. Chen et al. [55] also reported that purified SWNTs shows little weight loss indicating the presence of trace amount of impurities

in the SWNTs. Chen et al. [61] dispersed the MWNTs in concentrated acid mixture for three hours to achieve moderate oxidation and maintain high aspect ratio and suggested that the small amount of amorphous carbon and impurities represent the minor mass loss from TGA. They reported that ox-MWNTs shows 7% mass fraction of organic groups that are chemically bonded to MWNTs were eliminated at 600°C. Thermal behavior of CNTs was measured by TGA by Zhao et al. [52] and reported that the onset temperature of ox-MWNTs, 460°C which is dramatically lower than p-MWNTs, 615°C due to the organic contents attached.

## **4.2 Structural Properties of MWNTs / PEEK Composites**

### **4.2.1 XRD Results of MWNTs / PEEK Composites**

Figure 4.6(a) shows four main characteristic peaks of PEEK at  $2\theta$  of 18.6°, 20.7°, 23.2° and 28.9° which correspond to the diffraction of (110), (111), (200) and (211) crystalline planes of orthorhombic unit cell respectively [69]. In other words, the orthorhombic uniform structure of PEEK has interplanar distances of 4.72, 4.28, 3.88 and 3.09 Å [69]. Previous research on carbon nanotube / PEEK composites by Díez-Pascual et al. [5] which manipulated the fabrication method generally gives similar results. The semi-sharp diffraction patterns of PEEK show the characteristics of semicrystalline polymers [69].

Figure 4.6(b) and (c) shows five main peaks at  $2\theta$  of 18.6°, 20.7°, 23.2°, 28.9° and 39.1°. The four characteristic peaks of PEEK correspond to the diffraction of (110), (111), (200) and (211) crystalline planes of orthorhombic unit cell respectively. The fifth peak which is the new peak appears as small loading of p-MWNTs were added to the polymer. Peak at 43.1° of p-MWNTs in Figure 4.6(d) shifted to 39.1° when p-MWNTs were used to form composites with PEEK as in Figure 4.6(b) and (c). Incorporation of p-MWNTs into PEEK increases the intensity of the peaks at  $2\theta = 18.6^\circ$ ,  $20.7^\circ$  and  $23.2^\circ$ . On the other hand, the peak at  $2\theta = 18.6^\circ$ ,  $20.7^\circ$  and  $23.2^\circ$  becomes wider and smaller. The same observation was

reported by Díez-Pascual et al. [5] but appearance of new peak was not reported. Yin et al. [69] reported that small loading of p-MWNTs increases the crystallinity ratio of the polymer. However, the crystallinity ratio reduces as the loading of p-MWNTs increases.

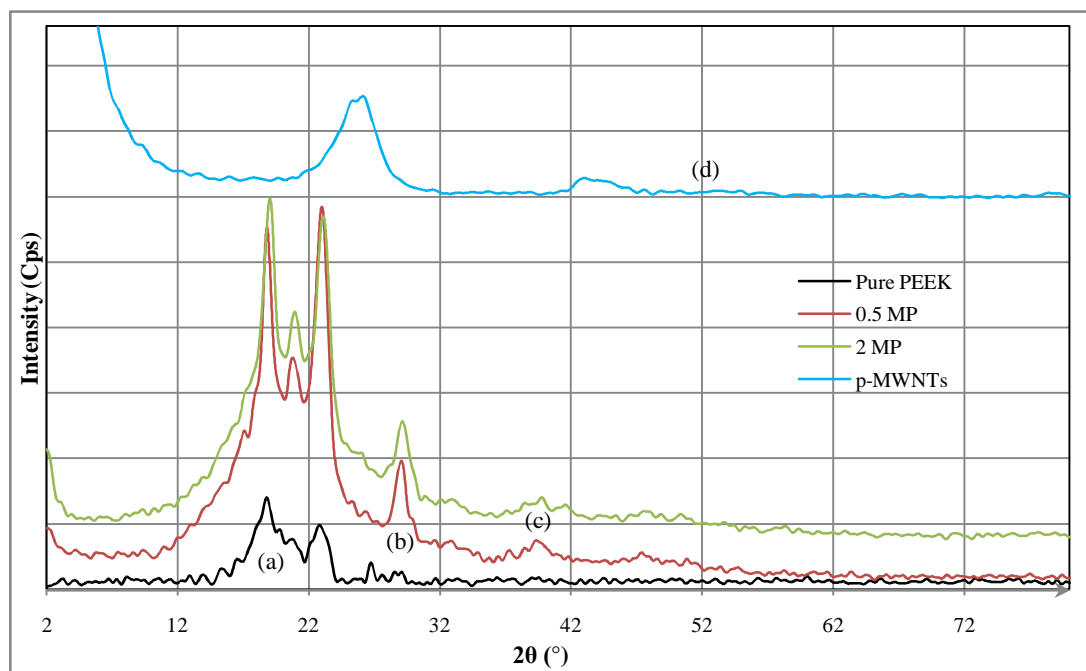


Figure 4.6: XRD pattern of p-MWNTs / PEEK composites

Figure 4.7 shows diffraction patterns displayed by ox-MWNTs / PEEK composites. The diffraction patterns are similar to that of p-MWNTs / PEEK composites. The intensity of the peaks at  $2\theta = 18.6^\circ$ ,  $20.7^\circ$  and  $23.2^\circ$  decreases with increasing MWNTs loading as seen in Figure 4.7(b) and (c). The similar results were obtained by Sahoo et al. [96], Zeng et al. [97] and Lai et al. [98] with their studies on MWNTs / polyurethane composites, MWNTs / polyamide1010 composites and MWNTs / poly(hydroxybutyrate-co-hydroxyvalerate) composites respectively. The intensity of peaks at  $2\theta = 18.6^\circ$ ,  $20.7^\circ$  and  $23.2^\circ$  increases intensively with 0.5% loading of MWNTs.

Pirilot et al. [58] in their study reported that the increased intensity of the peaks assigned to the MWNTs in the composite as a consequence of the increase in the charge of MWNTs in the film. They concluded that the preparation approach did not

cause alteration of the structure of the MWNTs. Zeng et al. [97] and supported by Lai et al. [98] reported that the increase in peak intensity of composites is because of the molecule of polymer that arranges and crystallizes around MWNTs. Another research by Chiu and Kao [95] on MWNTs / polyamide46 nanocomposites reported that the incorporation of modified MWNTs caused the slight decrease of peak intensity of the composites.

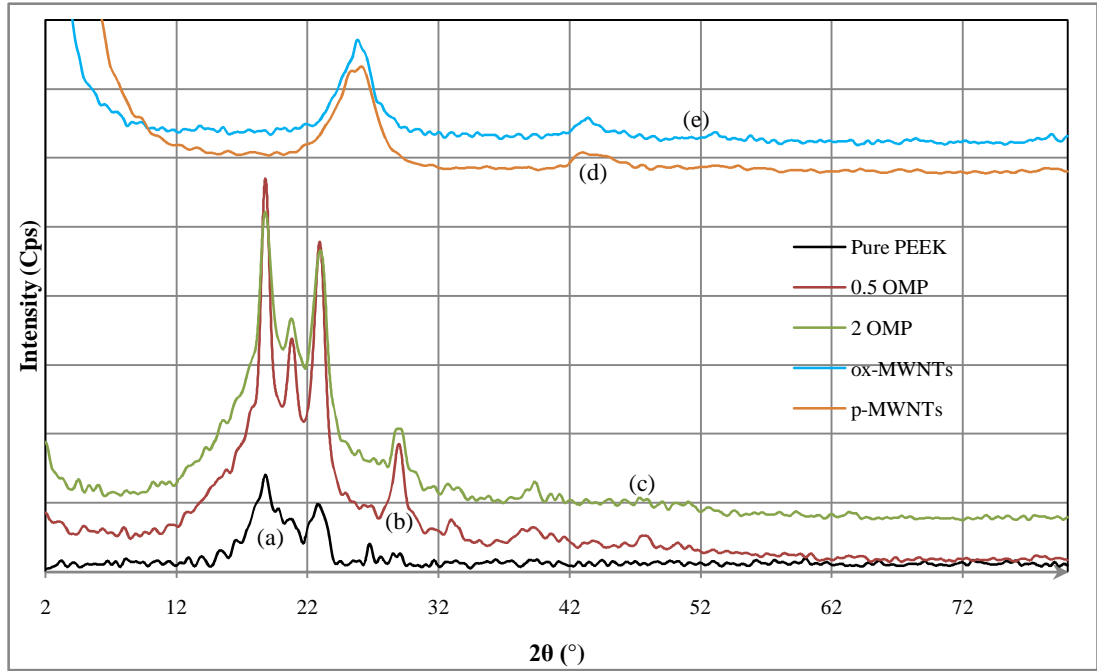


Figure 4.7: XRD of ox-MWNTs / PEEK composites

Figure 4.8 demonstrates the diffraction patterns of SPEEK-MWNTs / PEEK composites. Intensity of the peak at  $2\theta=18.8^\circ$  is higher than that displayed by p-MWNTs and ox-MWNTs with 0.5% addition of SPEEK-MWNTs (Figure 4.8(b)). Figure 4.8(b) and (c) shows that the intensity of the peaks at  $2\theta=18.8^\circ$ ,  $20.7^\circ$  and  $23.2^\circ$  decreases with increasing of SPEEK-MWNTs loading. This shows that the addition of SPEEK-MWNTs increases the crystallinity of the polymer more than that of p-MWNTs and ox-MWNTs.

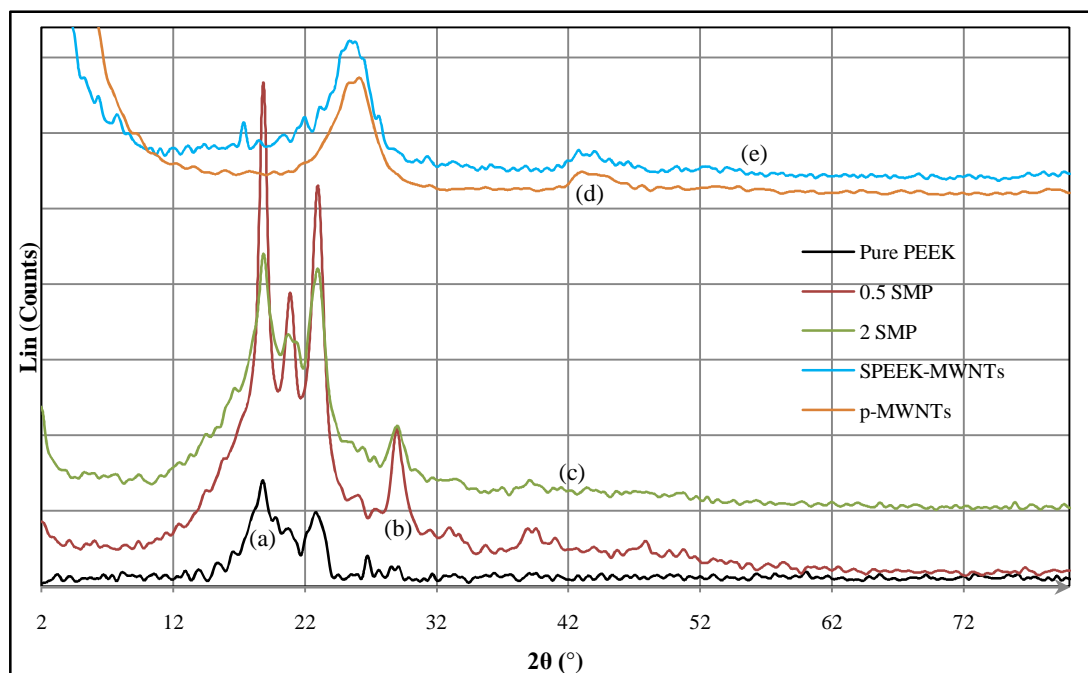


Figure 4.8: XRD of (SPEEK-MWNTs) / PEEK Composites

Based on the diffractograms, all composites display similar diffraction pattern to that of PEEK matrix, however, the patterns differs in peak width and peak intensity. In general, the intensity of the peaks at  $2\theta=18.8^\circ$ ,  $20.7^\circ$  and  $23.2^\circ$  decreases as the amount of MWNTs increased.

#### 4.2.2 FE-SEM on p-MWNTs / PEEK Composites

The pure PEEK was melted and hot-pressed to form PEEK films and analyzed utilizing respective analyzers. The morphology of fabricated PEEK is assessed by examining the fractured films with FE-SEM.

The purpose of fabricating composites is to achieve a good dispersion of CNTs in the polymer matrix with enhanced thermal and mechanical properties. However, it is commonly a difficult task because of the character of CNTs that tends to gather and form bundles [5]. The morphology and dispersion of fabricated composites are also assessed by examining the fractured film composites with FE-SEM. The samples were prepared by metallization with Au-Pd overlayer. The color of

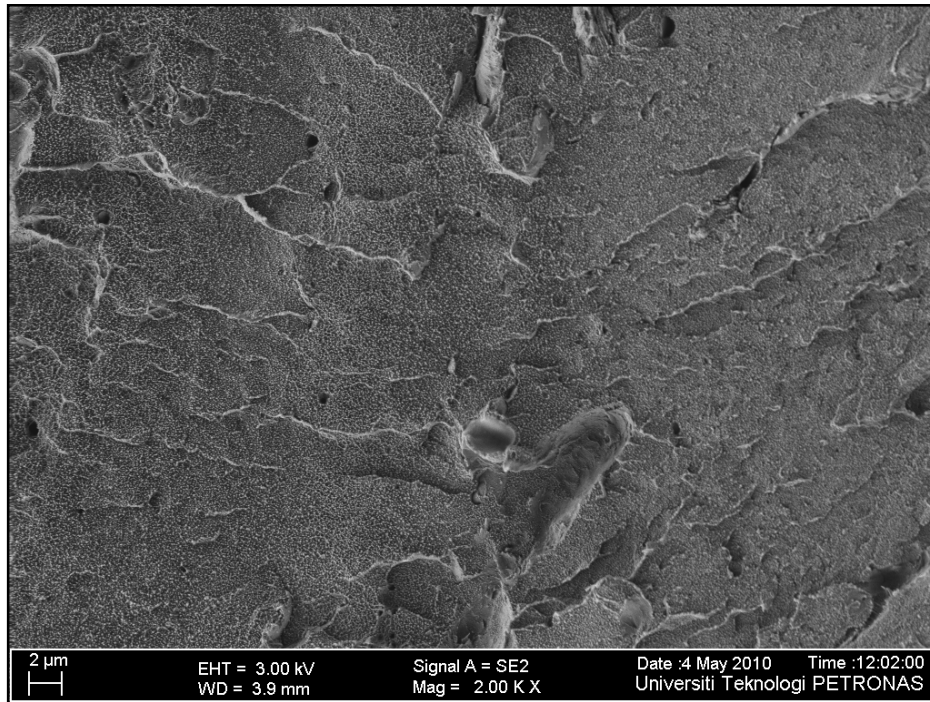


p-MWNTs / PEEK composites produced was dark gray even though the MWNTs loading are only 0.5%. The color of the composites turns to black as more MWNTs were added. Figure 4.9 compares the morphology of p-MWNTs / PEEK composites with pure PEEK film. The bright spots and lines (the marked arrows and circles on the images) are the end of the broken MWNTs. The MWNTs seem to severely agglomerate yet randomly oriented [20].

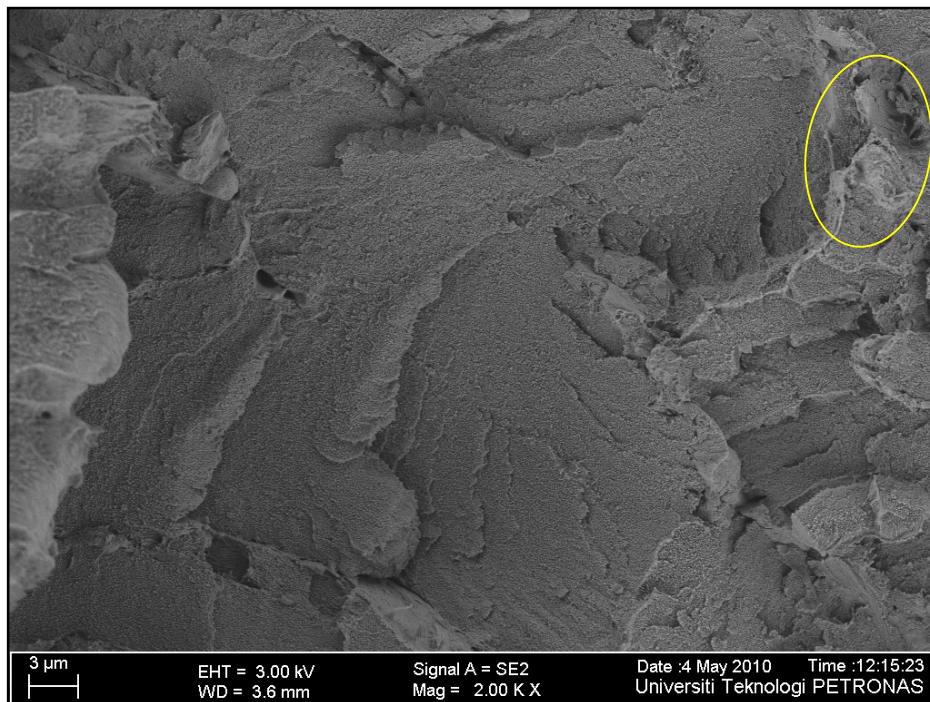
Choi et al. [87] reported that MWNTs / polystyrene (PS) nanocomposite produced was black in color with only 1 wt% of MWNTs addition. The MWNTs used in the study exhibited a distinct curved shape in all three dimensions as a result of interlocking between the MWNTs. They concluded that the structure and shape of nanotubes are randomly oriented in the polymer matrix which is agreed by Mago et al. [88].

Mago et al. [88] reported that the crystal structure of the composites begin to grow perpendicularly to the surface of the nanotubes resulting in nanohybrid-shish-kebab-like-structure especially for various types of semicrystalline polymers. The spherulitic morphologies that cover the surface of the nanotubes appear to have been cultivated upon the nucleation of multiple polymer chains on any nanotubes surface.

(a)



(b)



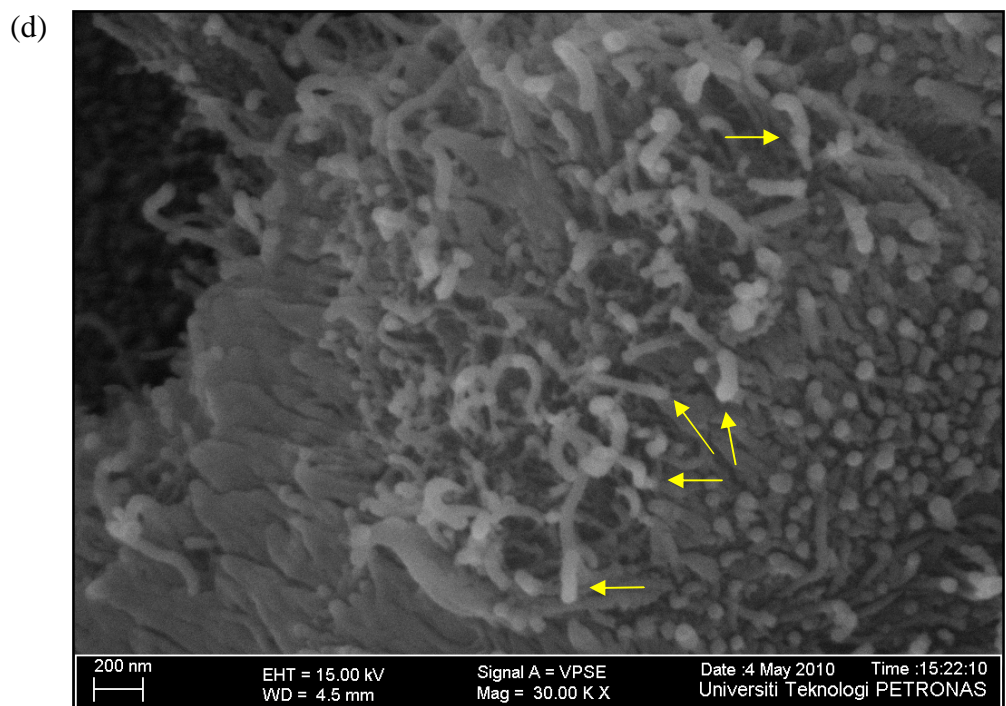
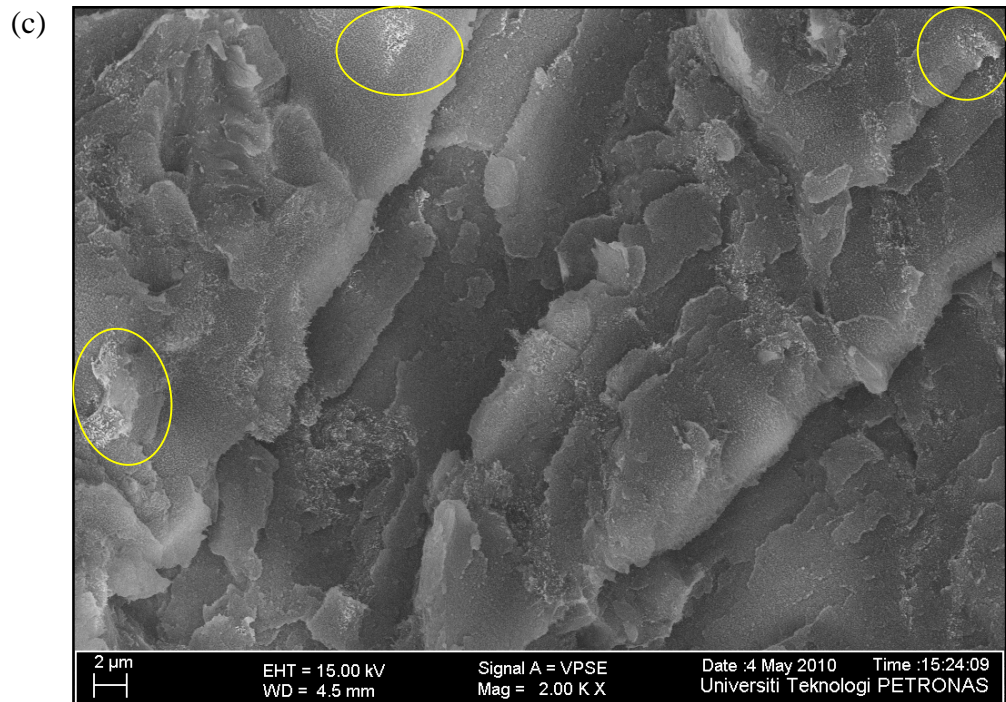


Figure 4.9: FE-SEM images of 100% PEEK and p-MWNTs / PEEK Composites; (a) Pure PEEK, (b) 0.5 MP and (c and d) 2 MP

### 4.2.3 FE-SEM on ox-MWNTs / PEEK Composites

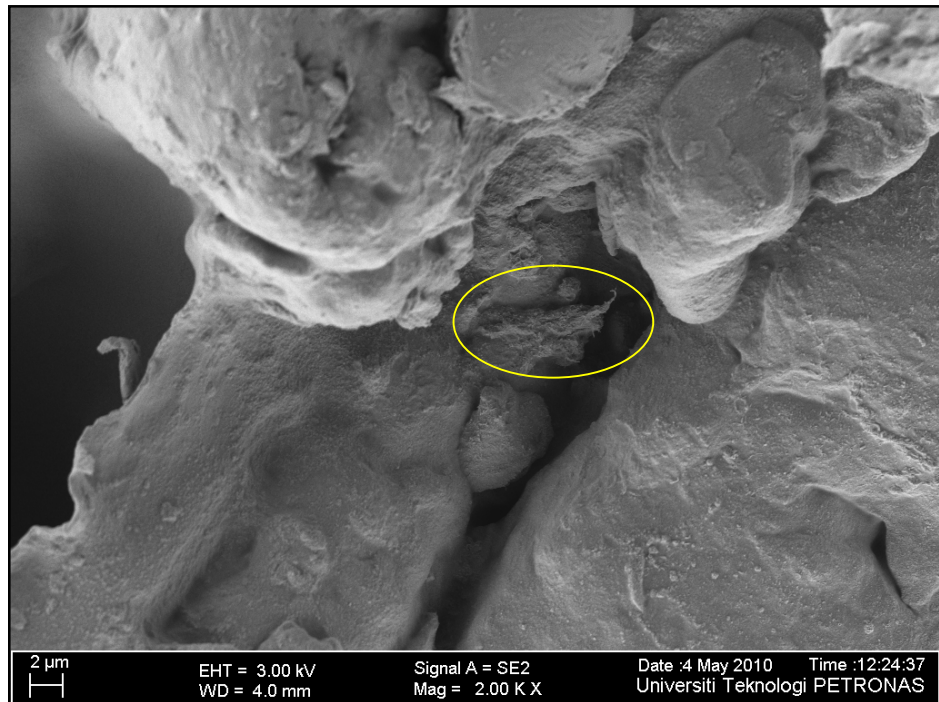
Figure 4.10 shows the micrographs of ox-MWNTs / PEEK systems. Similar to p-MWNTs / PEEK composites, the samples were metalized with Au-Pd overlayer. The color of MWNTs / PEEK composites produced was black even though only 0.5 wt% of MWNTs was added which similar to a study reported by Choi et al. [87]. This means that the distribution of ox-MWNTs in PEEK matrix is better than p-MWNTs. The MWNTs appear as bright spots (the marked circles and arrows on the images) and the micrographs shows that ox-MWNTs have better distribution in PEEK matrix than p-MWNTs without any favorable orientation and no obvious spots of agglomerated MWNTs is found.

Zhao et al. [20] reported that the major factors attributed to the difference in the dispersion of p-MWNTs and functionalized MWNTs in the poly(L-lactide) (PLLA) matrix is the electrostatic and van der Waals interactions between the MWNTs alone that lead to aggregation of the MWNTs. On the other hand, as the MWNTs is functionalized, the presence of the carbonyl groups on the surface of MWNTs assists a lot in improving the compatibility between functionalized MWNTs and the PLLA matrix. Hence, this prevents the apparent aggregation of MWNTs.

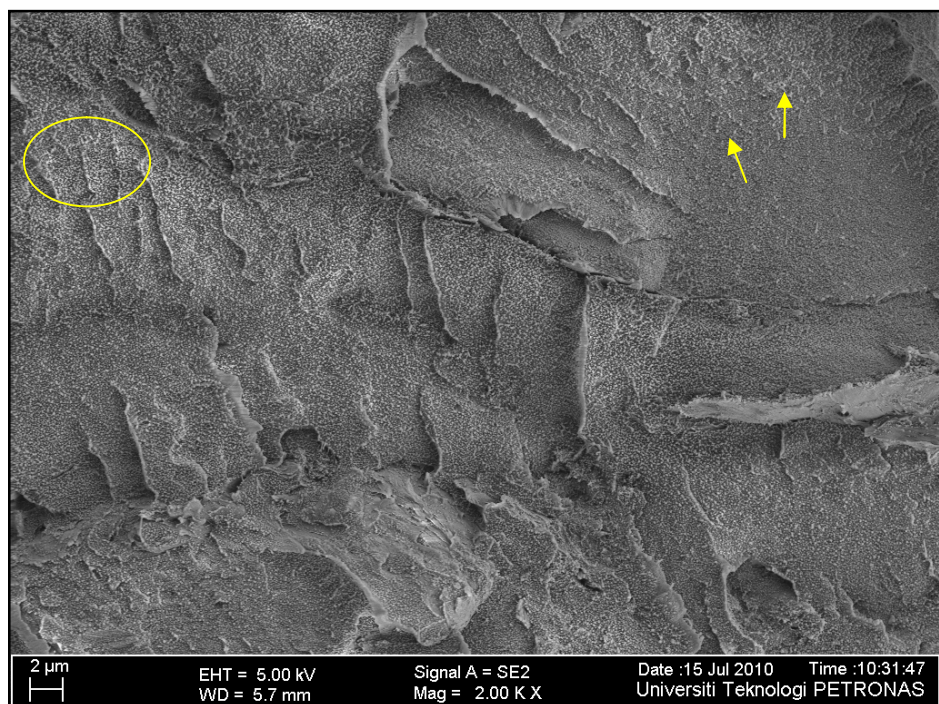
Figure 4.10(a) shows the micrograph of the edge of fractured surface of 0.5OMP sample. The agglomeration is due to the van der Waals forces between the nanotubes. The micrograph of 2OMP is shown in Figure 4.10(b) where the MWNTs disperse better as compared to 2MP. In Figure 4.10(c), the higher magnification micrograph of 2OMP, most of the MWNTs are broken and plenty of MWNTs are pulled out of the matrix before the breakage. There are also some MWNTs with their ends still strongly embedded in the matrix. This indicates that a strong interfacial adhesion occurred between the MWNTs and the matrix. As suggested by Zhao et al. [20] and supported by Nayak et al. [9], the load transfer takes place efficiently from the matrix to the nanotubes. This strong interfacial adhesion is accredited for the improvement of mechanical properties associated with the hydrophilicity of the PEEK macromolecules, while hydrophobic polymers like polypropylene usually possess weak bond to the nanotubes [70].



(a)



(b)



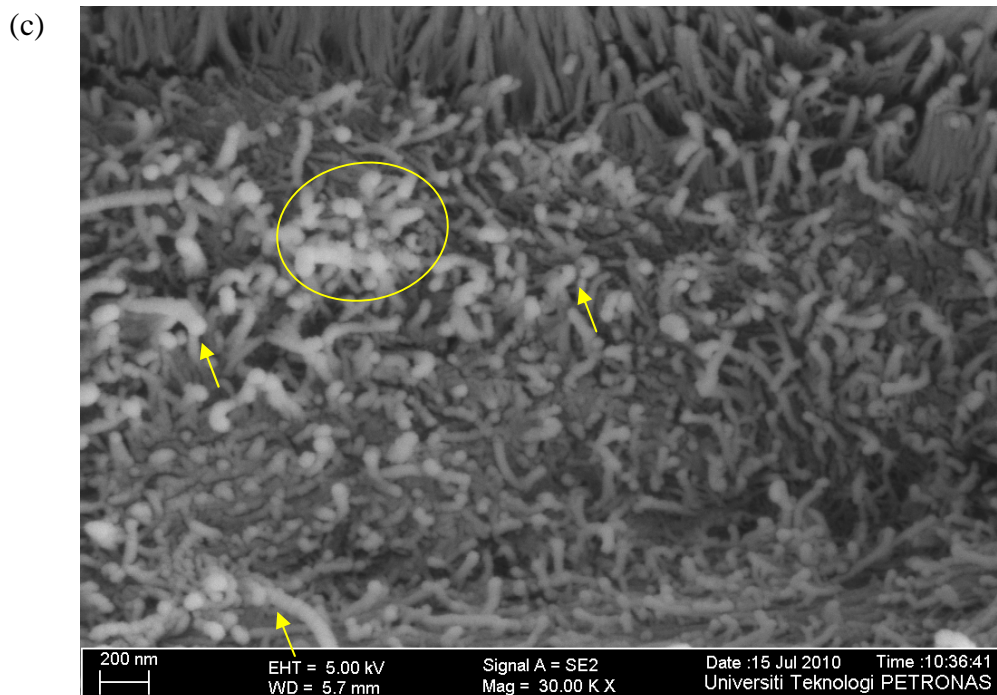


Figure 4.10: FE-SEM images of ox-MWNTs / PEEK Composites; (a) 0.5 OMP and (b and c) 2 OMP

#### 4.2.4 FE-SEM on SPEEK-MWNTs / PEEK Composites

Figure 4.11 shows typical micrographs of SPEEK-MWNTs / PEEK systems with different composition of MWNTs. The black-colored samples were also metalized with Au-Pd overlayer. The SPEEK-MWNTs (the marked arrows on the images) seems to disperse even better in PEEK matrix than ox-MWNTs / PEEK composites without favorable orientation and no obvious spots of agglomerated MWNTs is observed.

The existence of the functional groups on the surface of MWNTs assists in improving the compatibility between functionalized MWNTs and the PEEK matrix which leads to prevention of the apparent aggregation of MWNTs. This may lead to stronger interfacial adhesion between the MWNTs and the matrix and thus may contribute to an improvement in mechanical properties [20], [70].

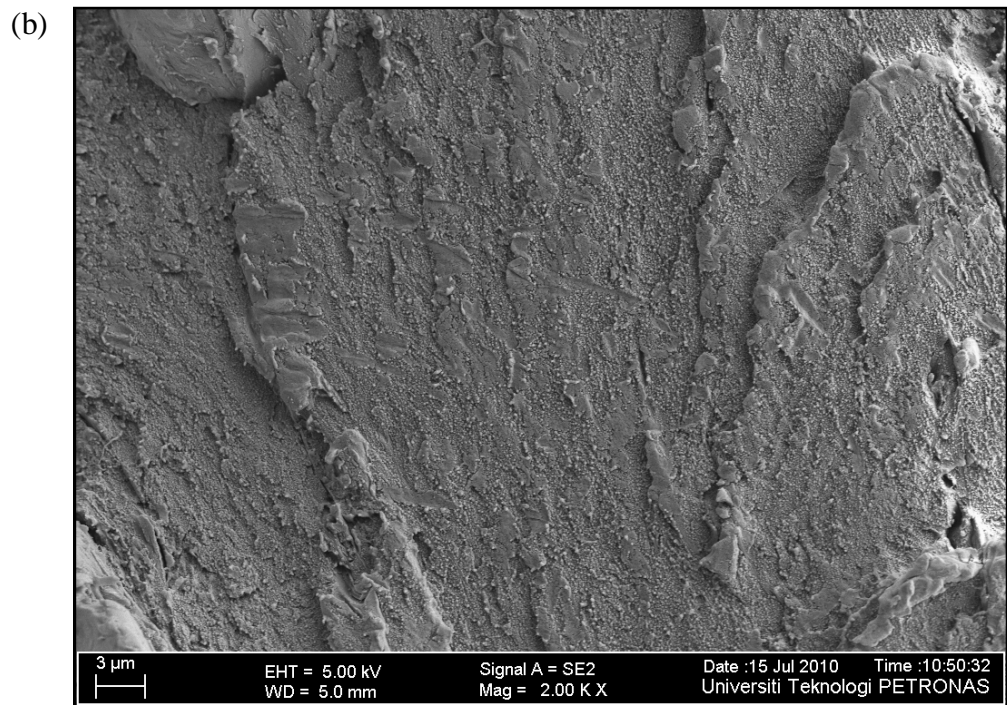
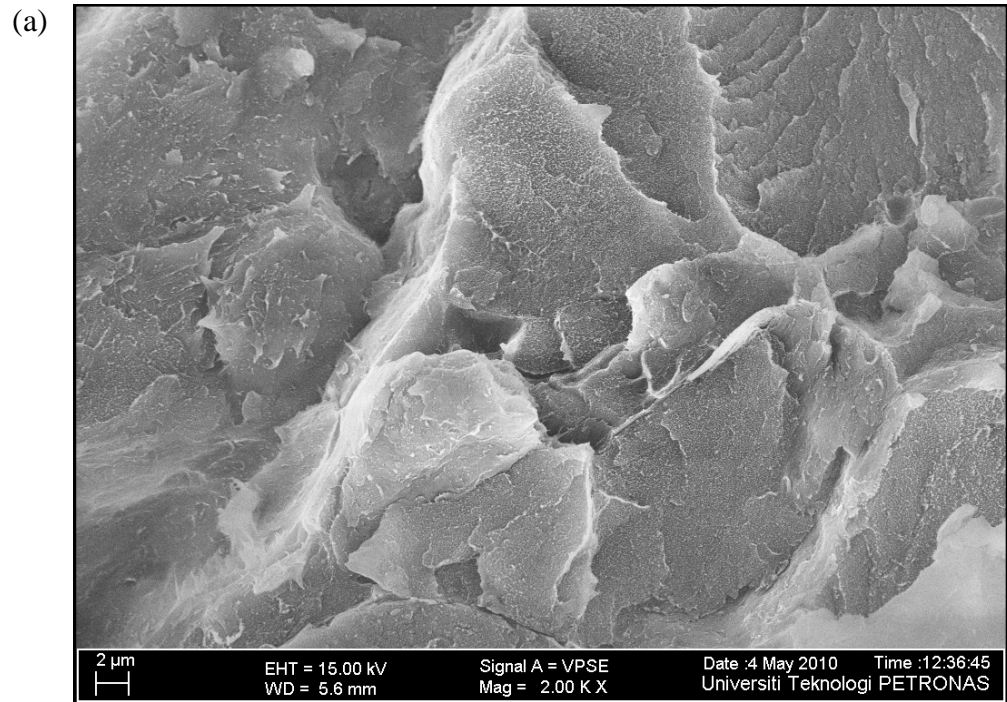


Figure 4.11: FESEM images of SPEEK-MWNTs / PEEK composites; (a) 0.5 SMP and (b) 2 SMP

Piriot et al. [58] reported that the degree of MWNTs dispersion in polymer matrix is assessed using low resolution of TEM resulted the aggregates of MWNTs appeared as well as some isolated nanotubes. Hence, TEM can be done in the future to confirm the results from FE-SEM.

### **4.3 Thermal Properties of PEEK Composites**

#### **4.3.1 TGA Results**

##### *4.3.1.1 TGA Results of p-MWNTs / PEEK Composites*

The thermal stability of the composites was studied from room temperature to 900°C under nitrogen atmosphere. Figure 4.12 shows that pure PEEK starts to decompose at 541°C and significant weight loss (6%) occurs between 541-585°C. A gradual weight loss continue to occur when pure PEEK was heated up to 900°C with 46% weight loss observed between 585-900°C. Fujihara et al. [8] reported that the onset temperature where the carbon fibre reinforced PEEK composites started to lose their thermal stability with approximately 2 % weight loss is at 561°C. On the other hand, Patel et al. [4] reported that the onset of thermal degradation of PEEK sample occurs between 575°C to 580°C.

Díez-Pascual et al. [5] suggested that the decomposition process takes place in a single stage involving decarboxylation, decarbonylation and dehydration processes. These processes lead to the formation of phenol groups, carbon dioxide and water, leaving the ether and aromatic structures to remain in the residue at elevated temperatures. The residual weight left from this study is relatively similar to the results reported by Díez-Pascual et al. [5] which is about 46% at 700°C. However, the onset temperature of pure PEEK observed by Díez-Pascual et al. [8] is up to 20°C higher than those observed in this study.



As reported by Yin et al. [69] and Patel et al. [4], pure PEEK has superior thermal degradation resistance with continuous use temperature of up to 260°C and melting point of 343°C [4]. The glass transition temperature has been reported as 143°C [69]. Onset decomposition temperature of PEEK is 575°C in nitrogen [4]. The thermal decomposition of PEEK differs in oxygen and nitrogen environment but both shows two decomposition steps where the first step is attributed to random chain scission of ether and ketone bonds which is the main mechanism. Carbonyl bond cleavage leads to formation of a more stable radical intermediate because of predominant resonance effects. Volatilisation of about 45% of polymer mass occurs rapidly just below 600°C with major weight loss and formation of carbonaceous char in the remaining polymer mass [4], [69], [72].

PEEK itself have high mechanical and thermal properties. Even if no improvement can be seen on the thermal behaviour of the composites, it should be expected to see some improvement on the mechanical properties and the effect of reinforcement on the thermal stability.

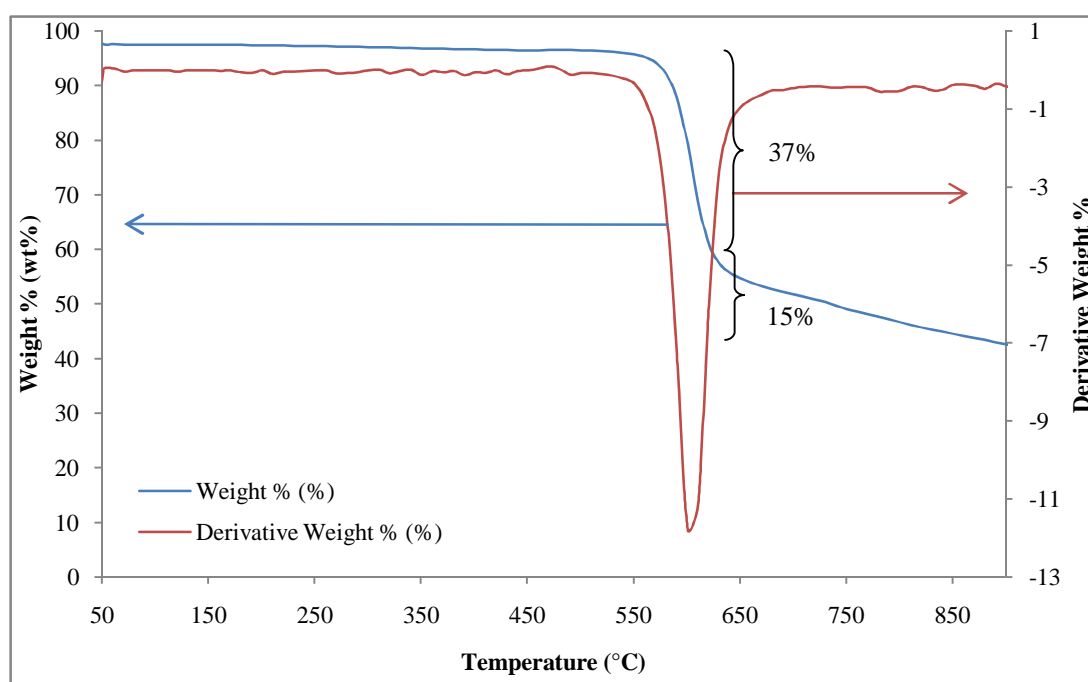


Figure 4.12: TGA of Pure PEEK

Cheng et al. [16] have reported that p-MWNTs are thermally stable in nitrogen environment below 1000°C while pure PEEK decompose drastically at 585°C with a total of 46% weight loss when the sample was heated up to 900°C. From Figure 4.13, the p-MWNTs / PEEK composite starts to lose weight at temperatures between 553-572°C even with different p-MWNTs loading. The onset degradation temperatures for 0.5% and 2% p-MWNTs loaded composites are 569°C and 576°C respectively. It can be seen that the onset degradation temperature of 0.5% p-MWNTs / PEEK composite is slightly lower than pure PEEK. This observation indicates that the p-MWNTs are not uniformly distributed where the interfacial adhesion between the filler and the matrix does not improve.

Hence, the thermal motion of the PEEK chains becomes less restricted, thus less stable [5]. This may be contributed by a few factors such as the preparation procedure and the impurities contained in the p-MWNTs. Choi et al. [87] and supported by Choi et al. [21] in their study on MWNTs / PS composite and MWNTs / polypropylene (PP) respectively reported that the enhanced distribution of MWNTs improve the thermal stability of the polymer matrix and also raises the surface area in the polymer matrix. Improvement in interfacial interaction increases the activation energy of degradation at interface between MWNTs and the polymer, and retards the degradation at the surface of the composites as a result of great thermal conductivity of CNTs [21].

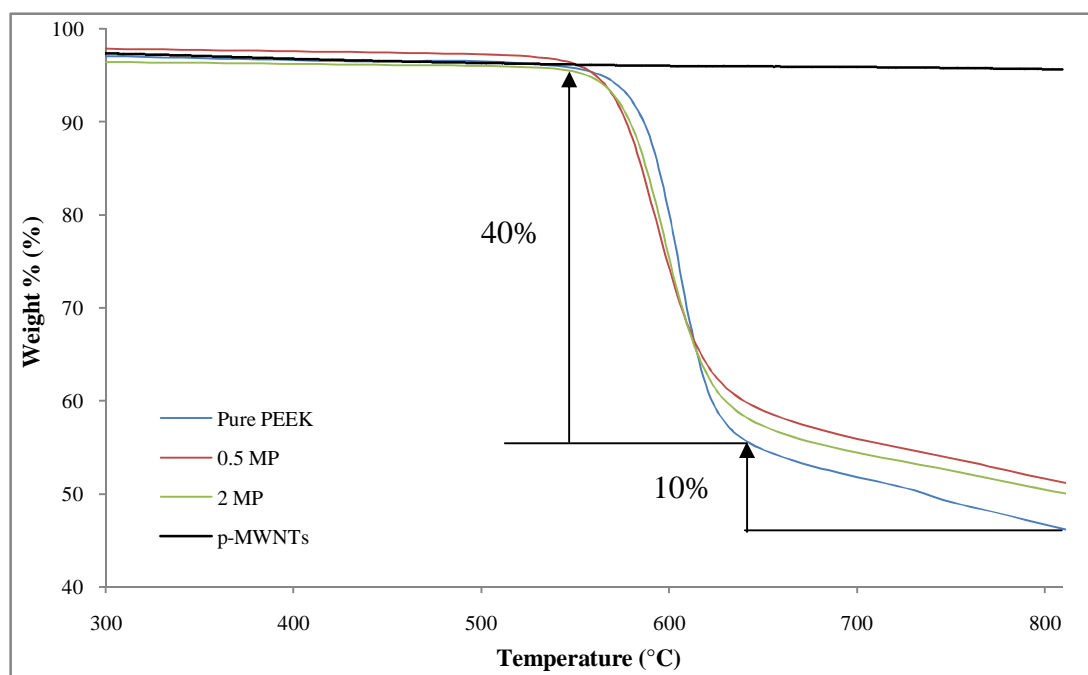


Figure 4.13: TGA of p-MWNTs / PEEK Composites

Similar results have been observed by Babooram and Narain [32] on SWNT / Silica composites. Díez-Pascual et al. [5] have reported that the incorporation of small amount of SWNTs which have been uniformly dispersed can stabilize the composite in an oxidative environment, raising the onset temperature of the matrix and delays the maximum rate temperature which progressively increases with increasing SWNTs loading. Furthermore, Nayak et al. [6] suggested that the chain mobility of polymer matrix is reduced with the incorporation of CNTs by imposing numbers of restriction sites which reduces the thermal vibration of the C-C bond. Hence, more thermal energy is required for the degradation of polymer matrix, which in turn increases their thermal stability. Another reason is the formation of char acting as the physical barrier between the polymer and the superficial zone where the combustion of the polymer is occurring [6].

#### 4.3.1.2 TGA Results of ox-MWNTs / PEEK Composites

Figure 4.14 shows that the onset temperatures for 0.5% and 2% ox-MWNTs / PEEK composites are at 580°C and 584°C respectively. It can be seen that the decomposition temperature for the composites is slightly lower than that of pure PEEK and the decomposition temperature decreases by 5°C as 0.5% MWNTs is loaded to the polymer as the loading of ox-MWNTs increases. This observation indicates that the ox-MWNTs disperse better in PEEK matrix. The interfacial adhesion between the filler and the matrix improved gradually as the MWNTs are oxidized. Enhanced thermal stability was also reported for Polyamide (PA) 46 / ox-MWNTs by Chiu et al. [95]. The improved thermal stability is contributed mainly by the well dispersed ox-MWNTs in the matrix [95]. The thermal motion of the PEEK chains becomes more restricted by imposing numbers of restriction sites that reduces thermal vibration of C-C bonds. This is in agreement with Nayak et al. [6]. Hence, ox-MWNTs / PEEK composites are more stable than p-MWNTs / PEEK. Nayak et al. [6] also suggested that the char formed during the combustion of the composites acts as the physical barrier between the polymer and the superficial zone of combustion.

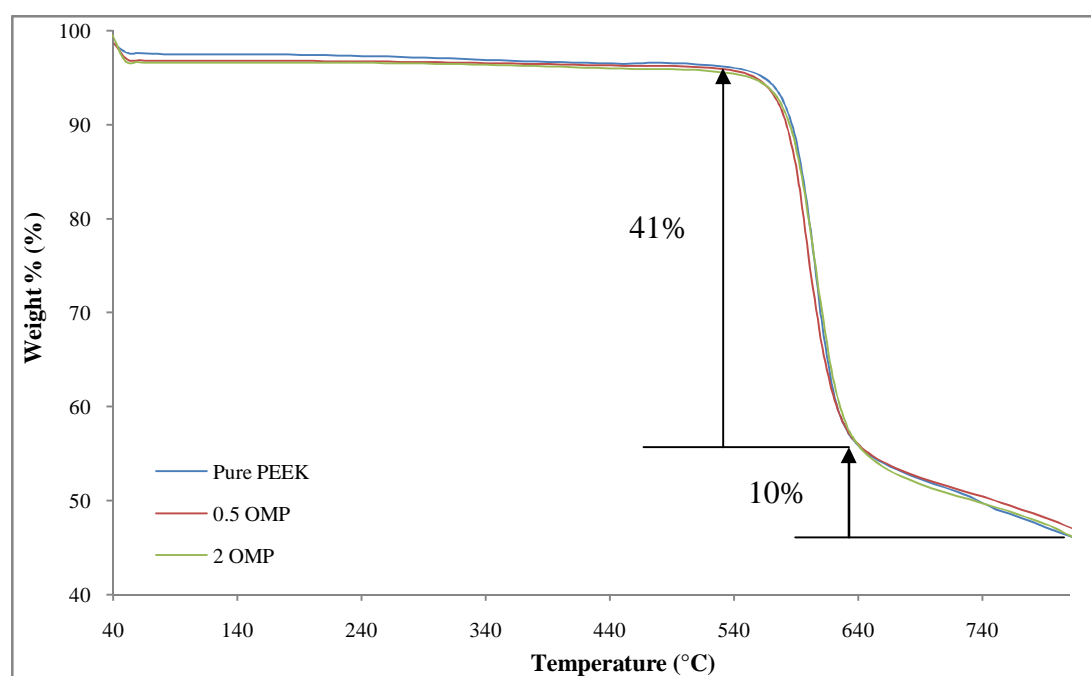


Figure 4.14: TGA of ox-MWNTs / PEEK Composites

#### 4.3.1.3 TGA Results of SPEEK-MWNTs / PEEK Composites

Figure 4.15 shows the onset temperatures for thermal degradation of 0.5% and 2% SPEEK-MWNTs / PEEK composites which are 581°C and 583°C respectively. It can be seen that the composites decomposition temperature is lower than pure PEEK by 4°C as 0.5% MWNTs is loaded to the polymer and this onset temperature increases slightly with increasing loading of SPEEK-MWNTs. This observation indicates that the distribution of the functionalized MWNTs is better than that of p-MWNTs but similar to that of ox-MWNTs / PEEK composites. The interfacial adhesion between the filler and the matrix improved gradually as the MWNTs are functionalized compared to p-MWNTs. The improved thermal stability is contributed mainly by the well dispersed ox-MWNTs in the matrix where thermal motion of the PEEK chains becomes more restricted by imposing numbers of restriction sites that reduces thermal vibration of C-C bonds [95]. This is in agreement with Nayak et al. [6]. Nayak et al. [6] also reported that the char formed during the combustion of the composites acts as the physical barrier between the polymer and the superficial zone of combustion. Hence, the thermal motion of the PEEK chains becomes more restricted and so more stable than p-MWNTs / PEEK.

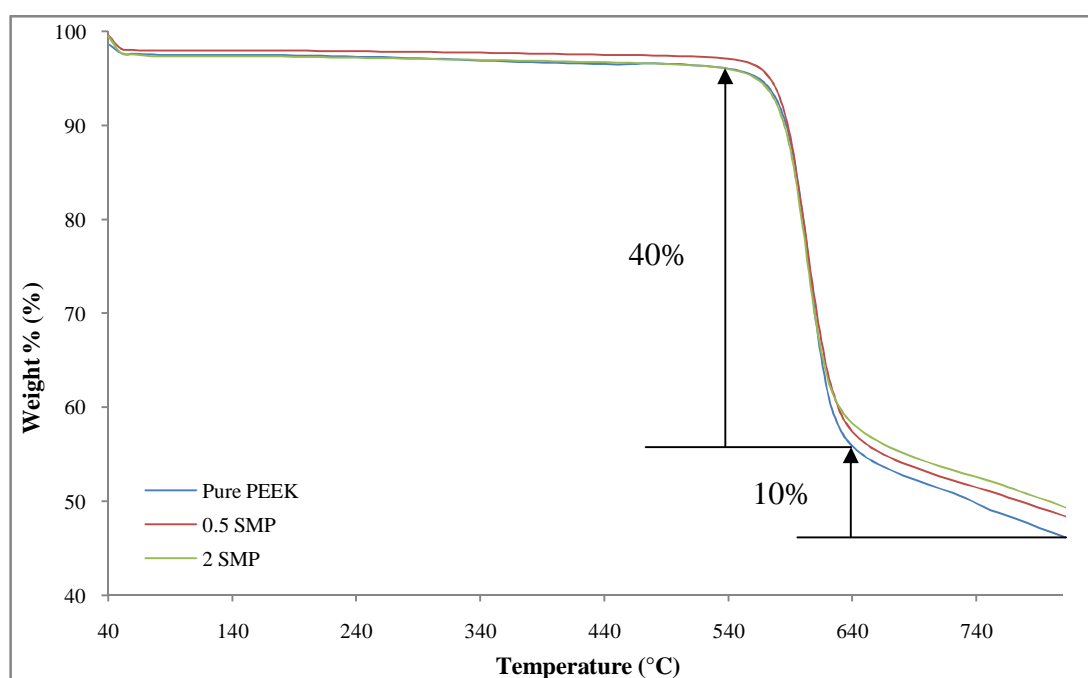


Figure 4.15: TGA of SPEEK-MWNTs / PEEK Composites

Sahoo et al. [96] reported that ox-MWNTs / polyurethane composites showed higher decomposition temperature and delayed decomposition temperature than that of pure polyurethane. Improvement of the properties also reported by Zeng et al. [97] on ox-MWNTs / reinforced nylon 1010 composites where the onset temperature increases proportionally. Zeng et al. [97] reported that the chain of nylon 1010 are intensely interconnected with MWNTs and that the MWNTs acts as radical scavengers that delays the onset of thermal degradation and results in improved thermal stability of nylon 1010; since polymer thermal degradation begins with chain cleavage and radical formation.

The TGA data for all the composites are compiled in Table 4.1. In general, the thermal stability of MWNTs / PEEK composites were not improved even after MWNTs were functionalized.

Table 4.1: TGA data of MWNTs / PEEK Composites

| Material | T <sub>onset</sub> (°C) | T <sub>mr</sub> (°C) | Weight loss (wt %) |
|----------|-------------------------|----------------------|--------------------|
| PEEK     | 585                     | 605                  | 46                 |
| 0.5 MP   | 569                     | 592                  | 52                 |
| 2 MP     | 576                     | 595                  | 50                 |
| 0.5 OMP  | 581                     | 600                  | 47                 |
| 2 OMP    | 584                     | 606                  | 48                 |
| 0.5 SMP  | 581                     | 602                  | 48                 |
| 2 SMP    | 583                     | 603                  | 50                 |

\* Residual weight percent is at 800°C

### 4.3.2 DSC Results

#### 4.3.2.1 DSC Results of *p*-MWNTs / PEEK Composites

The thermal properties of PEEK were studied with DSC to determine the glass transition of the polymer [5], [21]. Figure 4.16 shows the heating endotherms and crystallization exotherms for the PEEK film sample. When cooled down, PEEK crystallized at almost 315.25°C with crystallization enthalpy of around 25.52 J/g. These data are similar to those reported by Diez-Pascual et al. [5]. Pure PEEK shows an endothermic peak which is attributed to the melting temperature of PEEK at 349.3°C with the glass transition temperature,  $T_g$  at 156.38°C and a small variation of the specific heat related to the glass transition [5]. It is important to highlight again that the instrument can only be heated up to 350°C only. Diez-Pascual et al. [5] have reported that the melting point for pure PEEK is at 344.2°C while 150°C of  $T_g$ .

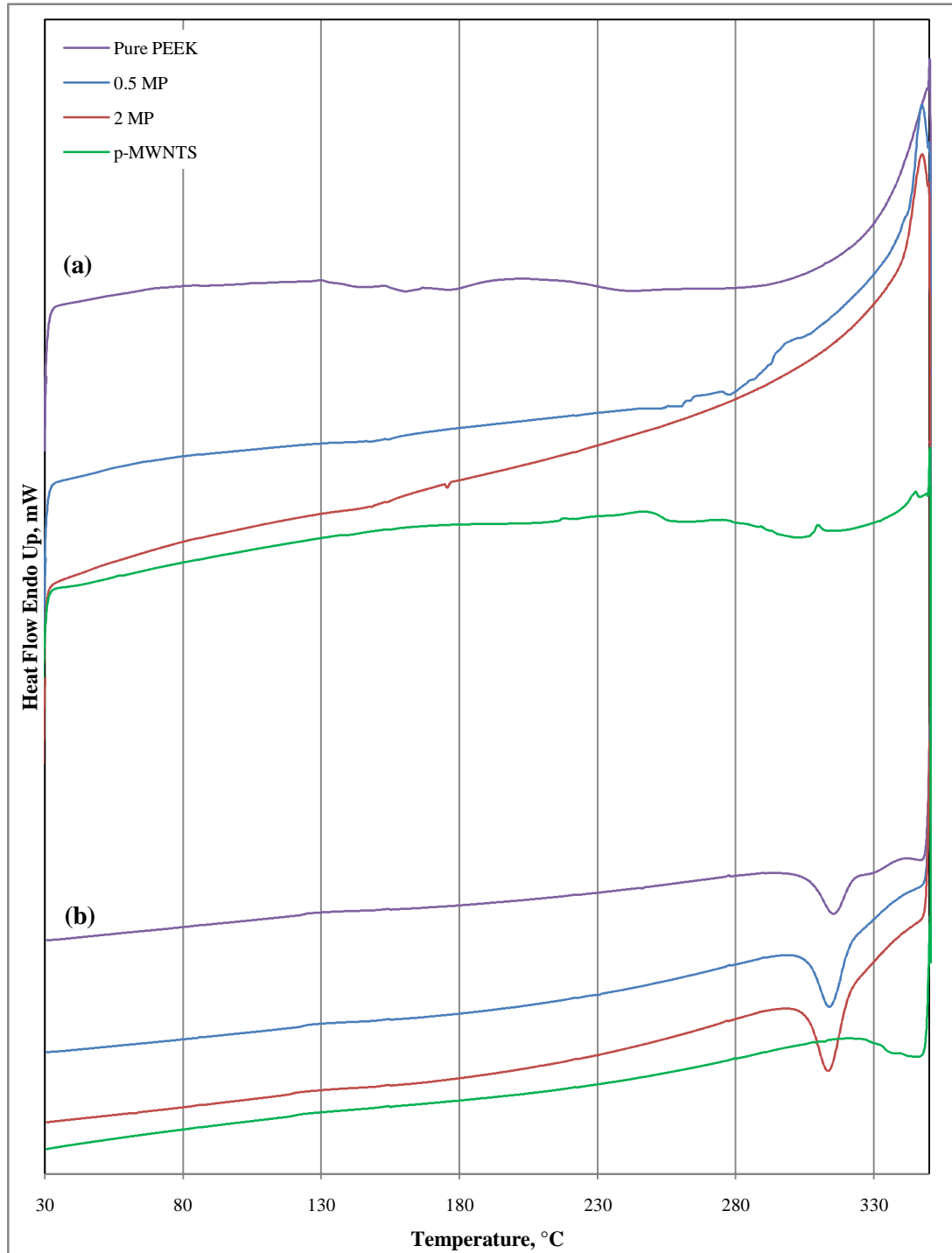


Figure 4.16: DSC scans of p-MWNTs / PEEK composites. (a) heating and (b) cooling curves.

The apparent crystallization enthalpy,  $\Delta H_c$  (J/g) is calculated as the normalized integral of the crystallization peak [5], [88]. On the basis of heat of fusion of 100 % crystalline PEEK,  $\Delta \hat{H}_c$  which is 130 J/g, the degree of crystallinity,  $(1-\lambda)_c$  of PEEK



and its composite are determined by the ratio of the crystallization enthalpy of the samples to that of 100 % crystalline PEEK. The degree of crystallinity obtained for pure PEEK sample is 19.63 %.

Figure 4.16 shows the DSC scans of pure PEEK and its composites with p-MWNTs. It can be observed that the peaks related to both the melting and crystallization of p-MWNTs / PEEK composites are narrower as compared to pure PEEK. This indicates a narrower crystallite size distribution in the matrix; hence heat supplied will be evenly distributed in the matrix [40]. Similar observations have been reported by Bhattacharyya et al. [40] on SWNTs / Polypropylene (PP) composites.

The characteristics of MWNTs which have higher thermal conductivity than the polymer contribute to the sharper crystallization and melting peaks. DSC analysis on MWNTs / PP filaments resulted in slight increment of heat of fusion of the composites due to a more ordered polymer packing obtained in the composites [21]. Choi et al. [21] suggested that the crystallization temperature is affected when MWNTs were added to polymer as it involves primary nucleation as well as spherulitic growth.

Utilizing MWNTs as a reinforcing material resulted in a progressive shift of the crystallization towards slightly lower temperature (Table 4.2). However, the apparent crystallization enthalpy,  $\Delta H_c$  increased dramatically from around 25.5 J/g for pure PEEK to 37.3 J/g when PEEK was loaded with 2 % p-MWNTs. These scenarios are interesting because the MWNTs acts as nucleating agents which improve the crystallization rate since the nucleation starts at multiple centers at the same time. Therefore, the  $T_c$  should be higher in the composites as compared to PEEK.

Table 4.2: DSC crystallization and melting data of p-MWNTs / PEEK Composites

| Material | $T_g$ (°C) | $T_m$ (°C) | $T_c$ (°C) | $\Delta H_c$ (J/g) | $(1-\lambda)_c$ (%) |
|----------|------------|------------|------------|--------------------|---------------------|
| PEEK     | 156.38     | 349.10     | 315.25     | 25.52              | 19.63               |
| 0.5 MP   | 153.87     | 347.23     | 314.03     | 35.86              | 27.72               |
| 2 MP     | 153.69     | 347.57     | 313.71     | 37.30              | 29.28               |

According to Díez-Pascual et al. [5], the network of CNTs enforces a confinement on the polymer chain diffusion and crystal growth. This decelerates the overall process for crystallization leading to lower  $T_c$  for the composites. Anyhow, results from this study are coherent with the behavior reported by Díez-Pascual et al. [5] in their work on SWNTs / PEEK composites. However, opposite observation was reported by Choi et al. [21] where they observed an increase of about 4.5°C in crystalline temperature ( $T_c$ ) as 1% MWNTs was incorporated. Vega et al. [41] also reported 1°C increment of  $T_c$  in 0.54% MWNTs / HDPE composite. The small increment is still considered significant in view of high nucleation density of polyethylene. Nevertheless, the  $T_m$  and crystallinity remain the same even by the presence of MWNTs [41]. Vega et al. [41] also reported that the process of crystallization occurs earlier than in pure HDPE with the entire crystallization process occurs faster.

The  $T_m$  is slightly affected as the MWNTs were incorporated in the PEEK matrix, where  $T_m$ s of the composites are modestly reduced to 347.5°C from 349.1°C observed with pure PEEK. Mago et al. [88] also reported similar observation where the melting temperature of MWNTs / poly (butylenes terephthalate) (PBT) reduced slightly from 208.6°C for pure PBT to 202.3°C for 2% MWNTs / PBT. These however are in contrast with the work reported by Díez-Pascual et al. [5] where they reported the average melting temperature of 343°C and it remains the same for all SWNTs / PEEK composites with  $T_g$ s of approximately 153.7°C in the composites and are lower than of the pure PEEK.

It is found that the  $(1-\lambda)_c$  of the composites increases with increasing of MWNTs loading (Table 4.2). The increment in crystallinity of PEEK is important before and after the MWNTs additions [20-21], [88]. Zhao et al. [20] reported that the addition of MWNTs to poly(L-lactide) (PLLA) shows slight effect on the  $T_m$  and  $T_c$  of PLLA, while the  $\Delta H_c$ ,  $\Delta H_m$ , and  $(1-\lambda)_c$  increases significantly in the composites. Mago et al. [88] suggested that increases in degree of crystallinity have a strong influence on the enhancement of various ultimate properties of the particular polymer.

#### 4.3.2.2 DSC Results of ox-MWNTs / PEEK Composites

The DSC scans of ox-MWNTs / PEEK composites are demonstrated in Figure 4.17. Similar to p-MWNTs / PEEK composites, the melting and crystallization peaks of the composites are narrower than that of pure PEEK which indicate narrower crystallite size distribution and evenly distributed heat in the matrix [40]. The characteristic of MWNTs was enhanced after oxidation process where the peak of 0.5 OMP is narrower than 0.5 MP. The value of  $T_g$ s is around 153.5°C in the nanocomposites which is 3°C lower than pure PEEK. However, the  $T_g$ s are similar with p-MWNTs / PEEK composites indicating that the  $T_g$ s are not affected even though the MWNTs have been oxidized (ox-MWNTs). Furthermore, the value of  $T_m$ s is around 347.5°C in the nanocomposites and slightly decreased than pure PEEK. This finding is similar to those observed in p-MWNTs / PEEK composites.

Table 4.3 shows the data obtained from DSC analysis where the values of  $H_c$  increase with increasing of ox-MWNTs loading from 0 to 2%. The degree of crystallinity also increases with increasing of ox-MWNTs loading. These increasing of  $H_c$  and degree of crystallinity are due to the restricted movements of polymer chains by the inorganic components. This is in agreement with work reported by Kuan et al. [30]. It is also observed that addition of ox-MWNTs has more effect on the  $T_g$ ,  $T_m$ ,  $T_c$  and  $H_c$  as compared to those using p-MWNTs as fillers. Yang et al. [29] reported that the  $T_g$ 's of a polymer are dependant to the free volume of the polymer that correlated with the similarity between the filler and polymer matrix. Thus, ox-MWNTs is suggested as a more suitable filler than p-MWNTs in enhancing

the crystallization of PEEK. This is in agreement with the work reported by Zhao et al. [20].

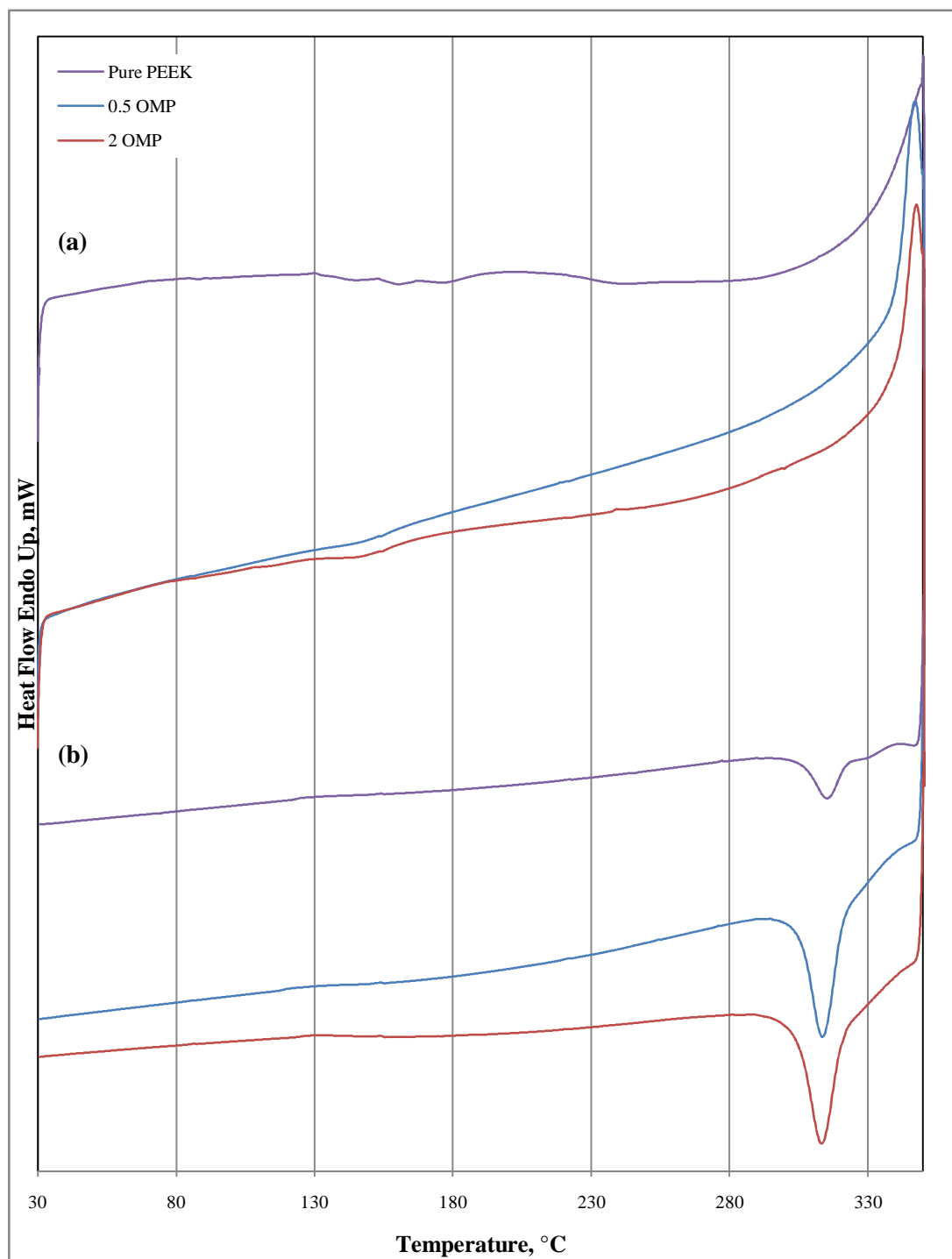


Figure 4.17: DSC scans of ox-MWNTs / PEEK composites. (a) Heating and (b) cooling curves.

Table 4.3: DSC data of ox-MWNTs / PEEK Composites

| Material | T <sub>g</sub> (°C) | T <sub>m</sub> (°C) | T <sub>c</sub> (°C) | ΔH <sub>c</sub> (J/g) | (1-λ) <sub>c</sub> (%) |
|----------|---------------------|---------------------|---------------------|-----------------------|------------------------|
| PEEK     | 156.38              | 349.10              | 315.25              | 25.52                 | 19.63                  |
| 0.5 OMP  | 153.65              | 347.22              | 313.71              | 37.06                 | 28.65                  |
| 2 OMP    | 153.98              | 347.85              | 313.33              | 39.59                 | 31.08                  |

#### 4.3.2.3 DSC Results of SPEEK-MWNTs / PEEK Composites

Figure 4.18 shows the DSC scans of SPEEK-MWNTs / PEEK composites. Similar to p-MWNTs / PEEK composites, the melting and crystallization peaks of the composites are narrower than that of pure PEEK which indicate narrower crystallite size distribution and evenly distributed heat in the matrix [40]. The characteristic of MWNTs was enhanced after functionalization where the peak of 0.5 SMP is narrower than 0.5 MP. The value of T<sub>g</sub>s is around 153.5°C in the nanocomposites which is 3°C lower than pure PEEK. However, the T<sub>g</sub>s are relatively similar with p-MWNTs / PEEK composites indicating that the T<sub>g</sub>s are not affected eventhough the MWNTs have been functionalized (SPEEK-MWNTs). Furthermore, the value of T<sub>m</sub>s is around 347.5°C in the nanocomposites and slightly decreased than pure PEEK. This finding is similar to those observed in p-MWNTs / PEEK composites.

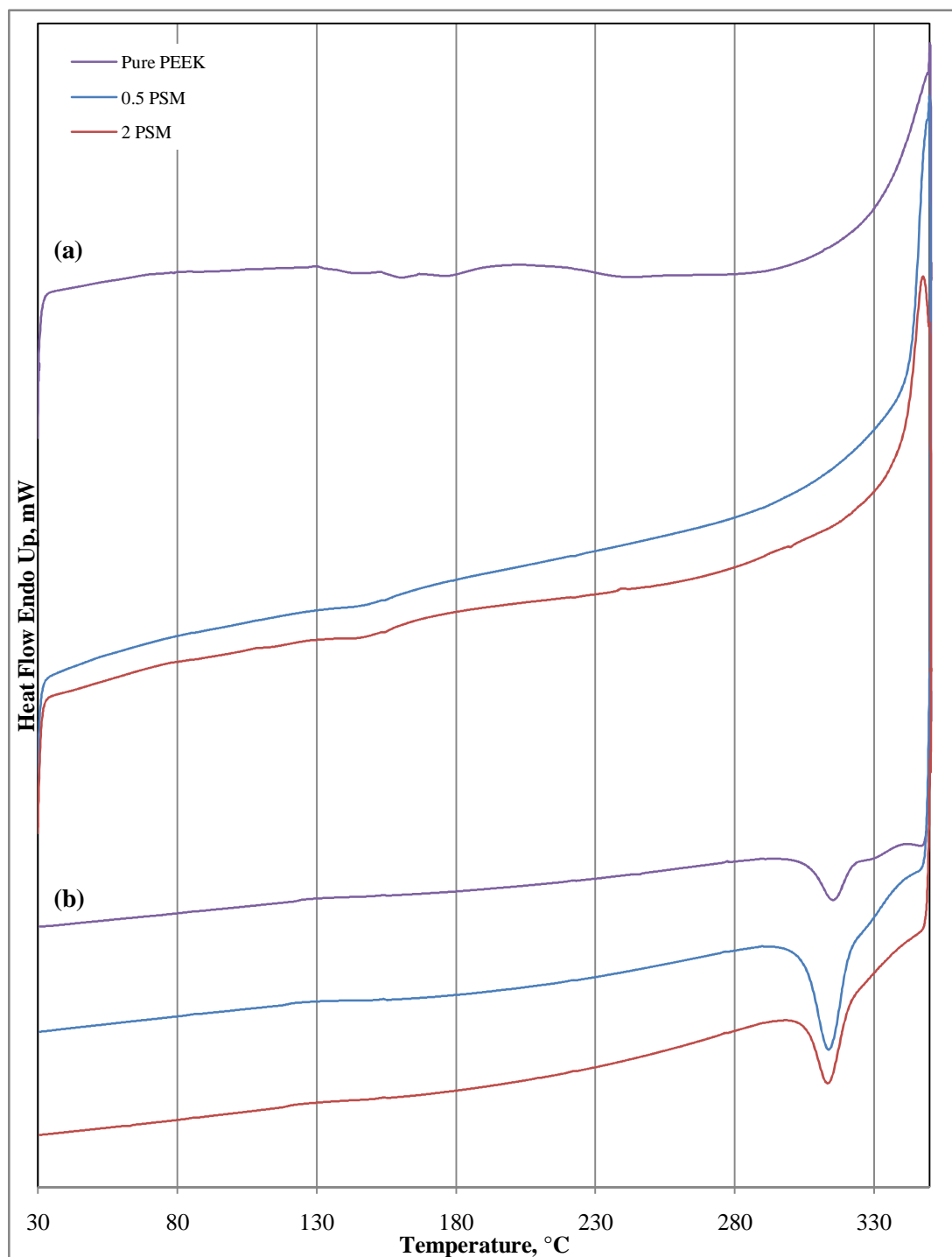


Figure 4.18: DSC scans of SPEEK-MWNTs / PEEK composites. (a) Heating and (b) cooling curves.

Table 4.4 shows the data obtained from DSC analysis where the values of  $H_c$  increase with increasing of SPEEK-MWNTs loading from 0 to 2%. The degree of crystallinity also increases with increasing of SPEEK-MWNTs loading. This shows

similar pattern of result as that of ox-MWNTs / PEEK composites. These increasing of  $H_c$  and degree of crystallinity are due to the restricted movements of polymer chains by the inorganic components [30]. It is also observed that addition of SPEEK-MWNTs has more effect on the  $T_g$ ,  $T_m$ ,  $T_c$  and  $H_c$  as compared to those using p-MWNTs as fillers yet does not improving more than that of ox-MWNTs / PEEK composites. Yang et al. [29] reported that the  $T_g$ 's of a polymer are dependant to the free volume of the polymer that correlated with the similarity between the filler and polymer matrix. Thus, SPEEK-MWNTs is suggested as a more suitable filler than p-MWNTs in enhancing the crystallization of PEEK.

Table 4.4: DSC data of SPEEK-MWNTs / PEEK Composites

| Material | $T_g$ (°C) | $T_m$ (°C) | $T_c$ (°C) | $\Delta H_c$ (J/g) | $(1-\lambda)_c$ (%) |
|----------|------------|------------|------------|--------------------|---------------------|
| PEEK     | 156.38     | 349.10     | 315.25     | 25.52              | 19.63               |
| 0.5 SMP  | 153.80     | 349.20     | 313.97     | 34.37              | 26.57               |
| 2 SMP    | 153.75     | 349.55     | 313.67     | 33.46              | 26.26               |

#### 4.4 Mechanical Properties of PEEK Composites

Table 4.5 shows that the Young's Modulus of p-MWNTs / PEEK and ox-MWNTs / PEEK composites increases as MWNTs loading was increased. The increment is expected since the Young's Modulus of MWNT is in range of 270 to 950 GPa. Incorporation of SPEEK-MWNTs in PEEK matrix however does not show any rise of Young's Modulus. Bhattacharyya et al. [40] prepared 1% SWNTs / PP nanocomposites by melt blending and reported unaffected mechanical properties with the presence of SWNTs. Bhattacharyya et al. [40] also suggested that large nanotubes aggregates nullify the effect of providing effective reinforcement.

Vega et al. [41] stated that good dispersion and adequate adhesion between the filler and the matrix are indicated by good mechanical properties. According to

previous studies, tensile strength and modulus enhancements are continually reported by Andrews and Weisenberger [39]. However, very little of the data achieve reinforcement predicted by a rule of mixtures approach especially at loadings beyond 10 vol.%.

Table 4.5: Mechanical properties of PEEK and MWNTs / PEEK Composites

| Sample    | Young's Modulus, E (GPa) | % Increment      |
|-----------|--------------------------|------------------|
| Pure PEEK | 3.962                    | <i>reference</i> |
| 0.5 MP    | 4.183                    | 5.58             |
| 2 MP      | 4.563                    | 15.17            |
| 0.5 OMP   | 4.211                    | 6.28             |
| 2 OMP     | 4.687                    | 18.30            |
| 0.5 SMP   | 4.001                    | 0.98             |
| 2 SMP     | 4.012                    | 1.26             |

Song et al. [70] observed ~40% increment in Young's Modulus of the sandwich-like SWNTs / PEEK composites as compared to the pure PEEK. Meanwhile, only slight improvement (4%) in the failure strength was observed. The SWNTs is in the form of a film and as more layers of SWNT film was incorporated to the PEEK film, some air bubbles were detected in the composites. This is one of the defects which resulted in pre-fracture of materials. Despite the defects, the mechanical properties of the composites are still better than neat PEEK. In another study, addition of MWNTs resulted in increase in the elastic modulus and the yield strength but decrease in the failure strain. The tensile modulus of composites containing 15 wt% MWNTs is 89% higher than that of pure PEEK [3], and they concluded that the incorporation of MWNTs is more effective in improving the mechanical properties of polymer above its glass transition temperature.

Nayak et al. [6] reported that the composites prepared using MWNTs and PEEK / liquid crystalline polymer (LCP) blend show better mechanical properties as compared to the pure PEEK / LCP blend. When 1 wt% MWNTs and functionalized



MWNTs were added to the polymer blend, Young's Modulus increases by 9% and 12%, respectively. Furthermore, the tensile strength increases by 12.5% and 38% respectively. However, the elongation at break decreases from 19.8% to 9.1% and 5.2%, respectively. This may be due to a decrease in ductility of the polymer blend as a result from incorporation of MWNTs to the polymer blend. The changes in crystallinity of the polymer affect the mechanical properties and permeability of the semicrystalline polymer.

## CHAPTER 5

### CONCLUSIONS AND RECOMMENDATIONS

#### 5.1 Conclusions

In this work, MWNTs were incorporated with PEEK polymer to form MWNTs/PEEK composite. The MWNTs were also functionalized via chemical modification to study the effect of different surface properties of the MWNTs to the morphology, thermal and mechanical properties of the MWNTs/PEEK composites.

The main finding of this research is the functionalized MWNTs. Several testing were done to conform that the MWNTs is successfully functionalized. SPEEK-MWNTs were in shorter length and were wrapped by a layer of polymer when probed with FE-SEM. Structural properties are further confirmed by TEM giving the diameter of SPEEK-MWNTs is in range of 7 to 15 nm with approximately 3.2 nm of wall thickness. Hence, MWNTs were successfully grafted with respective SPEEK. XRD patterns show no noticeable alteration was detected on the structure of the MWNTs. The second result for the MWNTs was tested using TGA. It is concluded that MWNTs are stable thermally in nitrogen at below 1000°C as agreed in previous researches.

The MWNTs were incorporated in PEEK matrix to study the effect of functionalization towards MWNTs. Structural properties by FE-SEM reveal that the dispersion of MWNTs is much improved after oxidation process and functionalization with SPEEK. The XRD patterns also have been tested to make sure the composites were successfully fabricated. It is found that the peaks of composites were similar with previous researchers. Results showed the crystallinity

of PEEK increased with small addition of MWNTs. This was confirmed with the DSC scans where the degree of crystallinity increased.

The second characteristic of the composites were tested using TGA. In this testing, pure PEEK has one stage of decomposition where dehydration takes place at the initial process. The onset decomposition of all the composites was consistent around 585°C and no large gap found. DSC scans were done on the composites and consistent results of glass transition temperature, melting temperature and crystallization temperature at 156°C, 349°C and 315°C respectively. However, the heat of crystallization increased reveals the increment of degree of crystallinity of the composites. Finally, the mechanical properties showed relatively no improvement even after the SPEEK-MWNTs is added to the polymer matrix. However, the optimum SPEEK amount of MWNTs is 2% where Young's Modulus increased as 21% for 2% ox-MWNTs / PEEK composites.

This study has successfully developed ox-MWNTs and SPEEK-MWNTs using chemical modification method. This research indicates the need for more study on polymer composites for industrial application especially using PEEK as polymer matrix. Additionally, the research demonstrates the need to determine not only the morphology, thermal properties and mechanical properties of the functionalized MWNTs / PEEK composites, but also its fire retardancy. The result would be more pleasant if variety of functionalized MWNTs could be developed and its application can be characterized owing to the interfacial interaction between functionalized MWNTs and PEEK.

## **5.2 Recommendations**

Future work should be focused on fire retardancy of the composites and also the photochemical behavior to understand more about the product. Mechanical properties shall be in more detail. On the other hand, it is possible to fabricate the composites using various methods in order to study the effect of fabrication method on the properties of the composites. It was proved that using other fabrication

method may affect the properties of particular polymer utilized as matrix. Therefore, it would be beneficial to develop polymers that have optimum condition. On top of that, other similar character of polymers shall be utilized to reconfirm the properties to be study. Moreover, smaller intervals of amount of carbon nanotubes could be set up to support the achievement of the product using variety of concentrations of polymers / fillers. On the other hand, MWNTs functionalized with other functional groups such as 4-phenylaniline could be studied in order to observe their effects on the polymer matrix.

## REFERENCES

- [1] M. M. Rabbani, C. H. Ko, J.-S. Bae, J. H. Yeum, S. Kim and W. Oh, "Comparison of some gold/carbon nanotube composites prepared by control of electrostatic interaction," *Colloids and Surfaces A: Physicochemical and Engineering Aspects*, vol. 336, pp. 183-186, 2009.
- [2] H. Z. Geng, R. Rosen, B. Zheng, H. Shimoda, L. Fleming, J. Liu, and O. Zhou, "Fabrication and Properties of Composites of Poly(ethylene oxide) and Functionalized Carbon Nanotubes," *Advanced Material*, vol. 14, no. 19, pp. 1387-1390, October 2002.
- [3] F. Deng, T. Ogasawara and N. Takeda, "Tensile Properties at Different Temperature and Observation of Micro Deformation of Carbon Nanotubes-Poly(Ether Ether Ketone) Composites," *Composites Science and Technology*, vol. 67, pp. 2959-2964, 2007.
- [4] P. Patel, T. R. Hull, R. W. McCabe, D. Flath, J. Grasmeder and M. Percy, "Mechanism of Thermal Decomposition of Poly(Ether Ether Ketone) (PEEK) from A Review of Decomposition Studies," *Polymer Degradation and Stability*, vol. 95, pp. 709-718, January 2010.
- [5] A. M. Diez-Pascual, M. Naffakh, M. A. Gomez, C. Marco, G. Ellis, M. T. Martinez, A. Anson, J. M. Gonzalez-Dominguez, Y. Martinez-Rubi and B. Simard, "Development and Characterization of PEEK/Carbon Nanotube Composites," *Carbon*, vol. 47, pp. 3079-3090, July 2009.
- [6] G. C. Nayak, R. Rajasekar, S. Bose And C. K. Das, "Effect of MWNTs and SiC-Coated MWNTs on Properties of PEEK/ LCP Blend," *J. Nanotechnology*, vol. 2009, article ID 759374, September 2009.
- [7] P. Werner, V. Altstädt, R. Jaskulka, O. Jacobs, J. K. W. Sandler, M. S. P. Shaffer and A. H. Windle, "Tribological Behavior of Carbon-Nanofibre-Reinforced Poly(Ether Ether Ketone)," *Wear*, vol. 257, pp. 1006-1014, July 2004.

- [8] K. Fujihara, Z.-M. Huang, S. Ramakrishna and H. Hamada, "Influence of Processing Conditions on Bending Property of Continuous Carbon Fiber Reinforced PEEK Composites," *Composites Science And Technology*, vol. 64, no. 16, pp. 2525-2534, July 2004.
- [9] M. R. Babaa, J.-L. Bantignies, L. Alvarez, P. Parent, F. Le Normand, M. Gulas, J. Mane Mane, P. Poncharal And B. Doyle, "NEXAFS Study of Multiwalled Carbon Nanotubes Functionalization with Sulfonated Poly(Ether Ether Ketone) Chains," *J. Nanosci. Nanotechnol.*, vol. 7, pp. 1-5, 2007.
- [10] M. C. Gupta and A. P. Gupta, "Introduction", "Polymer Matrix Materials" and "Fabrication of Polymer Composites" in *Polymer Composite*, New Delhi: New Age International (P) Limited, 2005, pp. 1-107.
- [11] The Society of the Plastic Industry, Inc. (2005, January). Plastics in Aerospace: the Right Stuff. *The IAPD Magazine* [Online]. Available: <http://www.theiapdmagazine.com/pdf/magazine-archives/224.pdf>.
- [12] W. Tang, M. H. Santare and S. G. Advani, "Melt Processing and Mechanical Property Characterization of Multi-Walled Carbon Nanotube/High Density Polyethylene (MWNT/HDPE) Composite Films," *Carbon*, vol. 41, pp. 2779-2785, August 2003.
- [13] S. G. Advani, *Processing and Properties of Nanocomposites*. USA:World Scientific, 2007, pp. 61-98.
- [14] P. Singh, R. M. Tripathi and A. Saxena, "Synthesis of Carbon Nanotubes and Their Biomedical Application," *J. Optoelectronics and Biomedical Materials*, vol. 2, pp. 91-98, June 2010.
- [15] Y. J. Kim, T. S. Shin, H. D. Choi, J. H. Kwon, Y.-C. Chung and H. G. Yoon, "Electrical Conductivity of Chemically Modified Multiwalled Carbon Nanotubes/Epoxy Composites," *Carbon*, vol. 43, pp. 23-30, 2005.
- [16] Q. Cheng, J. Wang, K. Jiang, Q. Li and S. Fan, "Fabrication and Properties of Aligned Multiwalled Carbon Nanotubes-Reinforced Epoxy Composites," *J. Material Res.*, vol. 23, no. 11, pp. 2975-2983, Nov 2008.
- [17] B. Viswanathan, "Composite Materials," *Nanomaterials*, 1st ed., U.K.:Alpha Science, 2009, ch. 12, pp. 12.1-12.15.

- [18] J. Shen, W. Huang, L. Wu, Y. Hu and M. Ye, "The Reinforcement Role of Different Amino-Functionalized Multi-Walled Carbon Nanotubes in Epoxy Nanocomposites," *Composites Science and Technology*, vol. 67, pp. 3041-3050, May 2007.
- [19] J. N. Coleman, U. Khan, W. J. Blau and Y. K. Gun'ko, "Small But Strong: A Review of the Mechanical Properties of Carbon Nanotubes-Polymer Composite," *Carbon*, vol. 44, pp. 1624-1652, 2006.
- [20] Y. Zhao, Z. Qiu and W. Yang, "Effect of Functionalization of Multiwalled Nanotubes on the Crystallization and Hydrolytic Degradation of Biodegradable Poly(L-lactide)," *J. Phys. Chem. B.*, vol. 112, pp. 16461-16468, September 2008.
- [21] S. Choi, Y. Jeong, G. -W. Lee and D. H. Cho, "Thermal and Mechanical Properties of Polypropylene Filaments Reinforced with Multiwalled Carbon Nanotubes Via Melt Compounding," *Fibers And Polymers*, vol. 10, no. 4, pp. 513-518, May 2009.
- [22] P. M. Ajayan and J. M. Tour. (2007, June 28). Nanotube Composites. *Nature*. vol. 447, pp. 1066-1068.
- [23] S. Reich, C. Thomsen and J. Maultzsch, "Introduction" In *Carbon Nanotubes: Basic Concepts and Physical Properties*, Germany: Wiley, 2004, pp. 1-2.
- [24] M. S. Dresselhaus, G. Dresselhaus and Ph. Avouris, "Introduction to Carbon Materials Research" in *Carbon Nanotubes: Synthesis, Structure, Properties and Applications*, New York: Springer, 2000, pp. 1-10.
- [25] S. Banerjee and S. S. Wong, "In Situ Quantum Dot Growth on Multiwalled Carbon Nanotubes," *J. Am. Chem. Soc.*, vol. 125, no. 34, pp. 10342-10350, May 2003.
- [26] Y. Bin, M. Kitanaka, D. Zhu and M. Matsuo, "Development of Highly Oriented Polyethylene Filled With Aligned Carbon Nanotubes By Gelation/Crystallization From Solutions," *Macromolecules*, vol. 36, pp. 6213-6219, May 2003.
- [27] R. Haggenueller, J. E. Fischer and K. I. Winey, "Single Wall Carbon Nanotubes/Polyethylene Nanocomposites: Nucleating and Templating Polyethylene Crystallites," *Macromolecules*, vol. 39, pp. 2964-2971, 2006.

- [28] M. Trujillo, M. L. Arnal, A. J. Müller, St. Bredeau, D. Bonduel, Ph. Dubois, I. W. Hamley and V. Castelletto, "Thermal Fractionation and Isothermal Crystallization of Polyethylene Nanocomposites Prepared by In Situ Polymerization," *Macromolecules*, vol. 41, pp. 2087-2095, January 2008.
- [29] K. Yang, M. Gu and Y. Pin, "Cure Behavior and Thermal Stability Analysis of Multiwalled Carbon Nanotubes/Epoxy Resin Nanocomposites," *Journal of Applied Polymer Science*, vol. 110, pp. 2980-2988, June 2008.
- [30] C.-F. Kuan, W.-J. Chen, Y.-L. Li, C.-H. Chen, H.-C. Kuan and C.-L. Chiang, "Flame Retardance and Thermal Stability of Carbon Nanotubes Epoxy Composite Prepared From Sol-Gel Method," *Journal of Physics and Chemistry Of Solids*, vol. 71, pp. 539-543, 2010.
- [31] X.-B. Yan, Z.-J. Han, Y. Yang and B.-K. Tay, "Fabrication of Carbon Nanotubes-Polyaniline Composites via Electrostatic Adsorption in Aqueous Colloids," *J. Phys. Chem. C*, vol. 111, pp. 4125-4131, 2007.
- [32] K. Babooram and R. Narain, "Fabrication of SWNT/Silica Composites by the Sol-Gel Process," *ACS Applied Materials & Interfaces*, vol. 1, no. 1, pp. 181-186, 2009.
- [33] S. Bal and S. S. Samal, "Carbon Nanotubes Reinforced Polymer Composites-A State of the Art," *Bull. Material Science*, vol. 30, no. 4, pp. 379-386, August 2007.
- [34] K. Mylvaganam and L. C. Zhang, "Nanotubes Functionalization and Polymer Grafting: An Ab Initio Study," *J. Phys. Chem. B.*, vol. 108, pp. 15009-15012, August 2004.
- [35] M. Endo, R. Saito, M. S. Dresselhaus and G. Dresselhaus, "From Carbon Fibres to Nanotubes," in *Carbon Nanotubes (Preparation and Properties)*, Boca Raton, Florida: CRC Press Inc., 1997, ch. 2, pp. 35-110.
- [36] J. B. Bai and A. Allaoui, "Effect of the Length and the Aggregate Size of MWNTs on the Improvement Efficiency of the Mechanical and Electrical Properties of Nanocomposites-Experimental Investigation," *Composites Part A: Applied Science and Manufacturing*, vol. 34, pp. 689-694, April 2003.



- [37] S. J. Park, S. T. Lim, M. S. Cho, H. M. Kim, J. Joo and H. J. Choi, "Electrical Properties Of Multi-Walled Carbon Nanotubes/Poly(Methyl Methacrylate) Nanocomposite," *Current Applied Physics*, vol. 5, pp. 302-304, May 2005.
- [38] J. N. Coleman, M. Cadek, R. Blake, V. Nicolosi, K. P. Ryan, C. Belton, A. Fonseca, J. B. Nagy, Y. K. Gun'ko and W. J. Blau, "High-Performance Nanotube-Reinforced Plastics: Understanding the Mechanism of Strength Increase," *Advanced Functional Materials*, vol. 14, no. 8, pp. 791-798, 2004.
- [39] A. Andrews and M. C. Weisenberger, "Carbon Nanotube Polymer Composites," *Current Opinion In Solid State & Materials Science*, vol. 8, pp. 31-37, 2004.
- [40] A. R. Bhattacharyya, T. V. Sreekumar, L. Tao, S. Kumar, L. M. Ericson, R. H. Hauge and R. E. Smalley, "Crystallization and Orientation Studies in Polypropylene/Single Wall Carbon Nanotubes Composite," *Polymer*, vol. 44, pp. 2373-2377, January 2003.
- [41] J. F. Vega, J. Martínez-Salazar, M. Trujillo, M. L. Arnal, A. J. Müller, S. Bredeau and Ph. Dubois, "Rheology, Processing, Tensile Properties and Crystallization of Polyethylene/Carbon Nanotubes Nanocomposites," *Macromolecules*, vol. 42, pp. 4719-4727, May 2009.
- [42] F. Hennrich, C. Chan, V. Moore, M. Rolandi and M. O'Connell, "The Element Carbon," in *Carbon Nanotubes (Properties and Applications)*, Boca Raton, Florida: CRC Press, 2006, ch. 1, pp. 1-18.
- [43] S. Iijima, "Helical Microtubules of Graphitic Carbon," *Nature*, vol. 354, pp. 56-58, 1991.
- [44] R. Streicher, "Carbon Nanotubes: Applications for Medical Devices," in *Carbon Nanotubes: Angels or Demons?*, Singapore: Pan Stanford Publishing, 2008, ch. 4, pp. 61-103.
- [45] A. Loiseau, P. Launois, P. Petit, S. Roche And J. -P. Salvetat, *Understanding Carbon Nanotubes: From Basics To Application*. Germany: Springer-Verlag, 2006, Preface.
- [46] D. Mann, "Synthesis of Carbon Nanotubes," in *Carbon Nanotubes (Properties and Applications)*, Boca Raton, Florida: CRC Press, 2006, ch. 2, pp. 19-49.

- [47] H. Dai, "Nanotube Growth and Characterization," in *Carbon Nanotubes*, Berlin Heidelberg: Springer-Verlag, 2001, pp. 29-53.
- [48] A. M. Rao and K. McGuire, "Characterization Techniques in Carbon Nanotube Research," in *Carbon Nanotubes: Science and Applications*, Boca Raton, Florida: CRC Press, 2004, ch. 5, pp. 117-136.
- [49] R. L. Vander Wal, T. M. Ticich and V. E. Curtis, "Diffusion Flame Synthesis of Single-Walled Carbon Nanotubes," *Chem. Phys. Lett.*, vol. 323, no. 3, pp. 217-223, June 2000.
- [50] K. Suggs and X.-Q. Wang, "Structural and Electronic Properties of Carbon Nanotubes-Reinforced Epoxy Resins," *Nanoscale*, vol. 2, pp. 385-388, 2010.
- [51] Z. L. Yao, N. Braidy, G. A. Botton and A. Adronov, "Polymerization from the Surface of Single-Walled Carbon Nanotubes – Preparation and Characterization of Nanocomposites," *Journals of the American Chemical Society*, vol. 125, no. 51, pp. 16015-16024, July 2003.
- [52] C. Zhao, L. Ji, H. Liu, G. Hu, S. Zhang, M. Yang and Z. Yang, "Functionalized Carbon Nanotubes Containing Isocyanate Groups," *J. of Solid State Chemistry*, vol. 177, pp. 4394-4398, November 2004.
- [53] Q. Shi, D. Yang, Y. Su, J. Li, Z. Jiang, Y. Jiang and W. Yuan, "Covalent functionalization of multi-walled carbon nanotubes by lipase," *Journal of Nanoparticle Research*, vol. 9, no. 6, pp. 1205-1210, 2007.
- [54] M. Jung, M. Huh, Y. Park, S. Kang, R. Russell, P. Holden and S. Yun, "Effect of CNT Functionalization on the Structure and Properties of Poly(3-Hydroxybutyrate)/MWCNT Biocomposites," presented at the 18<sup>th</sup> International Conference on Composite Materials, ICC Jeju, Korea, August 21-26, 2011, Paper M03-4.
- [55] S. Chen, W. Shen, G. Wu, D. Chen and M. Jiang, "A New Approach to the Functionalization of Single-Walled Carbon Nanotubes with Both Alkyl and Carboxyl Groups," *Chem. Phys. Lett.*, vol. 402, no. 4-6, pp. 312-317, January 2005.
- [56] J. Zhao, J.-P. Lu, J. Han and C.-K. Yang, "Non-covalent Functionalization of Carbon Nanotubes by Aromatic Organic Molecules," *Applied Physics Letters*, vol. 82, no. 21, pp. 3746-3748, May 2003.

- [57] A. Jorio, E. Kauppinen and A. Hassanien, "Carbon-Nanotube Metrology," in *Carbon Nanotubes: Advanced Topics in the Synthesis, Structure, Properties and Applications*, Berlin Heidelberg: Springer-Verlag, vol. 111, 2008, pp. 63-100.
- [58] C. Pirlot, I. Willems, A. Fonseca, J.B.Nagy and J.Delhalle, "Preparation and Characterization of Carbon Nanotube/Polyacrylonitrile Composites," *Advanced Eng. Materials*, vol. 4, no. 3, 2002.
- [59] S. L. Ruan, P. Gao, X. G. Yang and T. X. Yu, "Toughening High Performance Ultrahigh Molecular Weight Polyethylene Using Multiwalled Carbon Nanotubes," *Polymer*, vol. 44, pp. 5643-5654, July 2003.
- [60] B. Qu, Y.-T. Xu, S.-J. Lin, Y.-F. Zheng and L.Z. Dai, "Fabrication of Pt Nanoparticles Decorated PPy-MWNTs Composites and Their Electrocatalytic Activity for Methanol Oxidation," *Synthesis Metals*, vol. 160, pp. 732-742, February 2010.
- [61] W. Chen, M. L. Auad, R. J. J. Williams and S. R. Nutt, "Improving the Dispersion and Flexural Strength of Multiwalled Carbon Nanotubes-Stiff Epoxy Composites Through  $\beta$ -Hydroxyester Surface Functionalization Coupled With the Anionic Homopolymerization of the Epoxy Matrix," *European Polymer J.*, vol. 42, pp. 2765-2772, 2006.
- [62] J. Li, L. Tong, Z. Fang, A. Gu And Z. Xu, "Thermal Degradation Behavior of Multi-Walled Carbon Nanotubes/Polyamide 6 Composites," *Polymer Degradation and Stability*, vol. 91, pp. 2046-2052, September 2006.
- [63] T. Kashiwagi, E. Grulke, J. Hilding, R. Harris, W. Awad and J. Douglas, "Thermal Degradation and Flammability Properties of Poly(Propylene)/Carbon Nanotubes Composites," *Macromolecular Rapid Communications*, vol. 23, pp. 761-765, August 2002.
- [64] S. J. Park, M. S. Cho, S. T. Lim, H. J. Choi and M. S. Jhon, "Synthesis and Dispersion Characteristics of Multi-Walled Carbon Nanotubes Composite With Poly(Methyl Methacrylate) Prepared by In-Situ Bulk Polymerization," *Molecular Rapid Commun.*, vol. 24, pp. 1070-1073, 2003.
- [65] J. Li, Y. Lu, Q. Ye, M. Cinke, J. Han, and M. Meyyappan, "Carbon Nanotube Sensors for Gas and Organic Vapor Detection," *Nano Lett.*, vol. 3, pp. 929-933, 2003.

- [66] Y. Cheng and O. Zhou, "Electron Field Emission From Carbon Nanotubes," *Comptes Rendus Physique*, vol. 4, pp. 1021-1033, 2003.
- [67] P. Sarrazin, D. Blake, L. Delzeit, M. Meyyappan, B. Boyer, S. Snyder and B. Espinosa, "Carbon-Nanotube Field Emission X-Ray Tube for Space Exploration XRD/XRF Instrument," *JCDPS-International Centre for Diffraction Data 2004, Advances in X-Ray Analysis*, vol. 47, pp. 232-239, 2004.
- [68] L. H. Sperling, "Introduction to Polymer Science," in *Introduction of Physical Science Polymer*, 4th ed. Hoboken, New Jersey: John Wiley & Sons Inc., 2006, ch. 1, pp. 1-56.
- [69] J. Yin, A. Zhang, K. Y. Liew and L. Wu, "Synthesis of PEEK Assisted by Microwave Irradiation and Its Characterization," *Polymer Bulletin*, vol. 61, pp. 157-163, 2008.
- [70] L. Song, H. Zhang, Z. Zhang and S. Xie, "Processing and Performance Improvements of SWNT Paper Reinforced PEEK Nanocomposites," *Composites Part A: Applied Science and Manufacturing*, vol. 38, no. 2, pp. 388-392, January 2007.
- [71] W. Yin, P. Irwin and D. Schweickart, "Dielectric Breakdown of Polymeric Insulations Aged at High Temperatures," *IEEE Int. Power Modulators and High Voltage Conf., Proc. of the 2008*, pp. 537-542, May, 2008.
- [72] R. Walters and R. E. Lyon (2001, September), "Calculating Polymer Flammability from Molar Group Contributions," *U.S. Department of Transportation* [Online]. Available: <http://www.dtic.mil/cgi-bin/GetTRDoc?AD=ADA397200>.
- [73] P. D. Mangalgiri, "Composite Materials for Aerospace Applications," *Bulletin Material Science*, vol. 22, no. 3, pp. 657-664, May 1999.
- [74] V. K. Selvaraj, "Polymers and Fillers," in *Advanced Polymer Chemistry*, 1st ed. New Delhi: Campus Books, 2008, pp. 134-149.
- [75] A. K. Mikitaev, G. V. Kozlov and G. Zaikov, "The Nanocomposites, Filled by Carbon Nanotubes," in *Polymer Nanocomposites: Variety Of Structural Forms And Applications*, New York: Nova Science Publishers Inc., 2008, pp. 259-278.

- [76] K. Fujihara, Z. M. Huang, S. Ramakrishna, K. Satknanantham and H. Hamada, "Feasibility of Knitted Carbon / PEEK Composites for Orthopedic Bone Plates," *Biomaterials*, vol. 17, pp. 3877-3885, August 2004.
- [77] M. C. Kuo, C. M. Tsai, J. C. Huang and M. Chen, "PEEK Composites Reinforced By Nano-Sized SiO<sub>2</sub> and Al<sub>2</sub>O<sub>3</sub> Particulates," *Materials Chemistry and Physics*, vol. 90, pp. 185-195, 2005.
- [78] R. K. Goyal, Y. S. Negi and A. N. Tiwari, "Preparation of High Performance Composites Based on Aluminium Nitride / PEEK and Their Properties," *European Polymer Journal*, vol. 41, issue 9, September 2005.
- [79] J. P. Davim and R. Cardoso, "Tribological Behaviour of the Composite PEEK-CF30 at Dry Sliding against Steel Using Statistical Technology," *Material and Design*, vol. 27, issue 4, pp. 338-342, 2006.
- [80] H.-B. Qiao, Q. Guo, A. G. Tian, G.-L. Pan and L.-B. Xu, "A Study of Friction and Wear Characteristics of Nanometer Al<sub>2</sub>O<sub>3</sub> / PEEK Composites under the Dry Sliding Condition," *Tribology International*, vol. 40, issue 1, pp. 105-110, 2007.
- [81] R. K. Goyal, A. N. Tiwari, U. P. Mulik and Y. S. Negi, "Thermal Expansion Behaviour of High Performance PEEK Matrix Composites," *J. of Physics D: Applied Physics*, vol.41, no. 8, 2008.
- [82] D. S. Bangarusampath, H. Ruckdaschel, V. Altstadt, J. K. W. Sandler, D. Garraay and M. S. P. Shaffer, "Rheology and Properties of Melt-Processed PEEK / MWNT Composites," *Polymer*, vol. 50, issue 24, pp. 5803-5811, November 2009.
- [83] M. Mohiuddin and S. Van Hao, "Electrical Resistance of CNT - PEEK Composites under Compression at Different Temperatures," *Nanoscale Research Letters*, vol. 6, no. 419, 2011.
- [84] C. Vacogne and R. Wise, "Joining of High Performance Carbon Fibre / PEEK Composites," *Science and Technology of Welding and Joining*, vol. 16, no. 4, pp. 369-396, May 2011.

- [85] T. Ogasawara, T. Tsuda and N. Takeda, "Stress-Strain Behaviour of MWNT / PEEK Composites," *Composites Science and Technology*, vol. 71, issue 2, pp. 73-78, January 2011.
- [86] T. Tsuda, T. Ogasawara, F. Deng and N. Takeda, "Direct Measurements of Interfacial Shear Strength of MWNTs / PEEK Composite Using a Nano-Pullout Method," *Composite Science and Technology*, vol. 71, issue 10, pp. 1295-1300, July 2011.
- [87] Y.-J. Choi, S.-H. Hwang, Y. S. Hong, J.-Y. Kim, C.-Y. Ok, W. Huh and S.-W. Lee, "Preparation and Characterization of Ps/Multi-Walled Carbon Nanotubes Nanocomposites," *Polymer Bulletin*, vol. 53, pp. 393-400, February 2005.
- [88] G. Mago, F. T. Fisher and D. M. Kalyon, "Effect of Multiwalled Carbon Nanotubes on the Shear-Induced Crystallization Behavior of Poly(Butylenes Terephthalate)," *Macromolecules*, vol. 41, pp. 8103-8113, September 2008.
- [89] F. Du, J. E. Fischer, and K. I. Winey, "Coagulation Method For Preparing Single-Walled Carbon Nanotube / Poly (Methyl Methacrylate) Composites and Their Modulus, Electrical Conductivity And Thermal Stability," *J. of Polymer Science: Part B: Polymer Physics*, vol. 41, pp. 3333-3338, July 2003.
- [90] I. V. Dolbin, A. I. Burya and G. V. Kozlov, "The Structure and Thermal Stability of Polymer Materials: A Fractal Model," *High Temperature*, vol. 45, no. 3, pp. 313-316, 2007.
- [91] T. E. Chang, L. R. Jensen, A. Kisliuk, R. B. Pipes, R. Pyrz and A. P. Sokolov, "Microscopic Mechanism of Reinforcement in Single-Wall Carbon Nanotubes/Polypropylene Nanocomposite," *Polymer*, vol. 46, pp. 439-444, 2005.
- [92] V. Leon, R. Parret, R. Almairac, L. Alvarez, M.-R. Babaa, B. P. Doyle, P. Lenny, P. Parent, A. Zahab and J.-L. Bantignies, "Spectroscopic Study of Double-Walled Carbon Nanotube Functionalization for Preparation of Carbon Nanotube / Epoxy Composites," *Carbon*, In Press. Available: <http://dx.doi.org/10.1016/j.carbon.2012.06.007>.
- [93] R. Y. M. Huang, P. Shao, C. M. Burns and X. Feng, "Sulfonation of Poly(Ether Ether Ketone) (PEEK): Kinetic Study and Characterization," *J. of Applied Polymer Science*, vol. 82, pp. 2652-2660, January 2001.

- [94] K. Safarova, A. Dvorak, R. Kubinek and M. Vujtek, "Usage of AFM, SEM and TEM for the Research of Carbon Nanotubes," *Modern Research and Educational Topics in Microscopy*, vol. 2, pp. 513–519, 2007.
- [95] F.-C. Chiu and G.-F. Kao, "Polyamide 46/Multi-walled Carbon Nanotube Nanocomposites with Enhanced Thermal, Electrical, and Mechanical Properties," *Composites: Part A*, vol. 43, pp. 208-218, 2012.
- [96] N. G. Sahoo, Y. C. Jung, H. H. So and J. W. Cho, "Synthesis of Polyurethane Nanocomposites of Functionalized Carbon Nanotubes by *In-Situ* Polymerization Methods," *J. of the Korean Physical Society*, vol. 51, pp. S1-S6, July 2007.
- [97] H. Zeng, C. Gao, Y. Wang, P. C. P. Watts, H. Kong, X. Cui and D. Yan, "In Situ Polymerization Approach To Multiwalled Carbon Nanotubes-Reinforced Nylon 1010 Composites: Mechanical Properties and Crystallization Behavior," *Polymer*, vol. 47, pp. 113-122, 2006.
- [98] M. Lai, J. Li, J. Yang, J. Liu, X. Tong and H. Cheng, "The Morphology and Thermal Properties of Multi-Walled Carbon Nanotube and Poly(Hydroxybutyrate-co-hydroxyvalerate) Composite," *Polymer Int.*, vol. 53, pp. 1479-1484, February 2004.
- [99] G. S. Rani, M. K. Beera and G. Pugazhenthii, "Development of Sulphonated Poly (Ether Ether Ketone) / Zirconium Titanium Phosphate Composite Membranes for Direct Methanol Fuel Cell," *J. of Applied Polymer Science*, vol. 124, pp. E45-E56, 2012.
- [100] S. Ali, N. A. Mohd Zabidi and D. Subbarao, "Correlation between Fischer-Tropsch Catalytic Activity and Composition of Catalysts," *Chemistry Central Journal*, vol. 5, no. 68, pp. 1-8, 2011.
- [101] J. Zhang, H. Zou, Q. Qing, Y. Yang, Q. Li, Z. Liu, X. Guo and Z. Du, "Effect of Chemical Oxidation on the Structure of SWNTs," *J. Phys. Chem. B*, vol. 107, no. 16, pp. 3712-3718, 2003.





## APPENDIX A

### MSDS 1,6-HEXANEDIAMINE (HDA)



## SAFETY DATA SHEET

according to Regulation (EC) No. 1907/2006

Version 5.0 Revision Date 24.04.2012

Print Date 13.02.2013

GENERIC EU MSDS - NO COUNTRY SPECIFIC DATA - NO OEL DATA

### 1. IDENTIFICATION OF THE SUBSTANCE/MIXTURE AND OF THE COMPANY/UNDERTAKING

#### 1.1 Product identifiers

Product name : Hexamethylenediamine

Product Number : H11696  
Brand : Aldrich  
Index-No. : 612-104-00-9  
CAS-No. : 124-09-4

#### 1.2 Relevant identified uses of the substance or mixture and uses advised against

Identified uses : Laboratory chemicals, Manufacture of substances

#### 1.3 Details of the supplier of the safety data sheet

Company : Sigma-Aldrich (M) Sdn. Bhd.  
A-07-11, Empire Office, Empire Subang  
Jalan SS16/1, SS16  
47500 SUBANG JAYA-SELANGOR DARUL EHSAN  
MALAYSIA  
  
Telephone : +60 (603) 563 53321  
Fax : +60 (603) 563 54116

#### 1.4 Emergency telephone number

Emergency Phone # :

### 2. HAZARDS IDENTIFICATION

#### 2.1 Classification of the substance or mixture

##### Classification according to Regulation (EC) No 1272/2008 [EU-GHS/CLP]

Acute toxicity, Dermal (Category 4)  
Acute toxicity, Oral (Category 4)  
Specific target organ toxicity - single exposure (Category 3)  
Skin corrosion (Category 1B)

##### Classification according to EU Directives 67/548/EEC or 1999/45/EC

Causes burns. Harmful in contact with skin and if swallowed. Irritating to respiratory system.

#### 2.2 Label elements

##### Labelling according Regulation (EC) No 1272/2008 [CLP]

Pictogram



Signal word : Danger

Hazard statement(s)

H302 : Harmful if swallowed.  
H312 : Harmful in contact with skin.  
H314 : Causes severe skin burns and eye damage.  
H335 : May cause respiratory irritation.

Precautionary statement(s)

P261 : Avoid breathing dust/ fume/ gas/ mist/ vapours/ spray.  
P280 : Wear protective gloves/ protective clothing/ eye protection/ face protection.

P305 + P351 + P338

IF IN EYES: Rinse cautiously with water for several minutes. Remove contact lenses, if present and easy to do. Continue rinsing.  
Immediately call a POISON CENTER or doctor/ physician.

P310

Supplemental Hazard  
Statements

none

**According to European Directive 67/548/EEC as amended.**

Hazard symbol(s)



R-phrases(s)

R21/22

Harmful in contact with skin and if swallowed.

R34

Causes burns.

R37

Irritating to respiratory system.

S-phrases(s)

S22

Do not breathe dust.

S26

In case of contact with eyes, rinse immediately with plenty of water and seek medical advice.

S36/37/39

Wear suitable protective clothing, gloves and eye/face protection.

S45

In case of accident or if you feel unwell, seek medical advice immediately (show the label where possible).

## 2.3 Other hazards - none

## 3. COMPOSITION/INFORMATION ON INGREDIENTS

### 3.1 Substances

Synonyms : 1,6-Diaminohexane  
1,6-Hexanediamine

Formula : C<sub>6</sub>H<sub>16</sub>N<sub>2</sub>

Molecular Weight : 116,20 g/mol

| Component                   |              | Concentration |
|-----------------------------|--------------|---------------|
| <b>Hexamethylenediamine</b> |              |               |
| CAS-No.                     | 124-09-4     | -             |
| EC-No.                      | 204-679-6    |               |
| Index-No.                   | 612-104-00-9 |               |

## 4. FIRST AID MEASURES

### 4.1 Description of first aid measures

#### General advice

Consult a physician. Show this safety data sheet to the doctor in attendance.

#### If inhaled

If breathed in, move person into fresh air. If not breathing, give artificial respiration. Consult a physician.

#### In case of skin contact

Take off contaminated clothing and shoes immediately. Wash off with soap and plenty of water. Consult a physician.

#### In case of eye contact

Rinse thoroughly with plenty of water for at least 15 minutes and consult a physician.

#### If swallowed

Do NOT induce vomiting. Never give anything by mouth to an unconscious person. Rinse mouth with water. Consult a physician.

- 4.2 Most important symptoms and effects, both acute and delayed**  
burning sensation, Cough, wheezing, laryngitis, Shortness of breath, spasm, inflammation and edema of the larynx, spasm, inflammation and edema of the bronchi, pneumonitis, pulmonary edema, Material is extremely destructive to tissue of the mucous membranes and upper respiratory tract, eyes, and skin.
- 4.3 Indication of any immediate medical attention and special treatment needed**  
no data available
- 

## **5. FIREFIGHTING MEASURES**

- 5.1 Extinguishing media**  
**Suitable extinguishing media**  
Use water spray, alcohol-resistant foam, dry chemical or carbon dioxide.
- 5.2 Special hazards arising from the substance or mixture**  
Carbon oxides, nitrogen oxides (NOx)
- 5.3 Advice for firefighters**  
Wear self contained breathing apparatus for fire fighting if necessary.
- 5.4 Further information**  
no data available
- 

## **6. ACCIDENTAL RELEASE MEASURES**

- 6.1 Personal precautions, protective equipment and emergency procedures**  
Use personal protective equipment. Avoid dust formation. Avoid breathing vapors, mist or gas. Ensure adequate ventilation. Evacuate personnel to safe areas. Avoid breathing dust.
- 6.2 Environmental precautions**  
Prevent further leakage or spillage if safe to do so. Do not let product enter drains. Discharge into the environment must be avoided.
- 6.3 Methods and materials for containment and cleaning up**  
Pick up and arrange disposal without creating dust. Sweep up and shovel. Keep in suitable, closed containers for disposal.
- 6.4 Reference to other sections**  
For disposal see section 13.
- 

## **7. HANDLING AND STORAGE**

- 7.1 Precautions for safe handling**  
Avoid contact with skin and eyes. Avoid formation of dust and aerosols. Provide appropriate exhaust ventilation at places where dust is formed.
- 7.2 Conditions for safe storage, including any incompatibilities**  
Store in cool place. Keep container tightly closed in a dry and well-ventilated place.  
Hygroscopic. Store under inert gas.
- 7.3 Specific end uses**  
no data available
- 

## **8. EXPOSURE CONTROLS/PERSONAL PROTECTION**

- 8.1 Control parameters**  
**Components with workplace control parameters**
- 8.2 Exposure controls**  
**Appropriate engineering controls**  
Handle in accordance with good industrial hygiene and safety practice. Wash hands before breaks and at the end of workday.

## Personal protective equipment

### Eye/face protection

Face shield and safety glasses Use equipment for eye protection tested and approved under appropriate government standards such as NIOSH (US) or EN 166(EU).

### Skin protection

Handle with gloves. Gloves must be inspected prior to use. Use proper glove removal technique (without touching glove's outer surface) to avoid skin contact with this product. Dispose of contaminated gloves after use in accordance with applicable laws and good laboratory practices. Wash and dry hands.

The selected protective gloves have to satisfy the specifications of EU Directive 89/686/EEC and the standard EN 374 derived from it.

Immersion protection

Material: Nitrile rubber

Minimum layer thickness: 0,4 mm

Break through time: > 480 min

Material tested: Camatril® (Aldrich Z677442, Size M)

Splash protection

Material: Nitrile rubber

Minimum layer thickness: 0,11 mm

Break through time: > 30 min

Material tested: Dermatril® (Aldrich Z677272, Size M)

data source: KCL GmbH, D-36124 Eichenzell, phone +49 (0)6659 873000, e-mail sales@kcl.de, test method: EN374

If used in solution, or mixed with other substances, and under conditions which differ from EN 374, contact the supplier of the CE approved gloves. This recommendation is advisory only and must be evaluated by an Industrial Hygienist familiar with the specific situation of anticipated use by our customers. It should not be construed as offering an approval for any specific use scenario.

### Body Protection

Complete suit protecting against chemicals, The type of protective equipment must be selected according to the concentration and amount of the dangerous substance at the specific workplace.

### Respiratory protection

Where risk assessment shows air-purifying respirators are appropriate use a full-face particle respirator type N100 (US) or type P3 (EN 143) respirator cartridges as a backup to engineering controls. If the respirator is the sole means of protection, use a full-face supplied air respirator. Use respirators and components tested and approved under appropriate government standards such as NIOSH (US) or CEN (EU).

---

## 9. PHYSICAL AND CHEMICAL PROPERTIES

### 9.1 Information on basic physical and chemical properties

- |  |  |
|--|--|
| a) Appearance                              | Form: solid<br>Colour: colourless      |
| b) Odour                                   | no data available                      |
| c) Odour Threshold                         | no data available                      |
| d) pH                                      | 12,4 at 100 g/l at 25 °C               |
| e) Melting point/freezing point            | Melting point/range: 42 - 45 °C - lit. |
| f) Initial boiling point and boiling range | 204 - 205 °C                           |
| g) Flash point                             | 80 °C - closed cup                     |
| h) Evaporation rate                        | no data available                      |
| i) Flammability (solid, gas)               | no data available                      |

|    |  |  |
|----|--|--|
| j) | Upper/lower flammability or explosive limits | Upper explosion limit: 6,3 %(V)<br>Lower explosion limit: 0,7 %(V) |
| k) | Vapour pressure                              | no data available  |
| l) | Vapour density                               | 4,01 - (Air = 1.0)   |
| m) | Relative density                             | 0,89 g/cm <sup>3</sup> at 25 °C                                    |
| n) | Water solubility                             | no data available  |
| o) | Partition coefficient: n-octanol/water       | log Pow: 0,02  |
| p) | Autoignition temperature                     | no data available  |
| q) | Decomposition temperature                    | no data available  |
| r) | Viscosity                                    | no data available  |
| s) | Explosive properties                         | no data available  |
| t) | Oxidizing properties                         | no data available  |

## 9.2 Other safety information

no data available

---

## 10. STABILITY AND REACTIVITY

### 10.1 Reactivity

no data available

### 10.2 Chemical stability

no data available

### 10.3 Possibility of hazardous reactions

no data available

### 10.4 Conditions to avoid

no data available

### 10.5 Incompatible materials

acids, Acid chlorides, Acid anhydrides, Strong oxidizing agents, Carbon dioxide (CO<sub>2</sub>)

### 10.6 Hazardous decomposition products

Other decomposition products - no data available

---

## 11. TOXICOLOGICAL INFORMATION

### 11.1 Information on toxicological effects

#### Acute toxicity

LD50 Oral - rat - 750 mg/kg

LD50 Dermal - rabbit - 1.110 mg/kg

#### Skin corrosion/irritation

no data available

#### Serious eye damage/eye irritation

no data available

#### Respiratory or skin sensitization

no data available

#### Germ cell mutagenicity

no data available

#### Carcinogenicity

IARC: No component of this product present at levels greater than or equal to 0.1% is identified as probable, possible or confirmed human carcinogen by IARC.

**Reproductive toxicity**

no data available

**Specific target organ toxicity - single exposure**

May cause respiratory irritation.

**Specific target organ toxicity - repeated exposure**

no data available

**Aspiration hazard**

no data available

**Potential health effects**

**Inhalation**

May be harmful if inhaled. Material is extremely destructive to the tissue of the mucous membranes and upper respiratory tract. Causes respiratory tract irritation.

**Ingestion**

Harmful if swallowed. Causes burns.

**Skin**

Harmful if absorbed through skin. Causes skin burns.

**Eyes**

Causes eye burns.

**Signs and Symptoms of Exposure**

burning sensation, Cough, wheezing, laryngitis, Shortness of breath, spasm, inflammation and edema of the larynx, spasm, inflammation and edema of the bronchi, pneumonitis, pulmonary edema, Material is extremely destructive to tissue of the mucous membranes and upper respiratory tract, eyes, and skin.

**Additional Information**

RTECS: MO1180000

---

**12. ECOLOGICAL INFORMATION**

**12.1 Toxicity**

Toxicity to fish LC50 - Leuciscus idus (Golden orfe) - 62 mg/l - 96 h

Toxicity to daphnia and other aquatic invertebrates EC50 - Daphnia magna (Water flea) - 23,4 mg/l - 48 h

**12.2 Persistence and degradability**

Biodegradability Result: 56 % - Partially biodegradable.

**12.3 Bioaccumulative potential**

no data available

**12.4 Mobility in soil**

no data available

**12.5 Results of PBT and vPvB assessment**

no data available

**12.6 Other adverse effects**

Harmful to aquatic life.

---

**13. DISPOSAL CONSIDERATIONS**

**13.1 Waste treatment methods**

**Product**

Offer surplus and non-recyclable solutions to a licensed disposal company. Dissolve or mix the material with a combustible solvent and burn in a chemical incinerator equipped with an afterburner and scrubber.

**Contaminated packaging**

Dispose of as unused product.



---

**14. TRANSPORT INFORMATION****14.1 UN number**

ADR/RID: 2280

IMDG: 2280

IATA: 2280

**14.2 UN proper shipping name**

ADR/RID: HEXAMETHYLENEDIAMINE, SOLID

IMDG: HEXAMETHYLENEDIAMINE, SOLID

IATA: Hexamethylenediamine, solid

**14.3 Transport hazard class(es)**

ADR/RID: 8

IMDG: 8

IATA: 8

**14.4 Packaging group**

ADR/RID: III

IMDG: III

IATA: III

**14.5 Environmental hazards**

ADR/RID: no

IMDG Marine pollutant: no

IATA: no

**14.6 Special precautions for user**

no data available

---

**15. REGULATORY INFORMATION**

This safety datasheet complies with the requirements of Regulation (EC) No. 1907/2006.

**15.1 Safety, health and environmental regulations/legislation specific for the substance or mixture**

no data available

**15.2 Chemical Safety Assessment**

no data available

---

**16. OTHER INFORMATION****Further information**

Copyright 2012 Sigma-Aldrich Co. LLC. License granted to make unlimited paper copies for internal use only.

The above information is believed to be correct but does not purport to be all inclusive and shall be used only as a guide. The information in this document is based on the present state of our knowledge and is applicable to the product with regard to appropriate safety precautions. It does not represent any guarantee of the properties of the product. Sigma-Aldrich Corporation and its Affiliates shall not be held liable for any damage resulting from handling or from contact with the above product. See [www.sigma-aldrich.com](http://www.sigma-aldrich.com) and/or the reverse side of invoice or packing slip for additional terms and conditions of sale.

---

## APPENDIX B

MSDS N,N'-DICYCLOHEXYLCARBODIIMIDE (DCC)



## SAFETY DATA SHEET

according to Regulation (EC) No. 1907/2006

Version 5.0 Revision Date 26.04.2012

Print Date 13.02.2013

GENERIC EU MSDS - NO COUNTRY SPECIFIC DATA - NO OEL DATA

### 1. IDENTIFICATION OF THE SUBSTANCE/MIXTURE AND OF THE COMPANY/UNDERTAKING

#### 1.1 Product identifiers

Product name : *N,N'*-Dicyclohexylcarbodiimide

Product Number : 36650  
Brand : Fluka  
Index-No. : 615-019-00-5  
CAS-No. : 538-75-0

#### 1.2 Relevant identified uses of the substance or mixture and uses advised against

Identified uses : Laboratory chemicals, Manufacture of substances

#### 1.3 Details of the supplier of the safety data sheet

Company : Sigma-Aldrich (M) Sdn. Bhd.  
A-07-11, Empire Office, Empire Subang  
Jalan SS16/1, SS16  
47500 SUBANG JAYA-SELANGOR DARUL EHSAN  
MALAYSIA  
  
Telephone : +60 (603) 563 53321  
Fax : +60 (603) 563 54116

#### 1.4 Emergency telephone number

Emergency Phone # :

### 2. HAZARDS IDENTIFICATION

#### 2.1 Classification of the substance or mixture

##### Classification according to Regulation (EC) No 1272/2008 [EU-GHS/CLP]

Acute toxicity, Dermal (Category 3)  
Acute toxicity, Oral (Category 4)  
Serious eye damage (Category 1)  
Skin sensitization (Category 1)

##### Classification according to EU Directives 67/548/EEC or 1999/45/EC

Toxic in contact with skin. Harmful if swallowed. Risk of serious damage to eyes. May cause sensitization by skin contact.

#### 2.2 Label elements

##### Labelling according Regulation (EC) No 1272/2008 [CLP]

Pictogram



Signal word : Danger

Hazard statement(s)

H302 : Harmful if swallowed.  
H311 : Toxic in contact with skin.  
H317 : May cause an allergic skin reaction.  
H318 : Causes serious eye damage.

Precautionary statement(s)

P280 : Wear protective gloves/ eye protection/ face protection.  
P305 + P351 + P338 : IF IN EYES: Rinse cautiously with water for several minutes. Remove

P312 contact lenses, if present and easy to do. Continue rinsing.  
Call a POISON CENTER or doctor/ physician if you feel unwell.

Supplemental Hazard Statements none

**According to European Directive 67/548/EEC as amended.**

Hazard symbol(s)



R-phrases(s)

R22 Harmful if swallowed.  
R24 Toxic in contact with skin.  
R41 Risk of serious damage to eyes.  
R43 May cause sensitization by skin contact.

S-phrases(s)

S24 Avoid contact with skin.  
S26 In case of contact with eyes, rinse immediately with plenty of water and seek medical advice.  
S37/39 Wear suitable gloves and eye/face protection.  
S45 In case of accident or if you feel unwell, seek medical advice immediately (show the label where possible).

## 2.3 Other hazards - none

## 3. COMPOSITION/INFORMATION ON INGREDIENTS

### 3.1 Substances

Formula :  $C_{13}H_{22}N_2$   
Molecular Weight : 206,33 g/mol

| Component                       |              | Concentration |
|---------------------------------|--------------|---------------|
| <b>Dicyclohexylcarbodiimide</b> |              |               |
| CAS-No.                         | 538-75-0     | -             |
| EC-No.                          | 208-704-1    |               |
| Index-No.                       | 615-019-00-5 |               |

## 4. FIRST AID MEASURES

### 4.1 Description of first aid measures

#### General advice

Consult a physician. Show this safety data sheet to the doctor in attendance.

#### If inhaled

If breathed in, move person into fresh air. If not breathing, give artificial respiration. Consult a physician.

#### In case of skin contact

Take off contaminated clothing and shoes immediately. Wash off with soap and plenty of water. Take victim immediately to hospital. Consult a physician.

#### In case of eye contact

Rinse thoroughly with plenty of water for at least 15 minutes and consult a physician.

#### If swallowed

Do NOT induce vomiting. Never give anything by mouth to an unconscious person. Rinse mouth with water. Consult a physician.

### 4.2 Most important symptoms and effects, both acute and delayed

Depending on the intensity and duration of exposure, effects may vary from mild irritation to severe destruction of tissue., May cause blindness., Symptoms may be delayed., To the best of our knowledge, the chemical, physical, and toxicological properties have not been thoroughly investigated.

### 4.3 Indication of any immediate medical attention and special treatment needed

no data available

---

## **5. FIREFIGHTING MEASURES**

### **5.1 Extinguishing media**

#### **Suitable extinguishing media**

Use water spray, alcohol-resistant foam, dry chemical or carbon dioxide.

### **5.2 Special hazards arising from the substance or mixture**

Carbon oxides, nitrogen oxides (NO<sub>x</sub>)

### **5.3 Advice for firefighters**

Wear self contained breathing apparatus for fire fighting if necessary.

### **5.4 Further information**

no data available

---

## **6. ACCIDENTAL RELEASE MEASURES**

### **6.1 Personal precautions, protective equipment and emergency procedures**

Wear respiratory protection. Avoid dust formation. Avoid breathing vapors, mist or gas. Ensure adequate ventilation. Evacuate personnel to safe areas. Avoid breathing dust.

### **6.2 Environmental precautions**

Prevent further leakage or spillage if safe to do so. Do not let product enter drains.

### **6.3 Methods and materials for containment and cleaning up**

Pick up and arrange disposal without creating dust. Sweep up and shovel. Keep in suitable, closed containers for disposal.

### **6.4 Reference to other sections**

For disposal see section 13.

---

## **7. HANDLING AND STORAGE**

### **7.1 Precautions for safe handling**

Avoid contact with skin and eyes. Avoid formation of dust and aerosols. Provide appropriate exhaust ventilation at places where dust is formed.

### **7.2 Conditions for safe storage, including any incompatibilities**

Store in cool place. Keep container tightly closed in a dry and well-ventilated place.

Moisture sensitive.

### **7.3 Specific end uses**

no data available

---

## **8. EXPOSURE CONTROLS/PERSONAL PROTECTION**

### **8.1 Control parameters**

#### **Components with workplace control parameters**

### **8.2 Exposure controls**

#### **Appropriate engineering controls**

Avoid contact with skin, eyes and clothing. Wash hands before breaks and immediately after handling the product.

#### **Personal protective equipment**

##### **Eye/face protection**

Face shield and safety glasses Use equipment for eye protection tested and approved under appropriate government standards such as NIOSH (US) or EN 166(EU).

##### **Skin protection**

Handle with gloves. Gloves must be inspected prior to use. Use proper glove removal technique (without touching glove's outer surface) to avoid skin contact with this product. Dispose of contaminated gloves after use in accordance with applicable laws and good laboratory practices. Wash and dry hands.

The selected protective gloves have to satisfy the specifications of EU Directive 89/686/EEC and the standard EN 374 derived from it.

Immersion protection

Material: Nitrile rubber

Minimum layer thickness: 0,11 mm

Break through time: > 480 min

Material tested: Dermatrill® (Aldrich Z677272, Size M)

Splash protection

Material: Nitrile rubber

Minimum layer thickness: 0,11 mm

Break through time: > 30 min

Material tested: Dermatrill® (Aldrich Z677272, Size M)

data source: KCL GmbH, D-36124 Eichenzell, phone +49 (0)6659 873000, e-mail sales@kcl.de, test method: EN374

If used in solution, or mixed with other substances, and under conditions which differ from EN 374, contact the supplier of the CE approved gloves. This recommendation is advisory only and must be evaluated by an Industrial Hygienist familiar with the specific situation of anticipated use by our customers. It should not be construed as offering an approval for any specific use scenario.

### Body Protection

Complete suit protecting against chemicals, The type of protective equipment must be selected according to the concentration and amount of the dangerous substance at the specific workplace.

### Respiratory protection

Where risk assessment shows air-purifying respirators are appropriate use a full-face particle respirator type N100 (US) or type P3 (EN 143) respirator cartridges as a backup to engineering controls. If the respirator is the sole means of protection, use a full-face supplied air respirator. Use respirators and components tested and approved under appropriate government standards such as NIOSH (US) or CEN (EU).

---

## 9. PHYSICAL AND CHEMICAL PROPERTIES

### 9.1 Information on basic physical and chemical properties

- |   |  |
|---|--|
| a) Appearance                                   | Form: solid<br>Colour: colourless                                      |
| b) Odour  | no data available  |
| c) Odour Threshold                              | no data available  |
| d) pH   | no data available  |
| e) Melting point/freezing point                 | Melting point/range: 34 - 35 °C<br>Melting point/range: 34,5 - 37,0 °C |
| f) Initial boiling point and boiling range      | 122 - 124 °C at 8 hPa  |
| g) Flash point                                  | 113 °C - closed cup  |
| h) Evaporation rate                             | no data available  |
| i) Flammability (solid, gas)                    | no data available  |
| j) Upper/lower flammability or explosive limits | no data available  |
| k) Vapour pressure                              | no data available  |
| l) Vapour density                               | no data available  |
| m) Relative density                             | no data available  |
| n) Water solubility                             | no data available  |
| o) Partition coefficient: n-octanol/water       | no data available  |

- |    |                           |                   |
|----|---------------------------|-------------------|
| p) | Autoignition temperature  | no data available |
| q) | Decomposition temperature | no data available |
| r) | Viscosity                 | no data available |
| s) | Explosive properties      | no data available |
| t) | Oxidizing properties      | no data available |

## **9.2 Other safety information**

no data available

---

## **10. STABILITY AND REACTIVITY**

### **10.1 Reactivity**

no data available

### **10.2 Chemical stability**

no data available

### **10.3 Possibility of hazardous reactions**

no data available

### **10.4 Conditions to avoid**

no data available

### **10.5 Incompatible materials**

Strong oxidizing agents

### **10.6 Hazardous decomposition products**

Other decomposition products - no data available

---

## **11. TOXICOLOGICAL INFORMATION**

### **11.1 Information on toxicological effects**

#### **Acute toxicity**

LD50 Oral - rat - 1.499 mg/kg

LC50 Inhalation - rat - 6 h - 159 mg/m<sup>3</sup>

Remarks: Sense Organs and Special Senses (Nose, Eye, Ear, and Taste): Eye: Lacrimation.  
Vascular: Regional or general arteriolar or venous dilation. Skin and Appendages: Other: Hair.

LD50 Dermal - rabbit - 79,1 mg/kg

#### **Skin corrosion/irritation**

Skin - rabbit - Extremely corrosive and destructive to tissue. - 4 h

#### **Serious eye damage/eye irritation**

no data available

#### **Respiratory or skin sensitization**

May cause allergic skin reaction.

#### **Germ cell mutagenicity**

no data available

#### **Carcinogenicity**

IARC: No component of this product present at levels greater than or equal to 0.1% is identified as probable, possible or confirmed human carcinogen by IARC.

#### **Reproductive toxicity**

no data available

#### **Specific target organ toxicity - single exposure**

no data available



**Specific target organ toxicity - repeated exposure**

no data available

**Aspiration hazard**

no data available

**Potential health effects****Inhalation**

May be fatal if inhaled. Material is extremely destructive to the tissue of the mucous membranes and upper respiratory tract.

**Ingestion**

Harmful if swallowed. Causes burns.

**Skin**

May be fatal if absorbed through skin. Causes skin burns.

**Eyes**

Causes eye burns.

**Signs and Symptoms of Exposure**

Depending on the intensity and duration of exposure, effects may vary from mild irritation to severe destruction of tissue., May cause blindness., Symptoms may be delayed., To the best of our knowledge, the chemical, physical, and toxicological properties have not been thoroughly investigated.

**Additional Information**

RTECS: FF2160000

---

**12. ECOLOGICAL INFORMATION****12.1 Toxicity**

no data available

**12.2 Persistence and degradability**

no data available

**12.3 Bioaccumulative potential**

no data available

**12.4 Mobility in soil**

no data available

**12.5 Results of PBT and vPvB assessment**

no data available

**12.6 Other adverse effects**

no data available

---

**13. DISPOSAL CONSIDERATIONS****13.1 Waste treatment methods****Product**

Offer surplus and non-recyclable solutions to a licensed disposal company. Dissolve or mix the material with a combustible solvent and burn in a chemical incinerator equipped with an afterburner and scrubber.

**Contaminated packaging**

Dispose of as unused product.

---

**14. TRANSPORT INFORMATION****14.1 UN number**

ADR/RID: 2811

IMDG: 2811

IATA: 2811

**14.2 UN proper shipping name**

ADR/RID: TOXIC SOLID, ORGANIC, N.O.S. (Dicyclohexylcarbodiimide)

IMDG: TOXIC SOLID, ORGANIC, N.O.S. (Dicyclohexylcarbodiimide)

IATA: Toxic solid, organic, n.o.s. (Dicyclohexylcarbodiimide)

**14.3 Transport hazard class(es)**

ADR/RID: 6.1

IMDG: 6.1

IATA: 6.1

**14.4 Packaging group**

ADR/RID: II

IMDG: II

IATA: II

**14.5 Environmental hazards**

ADR/RID: no

IMDG Marine pollutant: no

IATA: no

**14.6 Special precautions for user**

no data available

---

**15. REGULATORY INFORMATION**

This safety datasheet complies with the requirements of Regulation (EC) No. 1907/2006.

**15.1 Safety, health and environmental regulations/legislation specific for the substance or mixture**

no data available

**15.2 Chemical Safety Assessment**

no data available

---

**16. OTHER INFORMATION****Further information**

Copyright 2012 Sigma-Aldrich Co. LLC. License granted to make unlimited paper copies for internal use only.

The above information is believed to be correct but does not purport to be all inclusive and shall be used only as a guide. The information in this document is based on the present state of our knowledge and is applicable to the product with regard to appropriate safety precautions. It does not represent any guarantee of the properties of the product. Sigma-Aldrich Corporation and its Affiliates shall not be held liable for any damage resulting from handling or from contact with the above product. See [www.sigma-aldrich.com](http://www.sigma-aldrich.com) and/or the reverse side of invoice or packing slip for additional terms and conditions of sale.

---

## APPENDIX C

### **FT-IR Spectroscopy Results of p-MWNTs and ox-MWNTs**

In this research, Infrared spectroscopy (FT-IR) analyses of the carboxylic acid groups present on CNTs surface were analyzed with Shimadzu Fourier Transform Infrared Spectrophotometer 8400-S. The samples were analyzed with a diamond Attenuated Total Reflectance (ATR) equipment where the samples were placed on the sample holder with the region observed from (4000–600  $\text{cm}^{-1}$ ).

Figure A illustrates the FT-IR spectrum of p-MWNTs and ox-MWNTs. Two strong C=C vibration of MWNTs in the range of 2069-1983  $\text{cm}^{-1}$  were detected along with weak aromatic ring of C=C in the range 1625 and 1535  $\text{cm}^{-1}$ . In addition, medium intensity of C-H bending bands in range from 650-600  $\text{cm}^{-1}$  can be seen in the figures below. Ox-MWNTs spectrum exhibits peaks in range of 1726-1612  $\text{cm}^{-1}$  and 1408-1375  $\text{cm}^{-1}$  corresponding C=O stretching and C-O-H bending vibrations. It can be seen that the vibrations are weak. This is because of the amount of the attached carboxylic group is small.

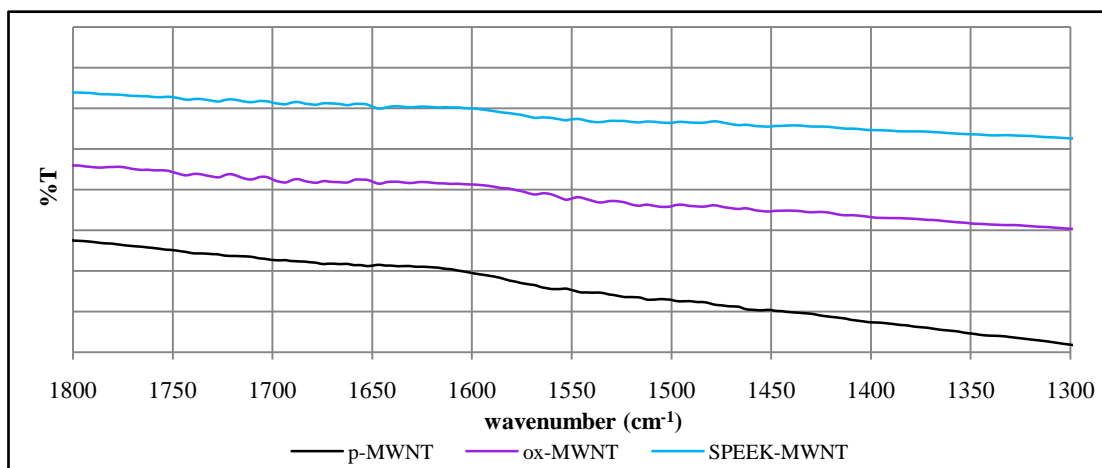


Figure A: FT-IR spectra of C=O bonding